State-dependent modulation of cortico-spinal networks

Dissertation

zur Erlangung des Grades eines

Doktors der Naturwissenschaften

der Mathematisch-Naturwissenschaftlichen Fakultät

und

der Medizinischen Fakultät

der Eberhard-Karls-Universität Tübingen

vorgelegt

von

Fatemeh Khademi
aus Hamedan,Iran

Oktober 2017

Tag der mündlichen Prüfung: 19.12.2017

Dekan der Math.-Nat. Fakultät: Prof. Dr. W. Rosenstiel
Dekan der Medizinischen Fakultät: Prof. Dr. I. B. Autenrieth

1. Berichterstatter: Prof. Dr. Alireza Gharabaghi

2. Berichterstatter: Prof. Dr. Christoph Braun

Prüfungskommission: Prof. Dr. Alireza Gharabaghi

Prof. Dr. Christoph Braun

Prof. Dr. Ingo Hertrich

Prof. Dr. Andreas Bartels

Erklärung / Declaration:

Ich erkläre, dass ich die zur Promotion eingereichte Arbeit mit dem Titel: *“ State-dependent modulation of cortico-spinal networks”* selbständig verfasst, nur die angegebenen Quellen und Hilfsmittel benutzt und wörtlich oder inhaltlich übernommene Stellen als solche gekennzeichnet habe. Ich versichere an Eides statt, dass diese Angaben wahr sind und dass ich nichts verschwiegen habe. Mir ist bekannt, dass die falsche Abgabe einer Versicherung an Eides statt mit Freiheitsstrafe bis zu drei Jahren oder mit Geldstrafe bestraft wird.

I hereby declare that I have produced the work entitled “State-dependent modulation of cortico-spinal networks”, submitted for the award of a doctorate, on my own (without external help), have used only the sources and aids indicated and have marked passages included from other works, whether verbatim or in content, as such. I swear upon oath that these statements are true and that I have not concealed anything. I am aware that making a false declaration under oath is punishable by a term of imprisonment of up to three years or by a fine.

Tübingen, den ....

Datum / Date Unterschrift /Signature

Table of contents

1. Abstract 5

2. Introduction 7

3. Chapters.....12

3.1. Distinct beta-band oscillatory circuits underlie corticospinal gain modulation …….....12

3.2. Brain-machine interface feedback shapes cortico-muscular control after stroke.....13

3.3. Brain-state dependent transcranial magnetic stimulation controlled by sensorimotor desynchronization induces robust increase of corticospinal excitability 14

3.4. Brain state-dependent stimulation enhances task-specific motor network connectivity.....15

3.5. Learned self-regulation of the lesioned brain with epidural electrocorticography.....17

4. Discussion.....18

5. References.....22

6. Statement of contributions.....28

7. Acknowledgement.....31

8. Included manuscripts 32

8.1. Manuscript 1.....32

8.2. Manuscript 2.....73

8.3. Manuscript 3.....122

8.4. Manuscript 4.....132

8.5. Manuscript 5.....168

Table of Abbreviations

BCI	Brain-computer interface
BMI	Brain-machine interface
ciCOH	Corrected imaginary part of coherence
CMC	Cortico-muscular coherence
CSE	Cortico-spinal excitability
ECoG	Electrocorticography
EEG	Electroencephalography
EMG	Electromyography
ERD	Event-related desynchronization
GABA	Gamma-aminobutyric acid
LFP	Local field potential
MEP	Motor evoked potential
MI	Motor imagery
PTN	Pyramidal tract neuron
RMT	Resting motor threshold
SRC	Stimulus-response curve
TEP	Transcranial evoked potential
TMS	Transcranial magnetic stimulation

1. Abstract

Beta-band rhythm (13-30 Hz) is a dominant oscillatory activity in the sensorimotor system. Numerous studies reported on links between motor performance and the cortical and cortico-spinal beta rhythm. However, these studies report divergent beta-band frequencies and are, additionally, based on differently performed motor-tasks (e.g., motor imagination, muscle contraction, reach, grasp, and attention). This diversity blurs the role of beta in the sensorimotor system. It consequently challenges the development of beta-band activity-dependent stimulation protocols in the sensorimotor system. In this vein, we studied the functional role of beta-band cortico-cortical and cortico-spinal networks during a motor learning task. We studied how the contribution of cortical and spinal beta changes in the course of learning, and how this modulation is affected by afferent feedback to the sensorimotor system. We furthermore researched the relationship to motor performance. Consider that we made our study in the absence of any residual movement to allow our findings to be translated into rehabilitation programs for severely affected stroke patients.

This thesis, at first, investigates evoked responses after transcranial magnetic stimulation (TMS). This revealed two different beta-band networks, i.e., in the low and high beta-band reflecting cortical and cortico-spinal activity. We, then, used a broader frequency range in the beta-band to trigger passive opening of the hand (peripheral feedback) or cortical stimulation (cortical feedback). While a unilateral hemispheric increase in cortico-spinal synchronization was observed in the group with peripheral feedback, a bilateral hemispheric increase in cortico-cortical and cortico-spinal synchronization was observed for the group with cortical feedback. An improvement in motor performance was found in the peripheral group only. Additionally, an enhancement in the directed cortico-spinal synchronization from cortex to periphery was observed for the peripheral group. Similar neurophysiological and behavioral changes were observed for stroke patients receiving peripheral feedback. The results

suggest two different mechanisms for beta-band activity-dependent protocols depending on the feedback modality. While the peripheral feedback appears to increase the synchronization among neural groups, cortical stimulation appears to recruit dormant neurons and to extend the involved motor network.

These findings may provide insights regarding the mechanism behind novel activity-dependent protocols. It also highlights the importance of afferent feedback for motor restoration in beta-band activity-dependent rehabilitation programs.

2. Introduction

The beta-band (13-30 Hz) oscillation is a prominent motor-related oscillatory activity in human and primates. However, different functional roles for this oscillatory rhythm were suggested. Modulation of both cortical and cortico-spinal beta was linked to performance and divergent motor task. This diversity increases as we include different sub-bands of 13-30 Hz. Here, some of these reports are introduced. Classen and colleague (1998) observed an intra- and inter-hemispheric increase in coherence (13-21 Hz) of electroencephalography signal (EEG) during a visuomotor task. The coherence was similar, when only the visual or motor task were performed; but it decreased when the subject was receiving a visual distractor. This finding suggests an information processing role for 13-21 Hz. In an awake behaving monkey, Fetz and colleagues (2000) showed that bursts of local field potential (LFP) oscillations in the motor cortex (20-40 Hz) but not for the electromyography (EMG) signal. This cortical modulation occurred during exploratory hand but not for wrist movements, suggesting an attentional role for 20-40 Hz rather than an involvement in motor execution. On the other side, during the hold period of a precision grip task performed by awake behaving monkey, Baker and colleagues (1997) showed bursts of 20-30 Hz LFP oscillation in the motor cortex and pyramidal tract neurons (PTN) coherent with EMG signals. This suggests a functional role for coherent cortical and spinal beta rhythms. All of these studies have in common is that the modulation of cortical and cortico-spinal beta activity is linked to different behavioral task (Khana and Carmena, 2015). Therefore, we used new protocol to overcome this diversity.

Cortico-muscular coherence (CMC) for 20-30 Hz was reported in stroke patients with upper limb discoordination during a reaching task (Fang et al., 2009). However, the control group of healthy subjects showed the CMC for 30-40 Hz. They (Fang et al., 2009), hence, concluded the CMC for 20-30 Hz might indicate the poor integration between sources of EEG and EMG signal for action processing. On the other side, 13-30 Hz and 30-41 Hz CMC was reported during static and dynamic

forces, respectively (Gewin and Ferris, 2012). Omlor and colleagues (2011) showed significant CMC for 15-30 Hz during a steady state and dynamic force generation in healthy subjects. The CMC was higher when processing was needed to predict the dynamic force, i.e., when the unpredictable amount of force was applied. They (Omlor et al., 2011) showed that the cortical beta power was lower during the task than rest. Specifically, it was lesser during unpredictable than predictable force. Moreover, they reported a linear relationship between the decrease in cortical beta power and an increase in beta CMC. However, in another study (Kriesteva et al., 2007), the high cortical beta (15-30 Hz) power was reported contingent with high beta CMC (15-30 Hz) for the group of subjects with good performance. These findings, also, blurred the role of beta CMC in the sensorimotor loop. It is not clear whether cortical beta is essential to reach motor performance or is an epiphenomenal observation, and rather cortico-spinal beta coherence is more relevant for motor-control.

Pharmacological studies revealed different mechanisms for the cortical and cortico-spinal beta using the benzodiazepines diazepam and carbamazepine (Baker et al., 2003; Riddle et al., 2004). Diazepam decreases the neural excitability by enhancing the neurotransmitter gamma-aminobutyric acid (GABA) at the GABA-A receptors. It decreases the chance of firing of the neurons by increasing the chloride inside the cell. Carbamazepine, on the other side, binds to the voltage-gated sodium channel and stops the repetitive firing of the neurons. Diazepam increased the cortical beta power (~ 20 Hz; Baker et al., 2003) in a precision grip task, but led to a slight decrease in cortico-muscular coherence (~20 Hz). This might suggest the involvement of GABAergic activity in intracortical inhibition of the local cortical circuits for beta (~20 Hz) oscillations. On the other hand, carbamazepine significantly increased cortico-muscular coherence (~21 Hz), in a precision grip task, with no modulation of cortical power (Riddle et al., 2004). These pharmacological studies suggest a partially independent role of cortical and cortico-spinal beta; and an important role of cortico-muscular coherence for motor-control.

In another study by Riddle and Baker (2005), manipulating the peripheral nerve by cooling the arm (Riddle and Baker, 2005) showed a decrease in CMC and caused a modulation in the respective phase delay. Specifically, Witham and colleagues (2011) could estimate the directed coherence for three different groups of subjects after estimating the phase-frequency relationships of their beta CMC: a group with significant directed coherence for the descending pathway, a group with significant directed coherence for the ascending pathway, and a group with no significant directed coherence (Witham et al., 2011). These findings provide remarkable evidence that afferent pathways play a relevant role in the generation of CMC (Riddle and Baker, 2005; Baker and Baker, 2003; Witham et al., 2011). Therefore, a model based on efferent pathways cannot sufficiently describe CMC. A current "closed neural group" theory (Aumann and Prut, 2015) proposes that sensorimotor beta (~20 Hz) is generated not only through the firing of cortical neurons, but rather as a result of recurrent loops between sensorimotor cortex and periphery. The idea is that the generated beta oscillations in the primary motor cortex (M1) will be conveyed to the periphery and returned to the primary sensory cortex (S1) via efferent and afferent pathways, respectively, and later from S1 to M1. This recurrent cortical-peripheral-cortical loop allows the resonant generation of beta oscillations within the motor system (Aumann and Prut, 2015).

In parallel to neurophysiological studies concerning the functional role of the beta-band, neuroprosthetic applications were developed in so-called brain-computer interface (BCI) platforms. In this platform the oscillatory activity of the cortex is transferred to a computer; and visual feedback is provided to the subject based on a linear classifier output (Schalk et al., 2004). Since beta-band oscillatory activity represents a repetitive modulation (Chen and Fetz, 2005; Witham and Baker, 2007) and has a topographical distribution (Neuper and Pfurtscheller, 2001; Pfurtcheler and da Silva, 1999) during movement preparation (Pfurtscheller et al., 1997; Pfurtschellerand da Silva, 1999; Salmelin and Hari, 1994) and motor execution (Tan et al., 2014; Tan et al., 2016), it was chosen as one of the target frequency bands for

neuroprosthetic applications.Importantly, kinesthetic motor imagery led to the similar functional and topographical modulations of the beta-band as movement execution (McFarland et al., 2000) by recruiting the neural population activated during active motor control (Pfurtscheller and Neuper 1997; Lotze et al. 1999; Neuper et al. 2005; Kaiser et al. 2011). The increase in CMC was also reported during kinesthetic motor imagery (Ridding and Rothwell 1999; Roosink and Zijdewind 2010; Stinear et al. 2006). Hence, BCI applications have been applied for patients with movement disorders using modulation of cortical beta-band (Gharabaghi et al., 2015; Sitaram et al., 2017) in a so-called brain-machine interface (BMI) platform. In this vein, a recent study (Kraus et al., 2016) demonstrated that BMI led a robust increase in cortico-spinal excitability (CSE). Current findings (Kraus et al., 2016) may suggest a beta-band activity-dependent protocol for plasticity induction in the human sensorimotor system (Gharabaghi et al., 2015; Kraus et al., 2016).

The contribution of state-dependent motor cortex oscillatory activity in CSE has been shown by Schulz and colleagues (2014). They used single TMS pulse after voluntary muscle contraction. They found a negative correlation between the power of cortical beta-band (15-30 Hz) and motor evoked potential (MEP) amplitude. Takemi and colleagues (2013) rather applied TMS pulse during kinesthetic motor imagery (7-26 Hz) and demonstrated that higher levels of event-related desynchronization (ERD) led to higher MEP amplitudes. A study by Kraus and colleagues highlights these findings. In this study, a correlation was found between the modulation level of 16-22 Hz desynchronization in the course of a BMI intervention and the MEP amplitude. For the intervention, they used a beta-band activity-dependent stimulation protocol. A robotic orthosis provided peripheral feedback by opening the hand of the subject contingent with 16-22 Hz desynchronization. They also showed an increase in the MEP amplitude but not in the area under the MEP curve after the intervention, suggesting an increase in the neural synchronization level (Kraus et al., 2016). The same beta-band activity-dependent protocol was used by Naros and colleagues (2016). They adjusted the

threshold for 16-22 Hz desynchronization detection and showed that subjects could enhance ERD across the sessions of the intervention. Importantly, they observed an improvement in motor performance. However, in none of the studies mentioned above (Takemi et al., 2013; Kraus et al., 2016; Naros et al., 2016) the cortico-spinal oscillatory activity was investigated. In one study, van Elswijk and colleague (2010) demonstrated the dependency of CSE on spinal beta. They applied a short-lasting TMS pulse during consecutive periods of voluntary muscle contraction and rest. They found the rising phase of the spinal beta oscillations to led to higher MEP amplitudes. They did not find any relationship concerning the phase of cortical beta oscillations.

We aimed to investigate the role of beta-band oscillations independent from any specific task first. The relationship between power and phase of cortical and spinal beta-band oscillations was quantified by the sensorimotor output, i.e., motor evoked potential (MEP). Then, the mechanism for a beta-band dependent stimulation protocol with contingent peripheral feedback with a robotic hand orthosis was explored. We, additionally, investigated the mechanism for the beta-band dependent stimulation protocol when peripheral feedback was replaced by cortical (TMS) feedback. The modulations of cortico-cortical and cortico-spinal connectivity were compared to a control group that was receiving the same peripheral or cortical feedback independent of the brain state. We also investigate da single ischemic stroke patient by moving from a non-invasive (EEG) to an invasive (electrocorticography, ECoG) platform for neurorehabilitation.

3. Chapters

3.1. Distinct beta-band oscillatory circuits underlie corticospinal gain modulation

Previous studies (van Elswijk et al., 2010; Keil et al., 2014) demonstrated phase-specific gain modulation in the motor system. However, the final conclusion regarding the optimal timing of the TMS pulse are contradictory. In this work, we intended to address these contradictory findings and provide information regarding the increased responsiveness of the beta-band oscillatory cycle. we investigated the modulatory effect of the ongoing cortical (EEG) and cortico-spinal rhythms (EMG) on the MEP amplitude. Additionally, we studied a potential confounding effect of power on phase.

During the experiment, the subjects were instructed to sit upright in a reclining chair and relax their arm. Single TMS pulses were applied to the right sensorimotor cortex of healthy subjects (Raco et al., 2017; Royter et al., 2016). We applied ten TMS pulses per eight different TMS intensities (90, 100, 110, 120, 130, 140, 145, and 150 % of resting motor threshold (RMT)). The pre-TMS power and phase of the EEG and EMG were estimated for 6-30 Hz in steps of 1 Hz per TMS intensities, and the MEP amplitude was estimated (van Elswijk et al., 2010). We observed an influence of pre-TMS power and phase of the EEG (14-17 Hz) on MEP amplitude only for the stimulation of 100% of RMT.

We, additionally, observed that pre-TMS phase, but not power, of EMG (20-24 Hz) oscillatory activity could determine the MEP amplitude. We, therefore, found two distinct beta networks, i.e. in the lower (14-17 Hz) and upper beta-band (20-24 Hz) for cortical and cortico-spinal oscillatory activity, respectively. This may suggest state-dependent and circuit-specific interventions for therapeutic applications. We, importantly, could demonstrate that the synaptic input is most efficient when it arrives at the rising phase of the cortical and cortico-spinal beta rhythm. Our findings,

confirm and extend the observations by van Elswijk and colleagues (2010). Further details can be found in the attached manuscript 1.

3.2. Brain-machine interface feedback shapes cortico-muscular control after stroke

Motor imagery-related (MI) neurofeedback is used as therapeutic tools for stroke rehabilitation (Sitaram et al., 2017). A recent study by Kraus et al. (2016) demonstrated that MI-related BMI intervention would increase CSE. Another study by Naros and colleagues (2016) showed the same intervention would increase cortical self-regulation of beta-band ERD, which was correlated with improvement in motor performance. However, the functional role of cortical beta-band ERD for the changes in motor performance remains unclear. In this study, we used a motor imagery (MI)-related peripheral intervention and studied the modulation of cortical and cotico-spinal beta and their relationships with improvement in performance.

For this study, we used desynchronization of 16-22 Hz of cortical oscillatory rhythm to provide contingent peripheral feedback. To quantify the effect of the peripheral feedback we investigated a control group which received visual feedback only. The effect of sensorimotor rhythm based visual feedback already has been shown for healthy subjects and stroke patients (Buch et al., 2008; Gomez-Rodiguez et al., 2011; Bai et al., 2015; Ang et al., 2010; Ramos-Murguialday et al., 2013). But, no study investigated the modulation of the cortico-spinal network and its phase-frequency relationship for the beta-band related brain-robot interface (BRI) and brain-computer interface (BCI) training. In this vein, we quantified the modulation of the cortico-spinal synchronization before and after the intervention. Additionally, the behavioral gain modulation was investigated before and after the beta-band related BRI and BCI training.

We measured the changes in beta-band ERD during the intervention. Both groups showed an increase in the beta-band ERD, but only the group with peripheral feedback reached to a significant increase in cortico-spinal synchronization. This effect was observed during the post-intervention isometric motor-task as well when the performance improved. The phase-frequency spectra of the modulated cortico-spinal synchronization showed significant changes in the slope of the fitted line. This suggests an enhanced directed coherence following the beta-band related BRI. The implementation of the same protocol, i.e., beta-band related BRI, for stroke patients led the similar physiological changes. The improvement in the upper-extremity Fugl-Meyer assessment suggests the therapeutic potential of this intervention. Further details can be found in the attached manuscript 2.

3.3. Brain-state dependent transcranial magnetic stimulation controlled by sensorimotor desynchronization induces robust increase of corticospinal excitability

It is known that desynchronization of cortical beta-band lead increase in cortico-spinal excitability. However, the cumulative effect of beta-band ERD contingent with TMS pulse remains unclear. In this study, the cumulative effect of cortical stimulation in the presence (experimental group) and absence (control group) of kinesthetic motor imagery was investigated. No peripheral feedback was provided and the cortical stimulation was paired with cortical beta-band ERD over the frequency range of 16-22 Hz. The pattern of brain state-dependent cortical stimulation during the intervention was copied and applied to the control group independent of the brain state.

The comparison between the spatial distribution of the ERD between the study and control group showed a significant difference for the modulated sensorimotor

cortex. The MEP amplitude and area under the curve showed a significant increase for the study group. This increase was observed in the range of 110-130% resting motor threshold (RMT). The increase in MEP amplitude with no changes in the area under the MEP curve suggests an increase in the synchronicity of neurons. In our study, however, we observed an increase in both MEP amplitude and the area under the curve, which suggest the recruitment of additional dormant neurons.

On the other side, no increase in MEP amplitude was observed for the control group in the range of 110-130% RMT. However, a decrease in the plateau values over the range of 131-160% was observed. The same changes were observed for the area under the MEP curve.

The cortical map of both study and control group was changed following the intervention. Brain state-dependent stimulation led to an increase in cortical excitability. Application of cortical stimulation independent of the state of the brain led to a decrease in cortical excitability. Further details can be found in the attached manuscript 3.

3.4. Brain state-dependent stimulation enhances task-specific motor network connectivity

In our previous study, MI-related ERD contingent with TMS pulse led the cortico-spinal excitability. It also suggested the recruitment of additional dormant neurons as a mechanism for the observed post-intervention increase in the MEP amplitude and area under the MEP curve. In this study, we aimed to reveal neurophysiological mechanisms underlying the effects of brain-state dependent cortical stimulation. We hypothesized that such protocol modulates cortical motor circuits and enhanced task-specific motor network connectivity.

Here, we analyzed the cortico-cortical and cortico-spinal connectivity of electrophysiological field potentials.

We observed that the amplitude of the transcranial evoked potential (TEP) for the late positive deflection was higher for the experimental group as compared to the control group. None of the other TEP components (P25, N45, P70, N100) showed significant modulation. The observed modulation of TEP amplitude was dominant in the left cortex, i.e., contra-lateral to the side of TMS pulse.

We, additionally, observed an increase in intra- and inter-hemispheric cortico-cortical connectivity. For the experimental group, the TMS-induced cortico-cortical functional connectivity (corrected imaginary part of coherence; ciCOH) was higher, specific to the feedback frequency band (16-22 Hz), and paralleled by an increase in the TMS-induced cortico-muscular coherence. These intra- and inter-hemispheric patterns suggest the recruitment of addition cortical areas during brain-state dependent cortical stimulation. Also, the modulation of the TEP amplitude suggests the involvement of GABAergic activity for inter-hemispheric connectivity. The phase-frequency relationships of the cortico-muscular coherence showed a different sign of the regression slope. While the right hemisphere showed a negative slope, indicating a directed coherence from the cortex to muscle, the left hemisphere showed a positive slope, indicating a directed coherence from the muscle to cortex.

The observed spatial distributions of the increased cortico-cortical and cortico-muscular coherence in the feedback frequency band (16-22 Hz) reoccurred after the intervention, i.e., during the isometric motor task in the absence of TMS. Importantly, this modulation was observed during the transition from finger flexion to extension. This pattern was thereby task-specific because participants performed kinesthetic motor imagery of hand opening during the intervention as well. Further details can be found in the attached manuscript 4.

3.5. Learned self-regulation of the lesioned brain with epidural electrocorticography

Electroencephalography (EEG) is used as a common platform for neurofeedback rehabilitation program of stroke patients. But EEG, in general, has low signal-to-noise ratio and may be contaminated with muscle artifact. On the other side, ECoG can provide better signal to noise ratio with less contamination of artifact and may suggest better platform for rehabilitation programs. In this study, we compared different recording modalities of cortical oscillatory activity, i.e., EEG and ECoG. One patient with an extended ischemic lesion of the cortex participated in two rehabilitation interventions, i.e. EEG-based and ECoG-based feedback. Each of the intervention periods lasted for one month and followed the same paradigm, i.e., feedback of ipsilesional sensorimotor activity (16-22 Hz).

EEG recordings were contaminated with muscle artifacts; they occurred during the "rest" period and to a lesser degree during the "move" period of the experiment. Since the closed-loop paradigm was using the oscillatory activity recorded during the "rest" period as a baseline for brain self-regulation, the patient learned to control the closed-loop paradigm by increasing and decreasing the muscle artifact. This learning correlated with the brain-machine interface performance.

During ECoG neurofeedback, no systematic changes in the number of muscle artifact were observed. Importantly, we did not find any evolution of the number of muscle artifact over the training period. Furthermore, the patient could modulate the MI-related ERD significantly above baseline in the course of the training period. Further details can be found in the attached manuscript 5.

4. Discussion

Two neural groups can effectively communicate when the input and output windows of the communication are open at the same time (Fries., 2005). In other words, only neural groups that oscillate coherently communicate efficiently (Fries., 2005). In this vein, the phase and the conduction delay of the frequency of the oscillatory neural groups should match (Fries., 2005). During unidirectional communication, however, the conduction delay can be translated to the phase of the frequency of the coherent oscillatory activity. This, specifically, can be addressed in the motor system. The coherent oscillatory activity between sensorimotor and spinal cord was repeatedly reported as a mechanism for the effective cortico-spinal communication (Schoffelen., 2005; Baker and Baker 2003). However convincing evidence for the relationship of the cortical phase and sensorimotor system output, measured by the amplitude of MEP, was not reported yet. However, the modulatory effect of the phase of the spinal beta on MEP was quantified by van Elswijk and colleagues (2010). On the other side, the relationship between cortical beta power and MEP amplitude was reported (Takemi et al.; 2013; Schulz et al., 2014; Keil et al., 2014); i.e., higher sensorimotor power led to lower MEP amplitude. A Recent study showed that using a beta-band activity-dependent protocol contingent with the modulation of cortical beta led to robust increases in CSE (Kraus et al., 2016). These finding might suggest cortical beta activity as a target frequency band for activity-dependent protocols (Gharabaghi et al., 2014; Naros et al., 2016) to induce cortico-spinal plasticity (Kraus et al., 2016). To facilitate the beta-band activity-dependent protocol for therapeutic applications (Gomez-Rodriguez et al., 2011; Gharabaghi et al., 2014; Bai et al., 2015) understanding the mechanism behind this protocol is crucial. Specifically, current theory (Aumann and Purt, 2015) suggests the beta rhythm as a recurrent propagation within a closed neural loop.

Hence, in this thesis, we investigated the effect of a beta-band activity-dependent stimulation protocol on cortico-cortical and cortico-spinal connectivity in the sensorimotor system with activity-dependent brain stimulation protocols. Before using any activity-dependent modulations, we quantified cortico-spinal connectivity with the motor system remained at rest, i.e., with no specific physical or mental task. We then perturbed the underlying networks with different TMS intensities. The optimal timing to apply the TMS pulse according to the state of the cortical and cortico-spinal sensorimotor rhythm was detected. Former studies during (van Elswijk et al., 2010) or after a motor task (Keil et la., 2014) had contradictory findings in this regard. Van Elswijk and colleagues (2010) found a phase-dependency for spinal, but not cortical activity. Keil and colleagues (2014) found a cortical phase dependency, but with two peaks of excitability within one oscillatory cycle. This observation, however, is in contradiction to previous reports of desynchronization and synchronization within one cycle of the beta rhythm (Baker, 2007; Fries et al., 2007; Lacey et al. 2014). Our study demonstrated cortical phase-specificity once per oscillatory beta cycle. Moreover, we detected two different networks on the cortical (14-17 Hz) and cortico-spinal (20-24 Hz) level. In line with former pharmacological studies, our work suggests different roles for cortical and cortico-spinal beta (Baker and Baker, 2003; Riddle et al. 2004).

We used 16-22 Hz frequency band for the activity-dependent protocols with peripheral and visual feedback. This frequency band, thereby, covered both of the networks mentioned above. Both groups (visual and peripheral feedback) enhanced ERD specific to the feedback frequency (16-22 Hz). However, only the peripheral group showed an increase in CMC contingent with a subsequent improvement in motor performance. Enhancement in cortical beta power in both groups independent from feedback modality is in line with reports from Thut and Miniussi (2009) and Jensen and Mazaheri (2010) that sensorimotor oscillation may modulate through

thalamo-cortical and cortico-cortical interactions. The relationship between CMC and performance is also in line with former reports and the role of beta CMC in motor-control (Baker et al., 1997; Kristeva et al., 2007). These findings complement Kraus and colleagues (2016) where the same intervention showed a robust increase in CSE. Therefore, pairing peripheral feedback with the sensorimotor ERD state of the cortex increased CSE (Mrachacz-Kersting et al., 2012, 2016). The recent study by Naros and colleagues (2016) also showed the improvement in motor performance to positively correlate with an increase in cortical desynchronization of beta-band activity. In this study, no quantification for the modulation in CMC has been done (Naros et al., 2016). In this context, our findings suggest beta-band CMC serves as a cortico-spinal functional gateway for the transfer of sensorimotor information (Omlor et al., 2011; Aumann and Prut, 2015). Moreover, the phase-frequency estimation showed changes in the directionality of the information flow. The results suggested an enhanced directed coherence from cortex to periphery at the end of the intervention with an extended motor network topography. This former studies (He et al., 1993; Kombos et al., 1999; Teitti et al., 2008; Schmidt et al., 2013) that showed extended cortico-spinal connections not restricted to the primary motor cortex. The same intervention led to improvements in motor performance in stroke patients. This could inform the therapeutic application of beta-band activity-dependent peripheral brain stimulation.

Replacing the peripheral feedback with cortical (TMS) feedback within the same experimental design led, however, to a different topographical distribution of the cortico-cortical and cortico-spinal networks. Different than previous approaches which applied the TMS pulse during the resting state (Bestmann et al., 2003; 2005; Veniero et al., 2013; Nettekoven et al., 2014, Volz et al., 2016) or voluntary movement (Bütefisch et al., 2004; Thabit et al., 2010; Bütefisch et al., 2011; Narayana et al., 2014.), we applied it contingent to 16-22 Hz ERD in the absence of

actual movement. We observed enhanced motor network (cortico-cortical and cortico-spinal) connectivity during the intervention (i.e., immediately following the TMS pulse) and after the intervention (i.e., during the post-intervention motor-task without TMS) in comparison to the control group (with the same pattern and number of pulses as an experimental group). Importantly, the same task-related network of imagined or real hand opening was activated during and after the intervention, respectively. This observation is in line with Rehme and colleagues (2013) who demonstrated activity-dependency of motor-network connectivity. Notably, the activated motor-network in our study was bilateral. The transcranial evoked response showed an increase in positivity for the P180 peak. This may suggest the involvement of GABAergic activity (Premoli et al., 2014 a, b) for beta-band activity-dependent cortical stimulation by TMS. The observed motor-network was extended to the contra-lateral hemisphere. This is in contrast to the unilateral cortico-spinal network which we observed for the peripheral feedback intervention. This suggests more the involvement of dormant neurons within an extended motor networks as a potential mechanism underlying this protocol in contrast to an increase in synchronization demonstrated by peripheral stimulation Kraus and colleagues (2016).

In summary, this thesis demonstrates that activity-dependent sensorimotor stimulation increases the synchronization within the sensorimotor loop and may thereby lead to the behavioral gains. This intervention may also increase the synchronization within an extended motor network and enhance its task-specific modulation. Moreover, the potential of peripheral feedback was demonstrated for stroke patients. This will need more consideration, e.g. regarding the platform applied for this therapeutic intervention. In one stroke, we demonstrated that EEG approaches may be compromised by artifacts. For these cases, ECoG platforms may be an alternative.

5. References

Ang KK, Guan C, Chua KSGC, Ang BT, Kuah C, Wang C, Phua KS, Chin ZY, Zhang H. Clinical Study of Neurorehabilitation in Stroke Using EEG-Based Motor Imagery Brain-Computer Interface with Robotic Feedback. Conf Proc IEEE Eng Med Biol Soc 2010; 5549–52.

Aumann TD, Prut Y. Do sensorimotor beta-oscillations maintain muscle synergy epresentations in primary motor cortex? Trends Neurosci 2015; 38:77-85.

Bai O, Lin P, Vorbach S, Floeter MK, Hattori N, Hallett M. A high performance sensorimotor beta rhythm-based brain-computer interface associated with human natural motor behavior. J Neural Eng 2015; 5:24-35.

Baker SN. Oscillatory interactions between sensorimotor cortex and the periphery. Curr Opin Neurobiol 2007; 17:649–55.

Baker MR, Baker SN. The effect of diazepam on motor cortical oscillations and corticomuscular coherence studied in man. J Physiol 2003; 546:931-42.

Baker SN, Olivier E, Lemon RN. Coherent oscillations in monkey motor cortex and hand muscle EMG show task-dependent modulation. J Physiol 1997; 501:225-41.

Bestmann S, Baudewig J, Siebner HR, Rothwell JC, Frahm J. Subthreshold high-frequency TMS of human primary motor cortex modulates interconnected frontal motor areas as detected by interleaved fMRI-TMS. Neuroimage 2003; 20:1685-96.

Bestmann S, Siebner HR, Rothwell JC, Frahm J BOLD MRI responses to repetitive TMS over human dorsal premotor cortex. Neuroimage 2005; 28:22-29.

Buch E, Weber C, Cohen LG, Braun C, Dimyan MA, Ard T, Mellinger J et al. Think to Move: A Neuromagnetic Brain-Computer Interface (BCI) System for Chronic Stroke. Stroke 2008; 39: 910–17.

Bütefisch C, Heger R, Schicks W, Seitz R and Netz J. Hebbian-Type Stimulation during Robot-Assisted Training in Patients with Stroke. Neurorehab Neural Repair 2011; 25: 645–55.

Bütefisch C, Khurana V, Kopylev L and Cohen LG. Enhancing Encoding of a Motor Memory in the Primary Motor Cortex by Cortical Stimulation. J Neurophysiol 2004; 91: 2110–16.

Chen D, Fetz EE. Characteristic membrane potential trajectories in primate sensorimotor cortex neurons recorded in vivo. J Neurophysiol 2005; 94:2713-25.

Classen J, Gerloff C, Honda M, Hallett M. Integrative visuomotor behavior is associated with interregionally coherent oscillations in the human brain. J Neurophysiol 1998; 79:1567-73.

Fang Y, Daly JJ, SunJ, Hvorat K, Fredrickson E, Pundik S, Sahgal V, Yue GH. Functional corticomuscular connection during reaching is weakened following stroke. Clin Neurophysiol 2009;120:994-1002.

Fetz EE, Chen D, Murthy VN, Matsumura M. Synaptic interactions mediating synchrony and oscillations in primate sensorimotor cortex. J Physiol Paris 2000; 94:323-31.

Fries P. A mechanism for cognitive dynamics: neuronal communication 680 through neuronal coherence. Trends Cogn Sci 2005; 9:474-80.

Fries P, Nikolić D, Singer W. The gamma cycle. Trends Neurosci 2007; 30:309–16.

GwinJT, Ferris DP. Beta- and gamma-range human lower limb corticomuscular coherence. Front Hum Neurosci. 2012; 6: 258.

Gharabaghi A, Kraus D, Leão MT, Spüler M,Walter A, Bogdan M, et al. Coupling brain-machine interfaces with cortical stimulation for brain-state dependent stimulation: enhancing motor cortex excitability for neurorehabilitation. Front Hum Neurosci 2014; 8:122.

Gharabaghi A, Naros G, Khademi F, Jesser J, Spueler M, Walter A, Bogdan M, Rosenstiel W, Birbaumer N. Learned self-regulation of the lesioned brain with epidural electrocorticography. Front Behav Neurosci 2015; 8:429.

Gomez-Rodriguez M, Peters J, Hill J, Schölkopf B, Gharabaghi A and Grosse-Wentrup M. 2011. Closing the Sensorimotor Loop: Haptic Feedback Facilitates Decoding of Motor Imagery. J Neural Eng 2011; 8: 036005.

He SQ, Dum RP, Strick PL. Topographic organization of corticospinal projections from the frontal lobe: motor areas on the lateral surface of the hemisphere. J Neurosci 1993;13:952-80.

Jensen O, Mazaheri A. Shaping functional architecture by oscillatory alpha activity: gating by inhibition. Front Hum Neurosci 2010; 4:186.

Kaiser V, Daly I, Pichiorri F, Mattia D, Müller-Putz GR and Neuper C. Relationship between Electrical Brain Responses to Motor Imagery and Motor Impairment in Stroke. Stroke 2012; 43: 2735–40.

Keil J, Timm J, Sanmiguel I, Schulz H, Obleser J, Schönwiesner M. Cortical brain states and corticospinal synchronization influence TMS-evoked motor potentials. J Neurophysiol 2014 ;111:513-9.

Khanna P, Carmena M. Neural oscillations: beta band activity across motor networks. Curr Opin Neurobiol 2015; 32:60-7.

Kombos T, Suess O, Kern BC, Funk T, Hoell T, Kopetsch O, Brock M. Comparison between monopolar and bipolar electrical stimulation of the motor cortex. Acta Neurochir (Wien) 1999;141:1295-301.

Kraus D, Naros G, Bauer R, Leao MT, Ziemann U, Gharabaghi A. Brain-robot interface driven plasticity: distributed modulation of corticospinal excitability. Neuroimage 2016; 125:522-32.

Kristeva R, Patino L, Omlor W. Beta-range cortical motor spectral power and corticomuscular coherence as a mechanism for effective corticospinal interaction during steady-state motor output. Neuroimage 2007; 36:785-92.

Lacey MG, Gooding-Williams G, Prokic EJ, Yamawaki N, Hall SD, Stanford IM, Woodhall GL. Spike Firing and IPSPs in Layer V Pyramidal Neurons 726 during Beta Oscillations in Rat Primary Motor Cortex (M1) In Vitro. PLoS One 2014; 727 9:e85109.

Lotze M, Montoya P, Erb M, Hülsmann E, Flor H, Klose U, Birbaumer N and Grodd W. Activation of Cortical and Cerebellar Motor Areas during Executed and Imagined Hand Movements: An fMRI Study. J Cogn Neurosci 1999;11: 491–501.

McFarland DJ, Miner LA, Vaughan TM, Wolpaw JR. Mu and beta rhythm topographies during motor imagery and actual movements. Brain Topogr 2000; 12:177–86.

Mrachacz-Kersting N, Kristensen SR, Niazi IK, Farina D. Precise temporal association between cortical potentials evoked by motor imagination and afference induces cortical plasticity. J Physiol 2012; 590:1669-82.

Mrachacz-Kersting N, Jiang N, Stevenson AJ, Niazi IK, Kostic V, Pavlovic A, Radovanovic S, Djuric-Jovicic M, Agosta F, Dremstrup K, Farina D. Efficient neuroplasticity induction in chronic stroke patients by an associative brain-computer interface. J Neurophysiol 2016; 115:1410-21.

Naros G, Naros I, Grimm F, Ziemann U, Gharabaghi A. Reinforcement learning of self-regulated sensorimotor β-oscillations improves motor performance. Neuroimage 2016; 134:142-52.

Narayana S, Zhang W, Rogers W, Strickland C, Franklin C, Lancaster JL, Fox PT 667. Concurrent TMS to the primary motor cortex augments slow motor 668 learning. Neuroimage 2014; 3:971-84.

Neuper C, Pfurtscheller G. Evidence for distinct beta resonance frequencies in human EEG related to specific sensorimotor cortical areas. Clin Neurophysiol 2001; 112:2084-97

Neuper C, Scherer R, Reiner M and Pfurtscheller G. Imagery of Motor Actions: Differential Effects of Kinesthetic and Visual-Motor Mode of Imagery in Single-Trial EEG. Brain Res Cogn Brain Res 2005; 668–77.

Nettekoven C, Volz LJ, Kutscha M, Pool EM, Rehme AK, Eickhoff SB, Fink GR, Grefkes C. Dose-dependent effects of theta burst rTMS on cortical excitability and resting-state connectivity of the human motor system. J Neurosci 2014; 34:6849-59.

Omlor W, Patino L, Mendez-Balbuena I, Schulte-Moenting J, Kristeva R. Corticospinal beta-range coherence is highly dependent on the pre-stationary motor state. J Neurosci 2011; 31:8037-45.

Pfurtscheller G, da Silva FL. Event-related EEG/MEG dynchronization and desynchronization: basic principles. Clin Neurophysiol 1999; 110:1842-57.

Pfurtscheller E, Stancfik A, Edlinger G. On the existence of different types of central beta rhythms below 30 Hz. Electron Clin Nero 1997; 102:316-25.

Raco V, Bauer R, Norim S, Gharabaghi A. Cumulative effects of single TMS pulses during beta-tACS are stimulation intensity-dependent. Brain Stimul 2017;

Ramos-Murguialday A, Brötz D, Rea M, Läer L, Yilmaz Ö, Brasil FL, Liberati G, et al. Brain-Machine Interface in Chronic Stroke Rehabilitation: A Controlled Study: BMI in Chronic Stroke. Ann Neurol 2013; 74: 100–8.

Rehme AK, Eickhoff SB, Grefkes C. State-dependent differences between functional and effective connectivity of the human cortical motor system. Neuroimage 2013; 67:237–46.

Ridding MC and Rothwell JC. Afferent Input and Cortical Organisation: A Study with Magnetic Stimulation. Exp Brain Res 1999; 126: 536–44.

Riddle CN, Baker MR, Baker SN. The effect of carbamazepine on human corticomuscular coherence. Neuroimage 2004; 22:333-40.

Riddle CN, Baker SN. Manipulation of peripheral neural feedback loops alters human corticomuscular coherence. J Physiol 2005; 566:625-39.

Roosink M and Zijdewind I. 2010. Corticospinal Excitability during Observation and Imagery of Simple and Complex Hand Tasks: Implications for Motor Rehabilitation. Behav Brain Res 213: 35–41.

Royter V, Gharabaghi A. Brain State-dependent closed-loop modulation of paired associative stimulation controlled by sensorimotor desynchronization. Front Cell Neurosci 2016;10:115.

Premoli I, Castellanos N, Rivolta D, Belardinelli P, Bajo R, Zipser C, Espenhahn S, Heidegger T, Mueller-Dahlhaus F, Ziemann U. TMS-EEG signatures of GABAergic neurotransmission in the human cortex. J Neurosci 2014a; 34:5603-12.

Premoli I, Rivolta D, Espenhahn S, Castellanos N, Belardinelli P, Ziemann U, Müller-Dahlhaus F. Characterization of GABAB-receptor mediated neurotransmission in the human cortex by paired-pulse TMS-EEG. Neuroimage 2014b; 103:152-62.

Salmelin R, Hari R. Characterization of spontaneous MEG rhythms in healthy adults. Electron Clin Neuro 1994; 91:237-48.

Schalk G, McFarland DJ, Hinterberger T, Birbaumer N, Wolpaw JR. BCI2000: a general-purpose brain-computer interface (BCI) system. IEEE Trans Biomed Eng 2004; 51:1034-43.

Schoffelen JM, Oostenveld R, Fries P. Neuronal coherence as a mechanism of effective corticospinal interaction. Science 2005; 308:111-3.

Schmidt S, Scholz M, Obermayer K, Brandt SA. Patterned Brain Stimulation, What a Framework with Rhythmic and Noisy Components Might Tell Us about Recovery Maximization. Front Hum Neurosci 2013;7:325.

Schulz H, Ubelacker T, Keil J, Müller N and Weisz N. Now I am Ready--Now I am not: The Influence of Pre-TMS Oscillations and Corticomuscular Coherence on Motor-Evoked Potentials. Cereb cortex 2013; 24:1708-19.

Sitaram R, Ros T, Stoeckel L, Haller S, Scharnowski F, Lewis-Peacock J, Weiskopf N, Blefari ML, Rana M, Oblak E, Birbaumer N, Sulzer J. Closed-loop brain training: the science of neurofeedback. Nat Rev Neurosci 2017; 18:86-100.

Stinear CM, Byblow WD, Steyvers M, Levin O and Swinnen SP. 2006. Kinesthetic, but Not Visual, Motor Imagery Modulates Corticomotor Excitability. Exp Brain Res 2006; 168:157-64.

Takemi M, Masakado Y, Liu M and Ushiba J. Event-Related Desynchronization Reflects down-Regulation of Intracortical Inhibition in Human Primary Motor Cortex. J Neurophysiol 2013;110:1158-66.

Tan H, Jenkinson N, Brown P. Dynamic neural correlates of motor error monitoring and adaptation during trial-to-trial learning. J Neurosci 2014; 34:5678-88.

Tan H, Wade C, Brown P. Post-movement beta activity in sensorimotor cortex indexes confidence in the estimations from internal models. J Neurosci 2016; 36:1516-28.

Teitti S, Määttä S, Säisänen L, Könönen M, Vanninen R, Hannula H, Mervaala E, Karhu J. Non-primary motor areas in the human frontal lobe are connected directly to hand muscles. Neuroimage 2008; 40:1243-50.

Thabit MN, Ueki Y, Koganemaru S, Fawi G, Fukuyama H and Mima T. Movement-Related Cortical Stimulation Can Induce Human Motor Plasticity. Journal Neurosci 2010; 30:11529–36.

Thut G, Miniussi C. New insights into rhythmic brain activity from TMS-EEG studies. Trends Cogn Sci 2009;13:182-9.

van Elswijk G, Maij F, Schoffelen JM, Overeem S, Stegeman DF, Fries P. Corticospinal beta-band synchronization entails rhythmic gain modulation. J Neurosci. 2010;30:4481-8.

Veniero D, Bortoletto M, Miniussi C. Cortical modulation of short-latency TMS-evoked potentials. Front Hum Neurosci 2012; 6:352.

Volz LJ, Rehme AK, Michely J, Nettekoven C, Eickhoff SB, Fink GR, Grefkes C. Shaping Early Reorganization of Neural Networks Promotes Motor Function after Stroke. Cereb Cortex 2016; 26:2882-94.

Witham CL, Baker SN. Network oscillations and intrinsic spiking rhythmicity do not covary in monkey sensorimotor areas. J Physiol 2007; 580:801-14.

Witham CL, Riddle CN, Baker MR, Baker SN. Contributions of descending and ascending pathways to corticomuscular coherence in humans. J Physiol 2011; 589:3789-800.

6. Statement of contributions

1. **Distinct beta-band oscillatory circuits underlie corticospinal gain modulation**

   Khademi F, Royter V, Gharabaghi A

   Under review

   Contributions:

   FK: Analysis, writing the manuscript

   VR: Data acquisition

   AG: Study design, analysis, writing the manuscript

2. **Brain-machine interface feedback shapes the cortico-muscular control after stroke**

   Khademi F, Naros G, Niksirat A, Kraus D, Gharabaghi A

   In submission

   Contributions:

   FK: Analysis, writing the manuscript

   GN: Study design, data acquisition

   AN: Data acquisition

   DK: Data acquisition

   AG: Study design, analysis, writing the manuscript

3. **Brain-state dependent transcranial magnetic stimulation controlled by sensorimotor desynchronization induces robust increase of corticospinal excitability**

   Kraus D, Naros G, Bauer R, Khademi F, Leão MT, Ziemann U and Gharabaghi A. (2016)

   Published in Brain Stimulation

   Contributions:

   DK: Data acquisition and analysis; writing the manuscript

   GN: Study design

   RB: Statistical analysis

   FK: Analysis

   MTL: Data acquisition

   UZ: Study design, editing the manuscript

   AG: Study design, writing the manuscript

4. **Brain state-dependent stimulation enhances task-specific motor network connectivity**

   Khademi F, Kraus D, Gharabaghi A

   In submission

   Contribution:

   FK: Analysis, writing the manuscript

   DK: Data acquisition

   AG: Study design, analysis, writing the manuscript

5. **Learned self-regulation of the lesioned brain with epidural electrocorticography**

   Gharabaghi A, Naros G, Khademi F, Jesser J, Spueler M, Walter A, Bogdan M, Rosenstiel W, Birbaumer N. (2015)

   Published in Frontiers Behavioral Neuroscience

   Contributions:

   AG: Study design, analysis, writing the manuscript

   GN: Study design, data acquisition, analysis.

   FK: Analysis

   JJ: Analysis

   MS: Study design; data acquisition

   AW: Study design; data acquisition

   MB: Study design

   WR: Study design

   NB: Study design, editing the manuscript

7. Acknowledgement

I want to thank Prof. Alireza Gharabaghi, who made this thesis possible. I would like to thank Prof. Christoph Braun and Dr. Robert Guggenberger for their valuable input during the thesis. I also would like to thank Prof. Christoph Braun and Prof. Ulf Ziemann for their valuable input during advisory board meetings. Additional thanks go to my fellow colleagues in the lab for data acquisition, Dr. Georgios Naros, Dr. Dominic Krause, Dr. Ali Nicksirat, and Mr. Vladimir Royter. I appreciate the support that I received from graduate training center (GTC) and Prof. Horst Herbert.

Distinct beta-band oscillatory circuits underlie corticospinal gain modulation

Short title: Distinct beta-band circuits predict gain modulation

Fatemeh Khademi, Vladimir Royter, Alireza Gharabaghi*

Author contributions: A.G. designed research; V.R. performed research; F.K. and A.G. analyzed data; F.K. and A.G. wrote the manuscript.

Division of Functional and Restorative Neurosurgery, and Centre for Integrative Neuroscience, Eberhard Karls University Tuebingen, Tuebingen, Germany

*To whom correspondence should be addressed

Professor Alireza Gharabaghi, Division of Functional and Restorative Neurosurgery, Eberhard Karls University Tuebingen, Otfried-Mueller-Str.45, 72076 Tuebingen, Germany. Email address: alireza.gharabaghi@uni-tuebingen.de

Acknowledgments

F.K. and V.R. were supported by the Graduate Training Centre of Neuroscience & International Max Planck Research School, Graduate School of Neural Information Processing (F.K.)and Graduate School of Neural and Behavioral Sciences (V.R.), Tuebingen, Germany. A.G. was supported by grants from the Baden-Wuerttemberg Foundation [NEU005] and the German Federal Ministry of Education and Research [BMBF 13GW0119B, IMONAS; 13GW0214B, INSPIRATION]. The authors declare no competing financial interests.

Abstract

Rhythmic synchronization of neurons is known to affect neuronal interactions. In the motor system, oscillatory power fluctuations modulate corticospinal excitability. However, previous research addressing phase-specific gain modulation in the motor system has resulted in contradictory findings. It remains unclear how many time windows of increased responsiveness each oscillatory cycle provides. Moreover, we still lack conclusive evidence as to whether the motor cortex entails an intrinsic response modulation along the rhythm cycle, as shown for spinal neurons. We investigated this question with single-pulse transcranial magnetic stimulation over the primary motor cortex at rest. Application of near-motor threshold stimuli revealed a frequency- and phase-specific gain modulation at both cortical and spinal level, independent of the spontaneous oscillatory power fluctuations at each level. We detected interhemispheric sensorimotor circuits in the lower beta-band (14-17 Hz) and unilateral corticospinal circuits in the upper beta-band (20-24 Hz). These findings provide novel evidence that intrinsic activity in the human motor cortex modulates input gain along the beta oscillatory cycle within distinct circuits.In accordance with periodic alternations of synchronous hyper- and depolarization, increased neuronal responsiveness occurred once per oscillatory beta cycle. This information may lead to new brain state-dependent and circuit-specific interventions for targeted neuromodulation.

Keywords: Corticospinal, gain modulation, sensorimotor, state-dependent, transcranial magnetic stimulation.

Introduction

Oscillatory neuronal activity occurs in distinct frequency bands and mediates the information flow between distant brain regions (Buzsáki, 2006). These neurons have a greater influence on each other when their temporal interaction windows open simultaneously, i.e., when the rhythmic synchronization within the groups is also synchronized between them (Womelsdorf et al. 2007). When the strength of such a neuronal interaction is dynamically modulated, itis referred to as gain modulation of neuronal connections (Salinas and Thier, 2000). It has been proposed that the synchronization of high-frequency bands determines this neuronal interaction strength (Fries, 2005). In the motor system, synchronized beta-band activity of spinal neurons during isometric contraction modulates the efficacy of synaptic input into this neuronal group along the rhythm cycle (van Elswijk et al. 2010). This spinal phase-dependent gain modulation revealed one peak of corticospinal excitability (CSE) per oscillatory cycle; minimum CSE occurred with a 180° phase shift. However, no response modulation was found in phase with the intrinsic oscillatory rhythm of the motor cortex. This was unexpected since the neuronal input in this study was mediated via transcranial magnetic stimulation (TMS) to the primary motor cortex (M1). Another study, performed during mild tonic contraction to keep the hand still,reported a phase-dependent CSE modulation in the oscillatory beta-band of both cortical and spinal activity (Keil et al. 2014). Surprisingly, however, this work described two CSE maxima in one cycle with a 180° phase shift, i.e., at both the peak and trough of the same oscillatory cycle. This contradicts the observations of van Elswijk and colleagues (2010) at spinal level and the known alternations of hyper- and depolarization within one beta oscillatory cycle (Baker, 2007; Fries et al. 2007; Lacey et al. 2014).

In a parallel line of research, where M1 rhythmic activity was artificially modulated, the findings were different.Specifically, when rhythmic activity in the beta-band was exogenously imposed on M1 by electrical (Pogosyan et al. 2009) or magnetic stimulation (Romei et al. 2016), corticomuscular coherence (CMC) increased in the stimulation frequency. Importantly, the entrainment effects depended on the precision with which the input was synchronized to the intrinsic cortical beta-rhythm (Romei et al. 2016). The technique of combining alternating current stimulation in the beta frequency band with concurrently applied and temporally targeted single-pulse TMS (Guerra et al. 2016; Nakazono et al. 2016; Raco et al. 2016) made it possible to detect the phase- and frequency-dependent characteristics of the different interneuronal populations in M1 (Guerra et al. 2016). Notably, these studies were performed when the subjects were at rest, thereby avoiding task-related modulations that might have altered the oscillatory characteristics of cortical interneuronal populations (Murthy and Fetz, 1996). However, conclusive evidence as to whether the intrinsic oscillations of the motor cortex entail a similar phase-specific response modulation independent of exogenously imposed rhythms is still lacking.

When searching for a phase-specific response modulation of M1 independent of exogenously imposed rhythms, task-related changes of interneuronal oscillatory characteristics are to be avoided, i.e., the study should be conducted at rest. Furthermore, to target distinct neuronal circuitries, the corticospinal pathway needs to be activated with different TMS intensities (Devanne et al. 1997; Di Lazzaro et al. 1998, 2001; Ziemann and Rothwell, 2000; Garry and Thomson, 2009). Moreover, a recent study confirmed earlier suggestions (Kiers et al. 1993; Devanne et al. 1997; Capaday et al. 1999) that the variability of motor-evoked potentials (MEPs) at rest was inversely related to the stimulation intensity and described by a logarithmic fit

(Klein-Fluegge et al. 2013). This finding, in turn, may imply that a potential phase- and frequency-dependent gain modulation of intrinsic oscillations can be detected by applying near-threshold TMS intensities when maximizing the response variability.

In the light of these considerations, the present study provides novel evidence for frequency- and phase-specific gain modulation along the beta rhythm cycle at both cortical and spinal level, independent of the spontaneous oscillatory power fluctuations at each level. Increased neuronal responsiveness occurred once per oscillatory cycle and was mediated by spectrally and spatially distinct neuronal networks.

Material and Method

Experimental design

Subjects

Sixty-one healthy, right-handed subjects (mean age, 24.32 ± 3.4 years, range 18-36 years, 38female), with no contraindications to TMS (Rossi et al. 2009) and no history of a psychiatric or neurological disease, were recruited for this study. Edinburgh handedness inventory (Oldfield, 1971) was used to confirm right-handedness. All subjects gave their written informed consent before participation in the study, which had been approved by the ethics committee of the Medical Faculty of the University of Tuebingen. This study conformed to the standards set by the latest version of the Declaration of Helsinki. Data acquisition was performed as recently described by our group and is cited here when performed in the same way (Kraus et al. 2016a; Royter and Gharabaghi, 2016):

Electromyography (EMG)

Ag/AgCIAmbuNeuroline 720 wet gel surface electrodes (Ambu GmbH, Bad Nauheim, Germany) were used to record electromyography (EMG) activity from the left Extensor Carpi Radialis (ECR) muscle. Two electrodes were placed 2 cm apart from each other on the muscle belly. Following filtering between 0.16 Hz and 1 kHz, signals were recorded with a 5 kHz sampling rate and downsampled to 1.1 kHz by the amplifier (antialiasing filter). The high-pass filter was 1^{st}-order (6 dB/Octave), and the low-pass filter was 5^{th}-orderButterworth filter (30 dB/Octave).

Electroencephalography (EEG)

For this study, Ag/AgCl electrodes (BrainCap for TMS, Brain Products GmbH, Gilching, Germany) and BrainVision software with DC amplifiers (low input impedance 10MΩ) and an inbuilt antialiasing filter (BrainAmp, Brain Products GmbH, Germany) were used to record electroencephalography (EEG) signals in a 64 channel setup that complied with the international 10–20 system (Fp1, Fp2, AF7, AF3, AF4, AF8, F7, F5, F3, F1, Fz, F2, F4, F6, F8, FT9, FT7, FC5, FC3, FC1, FCz, FC2, FC4, FC6, FT8, FT10, T7, C5, C3, C1, Cz, C2, C4, C6, T8, TP9, TP7, CP5, CP3, CP1, CPz, CP2, CP4, CP6, TP8, TP10, P7, P5, P3, P1, Pz, P2, P4, P6, P8, PO7, PO3, POz, PO4, PO8, O1, Oz, O2, and Iz with FCz as reference). Impedances at all electrodes were kept below 10 kΩ. Following filtering between 0.16 Hz and 1 kHz, EEG signals were recorded with a 5 kHz sampling rate and downsampled to 1.1 kHz by the amplifier (antialiasing filter). The high-pass filter was 1^{st}-order (6 dB/Octave), and the low-pass filter was 5^{th}-orderButterworth filter (30 dB/Octave). Since ambient noise could influence electrophysiological recordings we made every effort to remove any of its potential sources by unplugging superfluous power supplies and computers, etc. The corresponding effect, such as the decrease of 50

Hz line noise, was verified online (Kraus et al. 2016a; Royter and Gharabaghi, 2016).In this study, ipsilateral and contralateral electrodes refer to the site of the TMS pulse, i.e., the right hemisphere.

TMS protocol

A navigated TMS stimulator (MagPro-R30+MagOption, MagVenture, Willich, Germany) with a biphasic current waveform connected to a figure-8 MCF-B70coil (97mm outer diameter) was used to determine the MEP amplitude. A frameless stereotaxy (TMS Navigator, Localite GmbH, SanktAugustin, Germany) with a standard MNI dataset (MNI ICBM152 non-linear symmetric T1 Average Brain) was used for coil navigation. Subjects were requested to sit in a comfortable reclining chair and keep their muscles relaxed throughout the TMS measurements. The representation of their left forearm muscles in the right M1 was determined prior to the first TMS assessment. The TMS hotspot for the recorded muscle was determined as the cortical location in the right hemisphere, where the MEPs were robustly elicited with the lowest stimulation intensity. The hotspot search procedure started at a location on the scalp overlying the right parietal bone and corresponding to the C4 electroencephalogram (EEG) sensor (according to the international10/20 system) with a coil orientation perpendicular to the scalp and in the posterior-anterior direction. The initial TMS amplitude was set at 40% of the maximum stimulator output; stimulation was manually triggered as the coil was moved gradually around the initial position (Kraus and Gharabaghi, 2015). If the search did not elicit any discernable MEP, the intensity was increased in 5% steps, and the search was repeated. Once the location that robustly elicited the highest MEPs wasdetected (which was in the vicinity of C4), the stimulator intensity was reduced, using a staircase approach to diminish the current spread of the stimulation and hence

restricting the hotspot area eliciting MEPs (Kraus and Gharabaghi, 2015; Raco et al. 2017).We then determined the resting motor threshold (RMT) by the relative frequency method, i.e., by detecting the minimum stimulus intensity (in steps of 2% of MSO) that resulted in MEPs>50 μV in the peak-to-peak amplitude in at least 5 out of 10 consecutive trials (Groppa et al. 2012).

Our aim was to target distinct neuronal circuitries by activating the corticospinal pathway with different TMS intensities (Devanne et al. 1997; Di Lazzaro et al. 1998, 2001; Ziemann and Rothwell, 2000; Garry and Thomson, 2009). As explained elsewhere (Raco et al.2016), TMS over the primary motor cortex (M1) evokes multiple descending volleys,generated by direct (D-wave) and indirect (I-waves) activation of the corticospinal pathway (Di Lazzaro et al. 2001). The stimulation intensity determines the recruitment of neuronal structures (Di Lazzaro et al. 1998): TMS intensities below110% resting motor threshold (RMT) induce MEPs via the recruitment of early I-waves (Garry and Thomson, 2009), while later I-waves gradually mediate the propagation of the motor signals with increasing stimulation amplitude (Devanne et al. 1997; Di Lazzaro et al. 2001). These later waves are believed to be generated by a cortico-cortical circuitry that projects to the corticospinal neurons (Ziemann and Rothwell, 2000). When the stimulation intensity is increased further, the axons of the corticospinal neurons are directly activated (D-wave; Di Lazzaro et al.1998). When induced by specific TMS intensities only, a phase-dependency during TMS may thus provide information about the neural circuitry involved (Raco et al. 2016).

To avoid a bias by day-to-day variability, our study design aimed to examine different TMS intensities per subject in one session. We therefore had to restrict the number of stimuli per intensity to avoid carry-over effects. Since cumulative effects on

CSE have been described by the application of 200 single TMS pulses (Pellicciari et al. 2016), we chose an approach to minimize the absolute number of pulses applied, while still covering a broad range of different stimulation intensities. The experiment consisted of one session with eight blocks. Within each block, 10 TMS pulses were applied with the same intensity for 90, 100, 110, 120, 130, 140, 145, and 150% RMT (Fig. 1A). In all, 80 stimuli were applied during 10 minutes for each subject (Royter and Gharabaghi, 2016). Due to this relatively small number of stimuli per condition, pooling data was mandatory to enable us to compare the effects of different intensities. Potential issues with regard to pooling data are addressed in the statistics section (see below).

[Please insert Fig. 1 approximately here]

Data analysis

EEG/ EMG analysis was performed as described by van Elswijk and colleagues (2010) and is cited here when performed in the same way:

Electrophysiological signal preprocessing

Data were analyzed offline using the MATLAB (The MathWorks, Inc., Natick, Massachusetts, United States) and FieldTrip open source MATLAB toolbox (http://fieldtrip. fcdonders.nl/; MathWorks).This included visual artifact rejection (eye movement, eye blinking, and muscle artifacts), MEP<50μV removal, and linear detrending, yielding per TMS intensity an average of 348 ± 119 artifact-free trials across all subjects (an average of 6 ± 3 trials per subject). Since most of the trials from the stimulation block at 90% RMT had to be rejected due to MEP<50μV

removal, this block was not used for further analysis. For the near-threshold stimulation block at 100% RMT, the number of trials was, per definition, lower than for the stimulation blocks at higher RMT, since the100 % RMT condition was defined as having MEPs>50 μV in the peak-to-peak amplitude in at least 5 out of 10 consecutive trials (Groppa et al. 2012). To confirm the findings for the 100 % RMT condition, we also analyzed MEPs above the thresholds 40 μV, 30 μV, and 20 μV, respectively. The raw EEG and EMG signals were cut into epochs of ±1s around the TMS pulse. Only signals at 5 ms and before and at 15 ms and after the TMS artifact were included in the study.The pre-TMS EMG was subsequently rectified to estimate the EMG amplitude. Since the post-TMS EMG signal was required for determining the MEP amplitude (van Elswijk et al. 2010), it was not rectified, but estimated by its peak-to-peak amplitude, i.e., the difference between the lowest and highest value within 15–60 ms following the TMS pulse (Fig. 1C).

Assessing the group data

Since EEG/EMG power may differ across subjects, the absolute values of the latter cannot be compared. A normalization is thus necessary prior to group analysis. We therefore normalized the pre-TMS EEG/EMG power and MEP amplitude for each subject individually before group analysis. The MEP amplitude (and pre-TMS power accordingly) of each epoch was normalized for each subject with respect to the maximum MEP amplitude (power) across all epochs. We thereby acquired a relative measure of the maximum and minimum MEP amplitude and the corresponding pre-TMS EEG/EMG power. For the subsequent analysis of this study we quantified the effect of pre-TMS phase and power on the peak-to-peak MEP amplitude.By contrast, no normalization was required for computing the phase-dependency (spaced between -π and +π) of MEPs across subjects.

Spectral analysis of pre-stimulus epochs

The power of the EEG/EMG rhythm was estimated in 1 Hz intervals preceding the TMS pulse. Epochs were given a length of 360 ms before the TMS onset (5 ms before the onset of the TMS artifact) to ensure that they included at least two cycles of the respective frequency between 6-30 Hz. In detail, we chose a fixed time (Gross et al. 2013) window with sufficient window length to cover two cycles of the minimum frequency of interest (i.e., 6 Hz). In our setup, which had a sampling rate of 1100 Hz, this required a minimum of 367 samples. We therefore selected 400 samples, i.e.,360 ms, for our analysis. We chose this time window instead of a longer one (e.g., 1000 ms) to capture the effect of EEG oscillations close to the onset of the TMS pulse on the subsequent MEP. These were then Fourier transformed (with the zero-padding technique) to provide the power spectrum.

The phase of the EEG/EMG rhythm was estimated in 1 Hz intervals preceding the TMS pulse for from Fast Fourier analysis. Epochs had a length of two cycles at the respective frequency and ended prior to the TMS artifact. They were Fourier transformed to determine the phase at the respective frequency (vanElswijk et al. 2010).

Assessing the relationship between pre-TMS EEG and EMG phase and post-TMS MEP amplitude

In accordance with the procedure of van Elswijk and colleagues (2010), a frequency-wise estimation of the pre-TMS EEG/EMG phase was used to bin the epochs. Sixteen phase bins were defined on the unit circle,with their centers equally spaced between -π and +π. For the binning procedure, we assigned the epochs in which the

pre-TMS EEG/EMG phases were closest to the center phase of the bin. The MEP amplitudes were averaged for each group of epochs (bins) to obtain the mean MEP amplitude. In addition, the pre-TMS EEG/EMG phase was averaged for each group of epochs. This averaged phase, which may vary slightly from the center phase of the corresponding phase bin, was used for further analysis. With an average of 22 trials per phase bin, an F-test was performed to test whether MEP amplitude variance had an influence on the results. MEP amplitude variance across phase bins did not differ significantly with regard to stimulation intensity and EEG/EMG frequency. The minimum and maximum p-value for the corresponding analysis were 0.07 and 1, respectively. In line with this, the minimum and maximum F-statistic values were 0.32 and 3.15, respectively.This procedure provided us with 16 pairs (one per phase bin) of pre-TMS EEG/EMG phase and MEP amplitude per frequency. To quantify the relationship between the pre-TMS EEG/EMG phase and MEP amplitude, a cosine (least-squares) function was fitted to the MEP amplitudes as a function of the EEG/EMG phases (van Elswijk et al. 2010). Furthermore, the MEP amplitude was normalized by its SD, which was estimated by a jackknife procedure (Efron and Tibshirani, 1993; van Elswijk et al. 2010).We estimated the goodness of fit with a non-linear fitting model (NonLinearModel.fit function available in Matlab) by comparing the fitted model vs. zero model.

Assessing the relationship between pre-TMS EEG and EMG power and post-TMS MEP amplitude

Previous work indicates that the MEP amplitude correlates positively with EMG activity (Di Lazzaro et al. 1998; Mitchel et al. 2007) and inversely with sensorimotor rhythms in the EEG (Takemi et al. 2013; Schulz et al. 2014). We therefore also computed the linear relationship between pre-TMS EEG/EMG power and MEP

amplitude to estimate frequency-wise the Spearman's rank correlation coefficient between the pre-TMS EEG/EMG power and MEP amplitude for each EEG and EMG channel.

Assessing the pre-TMS EEG and EMG coherence

We investigated the synchronous oscillatory activity between the signal of the brain and the forearm muscle by analyzing the corticomuscular coherence (CMC).The epochs used for pre-TMS power estimation (i.e., 360 ms time window before TMS artifact, see above) were also used to assess the CMC between EEG and EMG. We calculated the CMC by estimating the cross-spectral density matrix per frequency between EEG channels and EMG channels (Schulz et al. 2014). The cross-spectral density matrix was calculated frequency wise by the multi-taper method (3 tapers) in the frequency range from 6 to 30 Hz in steps of 1 Hz using the zero-padding technique. The coherence values were obtained by normalizing the magnitudes of the summed cross-spectral density matrix for each frequency by the corresponding power values at that frequency (Schulz et al. 2014).

Assessing post-TMS MEP amplitude in relation to the pre-TMS CMC

To investigate the influence of the pre-TMS CMC on the MEP amplitude, we used the 16 bins described earlier in the methods section. We then estimated the CMC for each bin. The magnitude of the coherency is a function of the sample size (Maris et al. 2007). Since the number of epochs differed in each bin, we transformed the CMC values to z-values in each bin. This entailed using the number of degrees of freedom (d.f.) of the sample coherence. When CMC values were above 0.4 and the d.f. greater than 20, the latter represented the variance of the sample coherence and the CMC values could then be transformed to z-values (Enochson and Goodman, 1965; Maris et al. 2007). When the CMC values were below 0.4, we used d.f.as the

standard deviation. This led to a z-value transformation and coherence statistics comparable to the method proposed by Rosenberg and colleagues (1989). We used the following transformation:

$$Z(f) = \frac{tanh^{-1}\left(C(f)\right) - \left({}^{2}/_{(d.f.-2)}\right)^{2}}{\left({}^{2}/_{(d.f.-2)}\right)}$$

where the *C(f)* is the coherence at the frequency *f*. A nonparametric test (Maris et al. 2007) was then used to test the linear relation between CMC and MEP.The average of the z-values from the EEG channels of interest was estimated, yielding one z-value for each group of epochs. The average of the peak-to-peak MEP amplitude of each group of epochs was now used as the MEP amplitude for correlation with the corresponding bin. This procedure rendered 16 pairs of the transformed CMC and MEP values, which were used to test the linear relationship between pre-TMS CMC and MEP amplitude.

Statistical analysis

Since pooling data from different subjects was mandatory in our study design, we took the following precautions to avoid potential issues related to this approach:

(i) Both power and MEP amplitudes of each subject were normalized.

(ii) To rule out a bias during estimation by fixed-effects we also applied the Bootstrap method. By plotting the variance around the estimated effect, we assured that the former did not change across frequencies. Furthermore, the lower confidence limit was still above the threshold of the estimated bias for our observed significant result (see below). This analysis ensured that the findings were not compromised by specific subjects (outliers).

(iii) The significance of the effects was quantified by a randomization test (10,000 repetitions). For this purpose, we shuffled the independent versus dependent variables among subjects.

Testing the coefficient of variation for MEP and phase

By dividing the estimated standard deviation (SD) of the MEP amplitudes by the mean of the same population for each subject and TMS intensity, we calculated their coefficient of variation (CV) which we then used to assess the MEP variability (Klein-Fluegge et al. 2013). We assessed the variability of the phase distribution on the unit circle (Fig. 1D) for each frequency and TMS intensity by estimating the CV for the phase-lag between adjacent phases, i.e., the phase difference between neighboring phases. CV differences between stimulation intensities were tested with a one-way ANOVA for MEP and phase, respectively.

Testing significance of EEG and EMG power-dependent MEP amplitudes

We used a Spearman's rank correlation coefficient to assess the relationship between the pre-TMS power and MEP amplitude. To test the significance of the estimated effect, we applied the randomization approach. Our null hypothesis was that the pre-TMS power and MEP were not correlated. A cluster-based randomization test with 10,000 repetitions was therefore performed at each electrode (i.e., one-dimensional clustering for the frequency) for multiple frequency bins by shuffling the pre-TMS EEG/EMG amplitudes (independent variable) versus MEP amplitudes (dependent variable). We calculated the Spearman's rank correlation coefficient for each frequency bin and clustered adjacent frequency bins in the same set when the Spearman's rank correlation coefficient exceeded the threshold of $p<0.001$. We then calculated the cluster-level statistics by taking the sum of the Spearman's rank

correlation coefficient for each cluster. The maximum of the cluster-level statistics was used later for comparisons if multiple clusters were observed. The p-value to reject the null hypothesis was the proportion of cluster-based randomizations that resulted in larger test statistics than observed here (without randomization). We rejected the null hypothesis if $p \leq 0.0001$.

Testing significance of EEG and EMG phase-dependent MEP amplitudes

Our analysis showed that the relationship between pre-TMS EEG/EMG phase and MEP amplitude was cosine-shaped (Fig. 1E for the pre-TMS EEG). We therefore quantified this relationship by (least-squares) fitting a cosine function with the unconstrained phase (dashed line in Fig. 1E*).* The modulation depth (peak-to-peak difference) of the fitted cosine was used as an estimate of the strength of the relationship between pre-TMS EEG/EMG phase and MEP amplitude. Since the cosine fitted with the unconstrained phases, it had an amplitude with a positive bias (van Elswijk et al. 2010). We estimated this bias by randomly shuffling (100 repetitions) pre-TMS phase (independent variable) versus MEP amplitudes (dependent variable). At each randomization, we fitted the cosine function and estimated the modulation depth. After 100 repetitions, we averaged the modulation depth. The analysis described above was performed per frequency so that, by the end of the procedure, we had two spectra per intensity: one spectrum of the effect and one of the bias estimate (van Elswijk et al. 2010). To determine whether the estimated effect was significantly greater than the estimated bias, we designed a randomization test with the null hypothesis that the effect spectrum was no greater than the bias spectrum (vanElswijk et al. 2010). We conducted the following procedure: the sum of the modulation depth from the frequency bands, when greater than the estimated bias, was considered as the observed test statistics; we did not

386 consider single frequency bins but studied instead bands with a width of at least 3
387 Hz. Later, we randomly shuffled the pre-TMS phases (independent variable) versus
388 MEP amplitudes (dependent variable; as estimated for bias) with 10,000 repetitions.
389 We calculated the sum of the modulation depth for the frequency bands of interest for
390 each randomization (see above). The p-value to reject the null hypothesis was the
391 proportion of randomizations that resulted in larger test statistics than observed here.
392 We rejected the null hypothesis if p≤0.001.

393 **Testing for confounding of EEG phase and power**

394 For the EEG channel and frequency of interest (see results section), the average
395 power of those epochs resulting from the phase binning was used to fit a (least-
396 squares) cosine function. Other groups have suggested that low power of
397 sensorimotor rhythms predicts high MEP amplitude and vice versa (Takemi et al.
398 2013; Schulz et al. 2014).When EEG phase and power are confounded, we would
399 expect a cosine-shaped fitting curve (with the phase-lag of π) for power when the
400 fitting curve for phase and MEP is cosineshaped. This would indicate that the phase
401 which predicts high MEP also predicts low power.

402

403

404 **Testing significance of corticomuscular coherence**

405 For CMC, the significance level was calculated according to the procedure proposed
406 by Rosenberg and colleagues(1989).

$$C_{\alpha}^{lim} = 1 - (1 - {}^{\alpha}/_{100})^{{}^{1}/_{n-1}}$$

Where α is the confidence probability and n the number of epochs in which n-1 is the d.f. In our case, d.f. was 2* number of epochs (n) * number of tapers (k) (Maris et al.2007). We therefore calculated as follows:

$$C_{\alpha}^{lim} = 1 - (1 - {}^{\alpha}/_{100})^{{}^{1}/_{2*n*k}}$$

A confidence probability of α=0.999% (p=0.001)was chosen. The resulting confidence limit provided us with the significance level. The CMCs from the frequency bins above the significance level were considered as significant.

Testing significant correlation of CMC and MEP

We used a randomization test with 10,000 repetitions for the null hypothesis that the relationship between pre-TMS CMC and MEP was random. We shuffled pre-TMS CMC (independent variable) and MEP amplitude (dependent variable). At each randomization step, Spearman's rank correlation coefficient was used to estimate the test statistics. The proportion of the randomizations test that led to larger test statistics than observed here (without randomization) was used to reject the null hypothesis.

Results

The variability of corticospinal excitability(CSE), i.e., the coefficient of variation for MEP (CV_{MEP}), increased with lower stimulation intensities and was at its highest at near-threshold intensity. CV_{MEP} increased from 0.25 ± 0.15at 150% RMT to 0.85 ± 0.37 at 100% RMT(Fig. 1G). One-way ANOVA showed that CV_{MEP} differed significantly between intensities ($F(6,460)=51.49$, $p<0.00001$, ANOVA); the post-hoc test revealed a significant difference between CV_{MEP} at 100% RMT and at all other stimulation intensities ($t(120)=3.76$, $p<0.00001$, 110% RMT; $t(120)=5.98$, $p<0.00001$, 120% RMT; $t(120)=8.88$, $p<0.00001$, 130% RMT; $t(120)=10.09$, $p<0.00001$, 140% RMT; $t(120)=11.32$, $p<0.00001$, 145% RMT, and $t(120)=11.66$, $p<00001$, 150% RMT, unpaired t-test, p= 0.05 Bonferroni corrected to $p=0.0071$).

The phases' distribution on the unit circle (Fig. 1D, at the time of stimulation) did not differ significantly between the various intensities (Fig. 1H), i.e., the coefficient of variation for phase (CV_{phase}) remained unchanged across different stimulation intensities (average CV_{phase} of 2.33 ± 0.59), with no statistically significant difference of CV_{phase} between intensities ($F(6,168)=0.33$, $p=0.92$, ANOVA, Fig. 1H). Together, these findings suggest that the stimulation intensity-dependent findings were not biased by a potentially different distribution of phases at the time of stimulation. Further analysis revealed that robust predictions of CSE were possible only when stimuli were applied at near-threshold intensity (Fig. 2, Fig. 3).

At the cortical level, power (15-17 Hz; $p=0.0001$, randomization test,10,000repetitions) and phase (14-17 Hz; $p=0.001$,randomization test, 10,000 repetitions) in the lower beta-band predicted CSE in a frequency-specific way (Fig. 2B, 2E) and revealed a stable topographical pattern (Fig. 2C, 2F). This pattern

showed that CSE could be predicted at the site of stimulation (C4) and in a more distributed cortical network: specifically, by the oscillatory beta phase recorded at sensors projecting to the sensorimotor cortex ipsilateral (C4, CP4) and contralateral (C3, CP3) to the site of stimulation, and at contralateral FC3, CP5 and P5 (Fig. 2F); and by the beta power recorded at sensors projecting to the ipsilateral motor cortex (C2) and contralateral CP1, P5, P3, and PO3 (Fig. 2C).

[Please insert Fig. 2 approximately here]

At the spinal level, CSE was predicted in a frequency-specific way by the phase in the upper beta-band (20-24 Hz, Fig. 3D; p=0.001, randomization test, 10,000 repetitions), but not by power (Fig. 3B; p>0.16, randomization test, 10,000 repetitions). CMC coherence in this frequency band projected to the sensorimotor (C4, C6, CP4, CP6) and parietal cortex (P2, P4, P6, PO4) in the stimulated hemisphere (Fig. 3E;d.f.=690, p=0.001, significance level0.010). This pre-TMS CMC predicted post-TMS CSE (Fig. 4; r=0.63p=0.0031, Spearman's rank correlation, randomization test, 10,000 repetitions).

[Please insert Fig. 3 approximately here]

[Please insert Fig. 4 approximately here]

When the bins were sorted into 16 overlapping bins (Fig. 1D) according to the beta phase immediately preceding the neuronal input (TMS pulse), and the response modulation (MEP amplitude) was determined separately for each phase bin (Fig. 1E), the CSE resulted in a cosine-shaped function of pre-stimulus beta phase (Fig. 1E). This pattern occurred at both the cortical (EEG) and spinal (EMG) level in the lower (14-17 Hz) and upper (20-24 Hz) beta-band, respectively. Specifically, CSE was at its highest when stimuli arrived at the rising phase of cortical oscillations in the lower

beta-band (Fig. 5A; r-squared=0.108; F-statistic vs. zero model: 7.87;p=0.0066)or spinal oscillations in the upper beta-band (Fig. 5B; r-squared=0.246;F-statistic vs. zero model;16.30;p<0.0001), but at its lowest when stimuli arrived at the falling phase of cortical oscillations in the lower beta-band (Fig. 5C; r-squared= 0.094;F-statistic vs. zero model: 6.76; p=0.0115) or spinal oscillations (Fig. 5D; r-squared=0.162; F-statistic vs. zero model; 9.66; p=0.0031) in the upper beta-band (Fig. 5).

[Please insert Fig. 5 approximately here]

Notably, the phase of ipsilateral (C4, CP4) and contralateral (C3, CP3) sensorimotor beta-rhythms, which predicted CSE, was shifted by ~π radian (Fig. 6A). Moreover, the phase-dependent modulation of CSE was consistent across frequencies (14-17 Hz) and within each hemisphere, i.e., the maximum MEP mapped onto the corresponding spot in the rising phase of the oscillatory cycle for each of the frequencies that predicted CSE (Fig. 6A). Furthermore, the phase-dependent modulation of CSE remained stable during modification of the threshold of included MEPs (Fig. 7).

[Please insert Fig.6 approximately here]

[Please insert Fig. 7 approximately here]

Importantly, the phase-dependent CSE modulation at the cortical and spinal level was not confounded by the respective power fluctuation in the EEG and EMG. Specifically, EMG power did not predict CSE at all, whereas EEG power showed a significant inverse correlation with CSE in frequency bins (15-17 Hz) that overlapped with those showing the phase-dependent modulation (14-17 Hz). Pre-TMS phases preceding *high* MEPs might, therefore, be confounded by *low* beta power which preceded *high* MEPs as well, and vice versa. However, a cosine fitting to the average

power of each of the 16 bins that led to the cosine-shaped function of pre-stimulus beta phase resulted in a flat curve (Fig. 1F, dashed line), i.e., the phase modulation of CSE was not confounded by power fluctuations in the same frequency band.

Discussion

This study has demonstrated that the intrinsic beta-rhythm of the motor cortex entails rhythmical gain changes. This frequency- and phase-specific response modulation, mediated by spectrally and spatially distinct neuronal networks, occurred independent of spontaneous oscillatory power fluctuations at cortical and spinal levels.

Methodological consideration

The gain modulation was revealed only when stimuli were applied at near-threshold intensity, i.e., at 100% RMT. This might be due to the larger variability of the evoked MEP amplitudes compared to those elicited at higher stimulation intensities (Klein-Fluegge et al. 2013) or to the activation of distinct neuronal circuitries (Di Lazzaro et al.1998). Specifically, TMS intensities below 110% RMT induce MEPs by recruiting indirect circuits in the motor cortex, i.e., the early presynaptic activation of the corticospinal pathway (Di Lazzaro et al. 2001; Garry and Thomson, 2009). Alternatively, the gain modulation of intrinsic oscillations might have been detected due to the maximized response variability during the application of near-threshold TMS intensities (Fig. 1E). Since the phenomenon of gain modulation at near-threshold stimulation intensities was observed at both cortical (Fig. 2E) and spinal (Fig. 3D) level, the latter explanation appears more plausible in the light of the findings of the present study. The various stimulation intensities were, however,

examined in a predefined order in this study, i.e., incrementally increasing the TMS intensity from block to block. This might have prevented us from detecting gain modulation at higher TMS intensities, i.e., in later blocks within one session, since even these single TMS pulses can induce a systematic modulation of corticospinal excitability over time (Pellicciari et al. 2016). To minimize undesirable order effects, future studies investigating the influence of stimulation intensity on corticospinal gain modulation should therefore examine different intensities in a randomized order.

Power-related gain modulation

At the cortical and spinal level, spontaneous oscillatory power fluctuations played a different role in predicting CSE in this study. Specifically, EMG power did not predict CSE, which might be most parsimoniously explained by the fact that the experiment was performed in resting state. Albeit the observation that beta corticomuscular coherence could predict CSE may appear surprising in this context, Romei and colleagues (2016) recently proposed that, even while at rest, low-level tonic firing from spontaneous spiking in spinal motor neurons (Blankenship and Kuno, 1968) may occur in some motor units. Corticomuscular beta coherence could then ensue from increased temporal structuring at beta frequencies of this spontaneous spiking activity (Romei et al. 2016). This work provides evidence that such a *temporal structuring*occurs along the rhythm cycle of synchronized beta activity of spinal neurons even in the resting state, i.e., without overt movement.

Unlike the EMG power, the EEG power in the lower beta-band (15-17 Hz) predicted CSE even at rest. This was not surprising, given that sensorimotor oscillations are modulated by thalamo-cortical and cortico-cortical interactions (Thut and Miniussi, 2009; Jensen and Mazaheri, 2010) and reflect the current brain state (Salinas and Thier, 2000; Chance et al. 2002), i.e., high and low oscillatory power

indicate the inhibitory and excitatory state, respectively. Intrinsic fluctuations of oscillatory activity may thus determine the brain's responsiveness to external stimuli and at least partly account for the variability of CSE in this study.

The state of the motor system, i.e., rest or movement, and the influence of concurrent muscle activity might be responsible for the ambiguous results of previous studies on the oscillatory power-related gain modulation of the sensorimotor cortex. In particular, studies in which single TMS pulses were applied during rest revealed an inverse correlation between CSE and pre-stimulus power. There was, however, some ambiguity with regard to the frequency bands and cortical sites involved, i.e., ipsilateral sensorimotor cortex for the alpha- (Zarkowski et al. 2006; Sauseng et al. 2009) or beta-band (Lepage et al. 2008; Mäki and Ilmoniemi, 2010), and the posterior parietal cortex contralateral to the stimulation site in the beta-band (Keil et al. 2014). These diverse findings are probably related to the large variability of spontaneous oscillatory activity in the human sensorimotor cortex captured in relatively small sample sizes. Notably, studies that applied the same stimulation during movement tasks showed a correlation of the CSE with the pre-stimulus EMG activity in the beta-band (Mitchell et al. 2007; van Elswijk et al. 2010) or the cortico-muscular coherence in the alpha-band (Schulz et al. 2014) but not with the oscillatory power in stimulated sensorimotor cortex (Mitchell et al. 2007; van Elswijk et al. 2010). When the CSE correlated with cortical power, it tended to be located in a more distant fronto-parietal beta-network (Schulz et al. 2014). This ambiguity is probably related to the respective task designs, i.e., isometric contraction (Mitchell et al. 2007; van Elswijk et al. 2010) vs. post-movement beta-rebound (Schulz et al. 2014). Specifically, the task-related periods of increased cortical beta-power, i.e., reduced cortical excitability, were paralleled by elevated EMG power in the alpha- and beta-band during the isometric

contraction task (Kilner et al. 2000), which, in turn, correlated significantly with CSE. This suggests a more complex interaction between the oscillatory state of the peripheral and central motor system with respect to the stimulation-induced MEP, i.e., between the EMG activity immediately before the stimulus and the cortical excitability at the moment of stimulation (Mitchell et al. 2007).

In the present work, we reduced this complexity by studying the cortical gain modulation at rest by minimizing confounding EMG activity and by avoiding task-related modulations that can alter the oscillatory characteristics of cortical interneuronal populations (Murthy and Fetz, 1996). Furthermore, the robustness of the findings was ensured by the statistical approach chosen – the application of a randomization test with 10,000 repetitions to the frequency spectrum between 6-30 Hz in a rather large group of subjects.

Moreover, the spectrum and topography of the beta power, which correlated inversely with CSE, overlapped at least partially with the spectrum and topography of the phase-dependent modulation (see below), thereby underlining the consistency of the findings. Importantly, both power- and phase-dependency of CSE in the present study converged at the M1 site of stimulation (i.e., at the C4 sensor), while previous studies showed rather distributed cortical patterns (Schulz et al. 2014; Keil et al. 2014).

Phase-related gain modulation

Previous discrepancies with regard to the CSE phase-dependency might be related to methodological differences of data processing and phase estimation, e.g.,broad-band filtering with Fast Fourier Transform (van Elswijk et al.2010) vs. narrow-band filtering with Hilbert Transform (Keil et al. 2014). In particular, Keil and colleagues

(2014) did not show a phase dependency along the beta oscillatory cycle, whereas van Elswijk and colleagues (2010) fitted a cosine function to the MEP amplitudes. Instead, Keil and colleagues (2014) estimated an angular-linear correlation which showed two MEP peaks within one cycle for the very same 18 Hz frequency for which van Elswijk et al. (2010) had already demonstrated one MEP peak.

In the present work, we applied the data analysis proposed by van Elswijk and colleagues (2010), but removed the task-related muscle activity following the observations in the study of Keil and colleagues (2014). By fitting a cosine function to the MEP amplitudes, we observed a frequency-specific response modulation in-phase with the intrinsic oscillatory rhythm, i.e., along the beta rhythm cycle at both the cortical and spinal level. At the cortical level, the phase in the lower (14-17Hz) beta-band predicted CSE (Fig. 2E). At the spinal level, CSE was predicted by the phase in the upper (20-24Hz) beta-band (Fig. 3D). CMC coherence in this latter frequency band also predicted the post-TMS amplitude(Fig. 4).

Notably, CSE was highest when stimuli arrived at the rising phase of cortical or spinal beta oscillations (Fig. 6), thereby reflecting the responsiveness of the respective neuronal pools to a synaptic input. This was already known to be the case for spinal beta-rhythms during movement (van Elswijket al. 2010) and has now been extended to the resting state and the cortical level, suggesting a more general mechanism. This phase-dependent input gain is therefore probably attributable to the rhythmic inhibition after population spikes, depending systematically on the delay from the last population spike (Burchell et al. 1998; van Elswijket al. 2010).

Distinct beta-band oscillatory circuits

Our frequency-specific findings suggest a response modulation of CSE in two distinct neuronal circuitries: a cortical oscillatory circuit in the lower, and a corticospinal circuit in the upper beta-band. These two networks could also be distinguished on the basis of their topographical patterns. While the cortical network was characterized by an interhemispheric topography of homologous sensorimotor sensors (Fig. 2F), the corticospinal connectivity projected to a broader unilateral area of the sensorimotor and parietal cortex in the stimulated hemisphere (Fig. 3E).

Accordingly, previous pharmacological studies functionally dissociated the power of cortical beta oscillations (Baker and Baker, 2003) from the magnitude of corticomuscular beta coherence (Riddle et al.2004). Specifically, carbamazepine was shown to significantly increase beta CMC without affecting the power or frequency of cortical oscillations (Riddle et al. 2004). The same group also showed that diazepam could double the power of cortical beta oscillations without altering the magnitude of CMC (Baker and Baker, 2003). Our work complements these findings by proposing that the effective information flow within these distinct beta circuits is mediated in a frequency- and phase-dependent way.

The network showing a significant inverse correlation of beta power (15-17 Hz) with CSE overlapped at least partly with the spectrum (14-17 Hz) and topography (specifically at the C4 sensor, i.e., at the site of stimulation) of the network revealing a phase-dependent modulation. This suggests that different motor system circuits converge (Fig. 2) prior to signal propagation to downstream spinal motor neurons. Importantly, however, the phase modulation of CSE was not confounded by power fluctuations in the same frequency band (Fig. 1F).

In conclusion, these findings provide novel evidence that intrinsic activity in the human motor cortex modulates phase- and frequency-specific input gain along the beta oscillatory cycle.In accordance with periodic alternations of synchronous hyper- and depolarization, increased neuronal responsiveness occurred once per oscillatory beta cycle. These findings may lead to novel brain state-dependent and circuit-specific interventions (Kraus et al. 2016a, 2016b; Naros et al. 2016) for addressing neurorehabilitation of motor function after stroke (Belardinelli et al.2017; Naros and Gharabaghi, 2017).

References

Baker SN. 2007. Oscillatory interactions between sensorimotor cortex and the periphery. Curr Opin Neurobiol. 17:649–655.

Baker MR, Baker SN. 2003. The effect of diazepam on motor cortical oscillations and corticomuscular coherence studied in man. J Physiol. 546:931-942.

Belardinelli P, Laer L, Ortiz E, Braun C, Gharabaghi A.2017. Plasticity of premotor cortico-muscular coherence in severely impaired stroke patients with hand paralysis. Neuroimage Clin. 14:726-733.

Blankenship JE, Kuno M. 1968. Analysis of spontaneous subthreshold activity in spinal motoneurons of the cat. J Neurophysiol. 31:195-209.

Burchell TR, Faulkner HJ, Whittington MA. 1998. Gamma frequency oscillations gate temporally coded afferent inputs in the rat hippocampal slice. Neurosci Lett. 255:151-154.

Buzsaki G. 2006. Rhythms of the brain. New York, NY: Oxford University Press.

Capaday C, Lavoie BA, Barbeau H, Schneider C, Bonnard M. 1999. Studies on the corticospinal control of human walking. I. Responses to focal transcranial magnetic stimulation of the motor cortex. J Neurophysiol. 81:129-139.

Chance FS, Abbott LF, Reyes AD. 2002. Gain modulation from background synaptic input. Neuron. 35:773-782.

Devanne H, Lavoie BA, Capaday C. 1997. Input-output properties and gain changes in the human corticospinal pathway. Exp Brain Res. 114:329-338.

Di Lazzaro V, Restuccia D, Oliviero A, Profice P, Ferrara L, Insola A, Mazzone P, Tonali P, Rothwell JC. 1998. Effects of voluntary contraction on descending volleys evoked by transcranial stimulation in conscious humans. J Physiol. 508:625-633.

Di Lazzaro V, Oliviero A, Profice P, Meglio PM, Cioni B, Tonali P, Rothwell JC. 2001. Descending spinal cord volleys evoked by transcranial magnetic and electrical stimulation of the motor cortex leg area in conscious humans. J Physiol. 537:1047-1058.

Fries P. 2005. A mechanism for cognitive dynamics: neuronal communication through neuronal coherence. Trends Cogn Sci. 9:474-480.

Fries P, Nikolić D, Singer W. 2007. The gamma cycle. Trends Neurosci. 30:309–316.

Efron B, Tibshirani RJ. 1993. An introduction to the bootstrap. Boca Raton, FL: Chapman and Hall/CRC.

Enochson LD, Goodman NR. 1965. Gaussian approximation for the distribution of sample coherence. Tech Rep TR:65-57. Ohio: Air Force Flight Dynamics Laboratory, Wright-Patters on AFB.

Garry MI, Thomson RH. 2009. The effect of test TMS intensity on short-interval intracortical inhibition in different excitability states. Exp Brain Res. 193:267-274.

Groppa S, Oliviero A, Eisen A, Quartarone A, Cohen LG, Mall V, et al. 2012. Apractical guide to diagnostic transcranial magnetic stimulation: report of an IFCN committee. Clin Neurophysiol. 123:858-882.

Gross, J., Baillet, S., Barnes, G.R., Henson, R.N., Hillebrand, A., Jensen, O., Jerbi, K., Litvak, V., Maess, B., Oostenveld, R., Parkkonen, L., Taylor, J.R., van Wassenhove, V., Wibral, M., Schoffelen, J.-M. 2013. Good practice for conducting and reporting MEG research. Neuroimage. 65: 349-363.

Guerra A, Pogosyan A, Nowak M, Tan H, Ferreri F, Di Lazzaro V, Brown P. 2016.Phase Dependency of the human primary motor cortex and cholinergic inhibition cancelation during beta tACS. Cereb Cortex. 26:3977-3990.

Jensen O, Mazaheri A. 2010. Shaping functional architecture by oscillatory alpha activity: gating by inhibition.Front Hum Neurosci. 4:186.

Keil J, Timm J, Sanmiguel I, Schulz H, Obleser J, Schönwiesner M. 2014. Cortical brain states and corticospinal synchronization influence TMS-evoked motor potentials. J Neurophysiol. 111:513-519.

Kiers L, Cros D, Chiappa KH, Fang J. 1993. Variability of motor potentials evoked by transcranial magnetic stimulation. Electroencephalogr Clin Neurophysiol. 89:415-423.

Kilner JM, Baker SN, Salenius S, Hari R, Lemon RN. 2000. Human cortical muscle coherence is directly related to specific motor parameters. J Neurosci. 20:8838–8845.

Klein-Fluegge MC, Nobbs D, Pitcher JB, Bestmann S. 2013. Variability of human corticospinal excitability tracks the state of action preparation. J Neurosci. 33:5564-5572.

Kraus D, Gharabaghi A. 2015. Projecting navigated TMS sites on the gyral anatomy decreases inter-subject variability of cortical motor maps. Brain Stimul. 8:831-837.

Kraus D, Naros G, Bauer R, Khademi F, Leão MT, Ziemann U, Gharabaghi A. 2016a. Brain state-dependent transcranial magnetic closed-loop stimulation controlled by sensorimotor desynchronization induces robust increase of corticospinal excitability. Brain Stimul. 9:415-424.

Kraus D, Naros G, Bauer R, Leão MT, Ziemann U, Gharabaghi A. 2016b. Brain-robot interface driven plasticity: distributed modulation of corticospinal excitability. Neuroimage. 125:522-532

Lacey MG, Gooding-Williams G, Prokic EJ, Yamawaki N, Hall SD, Stanford IM, Woodhall GL. 2014. Spike Firing and IPSPs in Layer V Pyramidal Neurons during Beta Oscillations in Rat Primary Motor Cortex (M1) In Vitro. PLoS One. 9:e85109.

Lepage J-F, Saint-Amour D, Théoret H. 2008. EEG and neuronavigated single-pulse TMS in the study of the observation/execution matching system: are both techniques measuring the same process? J Neurosci Methods. 175:17–24.

Mäki H, Ilmoniemi RJ. 2010. EEG oscillations and magnetically evoked motor potentials reflect motor system excitability in overlapping neuronal populations. Clin Neurophysiol. 121:492–501.

Maris E, Schoffelen JM, Fries P. 2007. Nonparametric statistical testing of coherence differences. J Neurosci Methods. 163:161-175.

Mitchell WK, Baker MR, Baker SN. 2007. Muscle responses to transcranial stimulation in man depend on background oscillatory activity. J Physiol. 583:567–579.

Murthy VN, Fetz EE. 1996. Oscillatory activity in sensorimotor cortex of awake monkeys: synchronization of local field potentials and relation to behavior. J Neurophysiol. 76:3949-3967.

Nakazono H, Ogata K, Kuroda T, Tobimatsu S. 2016. Phase and frequency-dependent effects of transcranial alternating current stimulation on motor cortical excitability. PLoS One. 11:e0162521.

744 Naros G, Gharabaghi A. 2017. Physiological and behavioral effects of β-tACS on
745 brain self-regulation in chronic stroke. Brain Stimul. 10:251-259.

746 Naros G, Naros I, Grimm F, Ziemann U, Gharabaghi A. 2016. Reinforcement learning
747 of self-regulated sensorimotor β-oscillations improves motor performance.
748 Neuroimage. 134:142-152.

749 Oldfield RC. 1971. The assessment and analysis of handedness: the Edinburgh
750 inventory. Neuropsychologia. 9:97-113.

751 PellicciariMC, Miniussi C, Ferrari C, Koch G, Bortoletto M. 2016. Ongoing cumulative
752 effects of single TMS pulses on corticospinal excitability: an intra- and inter-
753 block investigation. Clin Neurophysiol. 127:621-628.

754 Pogosyan A, Gaynor LD, Eusebio A, Brown P. 2009. Boosting cortical activity at
755 Beta-band frequencies slows movement in humans. Curr Biol. 19:1637-1641.

756 Raco V, Bauer R, Tharsan S, Gharabaghi A. 2016. Combining TMS and tACS for
757 closed-loop phase-dependent modulation of corticospinal excitability: a
758 feasibility study. Front Cell Neurosci.10:143.

759 Raco V, Bauer R, Norim S, Gharabaghi A. 2017. Cumulative effects of single TMS
760 pulses during beta-tACS are stimulation intensity-dependent. Brain Stimul.

761 Riddle CN, Baker MR, Baker SN. 2004. The effect of carbamazepine on human
762 corticomuscular coherence. Neuroimage. 22:333-340.

763 Romei V, Bauer M, Brooks JL, Economides M, Penny W, Thut G, Driver J, Bestmann
764 S. 2016. Causal evidence that intrinsic beta-frequency is relevant for
765 enhanced signal propagation in the motor system as shown through rhythmic
766 TMS. Neuroimage. 126:120-130.

767 Rosenberg JR, Amjad AM, Breeze P, Brillinger DR, Halliday DM. 1989. The Fourier
768 approach to the identification of functional coupling between neuronal spike
769 trains. Prog Biophys Mol Biol.53:1-31.

770 Rossi S, Hallett M, Rossini PM, Pascual-Leone A, Safety of TMS Consensus Group.
771 2009. Safety, ethical considerations, and application guidelines for the use of
772 transcranial magnetic stimulation in clinical practice and research. Clin
773 Neurophysiol. 120:2008-2039.

774 Royter V, Gharabaghi A. 2016. Brain State-dependent closed-loop modulation of
775 paired associative stimulation controlled by sensorimotor desynchronization.
776 Front Cell Neurosci.10:115.

777 Salinas E, Thier P. 2000. Gain modulation: a major computational principle of the
778 central nervous system. Neuron. 27:15-21.

779 Sauseng P, Klimesch W, Gerloff C, Hummel FC. 2009. Spontaneous locally
780 restricted EEG alpha activity determines cortical excitability in the motor
781 cortex. Neuropsychologia. 47:284–288.

782 Schulz H, Ubelacker T, Keil J, Müller N, Weisz N. 2014. Now I am ready-nowI am
783 not: the influence of pre-TMS oscillations and corticomuscular coherence on
784 motor-evoked potentials. Cereb Cortex. 24:1708-1719.

785 Takemi M, Masakado Y, Liu M, Ushiba J. 2013. Event-related desynchronization
786 reflects downregulation of intracortical inhibition in human primary motor
787 cortex. J Neurophysiol. 110:1158-1166.

788 Thut G, Miniussi C. 2009. New insights into rhythmic brain activity from TMS-EEG
789 studies. Trends Cogn Sci.13:182-189.

790 van Elswijk G, Maij F, Schoffelen JM, Overeem S, Stegeman DF, Fries P.
791 2010.Corticospinal beta-band synchronization entails rhythmic gain
792 modulation. J Neurosci. 30:4481-4488.

793 Womelsdorf T, Schoffelen JM, Oostenveld R, Singer W, Desimone R, Engel AK,
794 Fries P. 2007. Modulation of neuronal interactions through neuronal
795 synchronization. Science. 316:1609-1612.

796 Zarkowski P, Shin CJ, Dang T, Russo J, Avery D. 2006. EEG and the variance of
797 motor evoked potential amplitude. Clin EEG Neurosci. 37:247–251.

798 Ziemann U, Rothwell JC. 2000. I-waves in motor cortex. J Clin Neurophysiol. 17:397-
799 405.

800

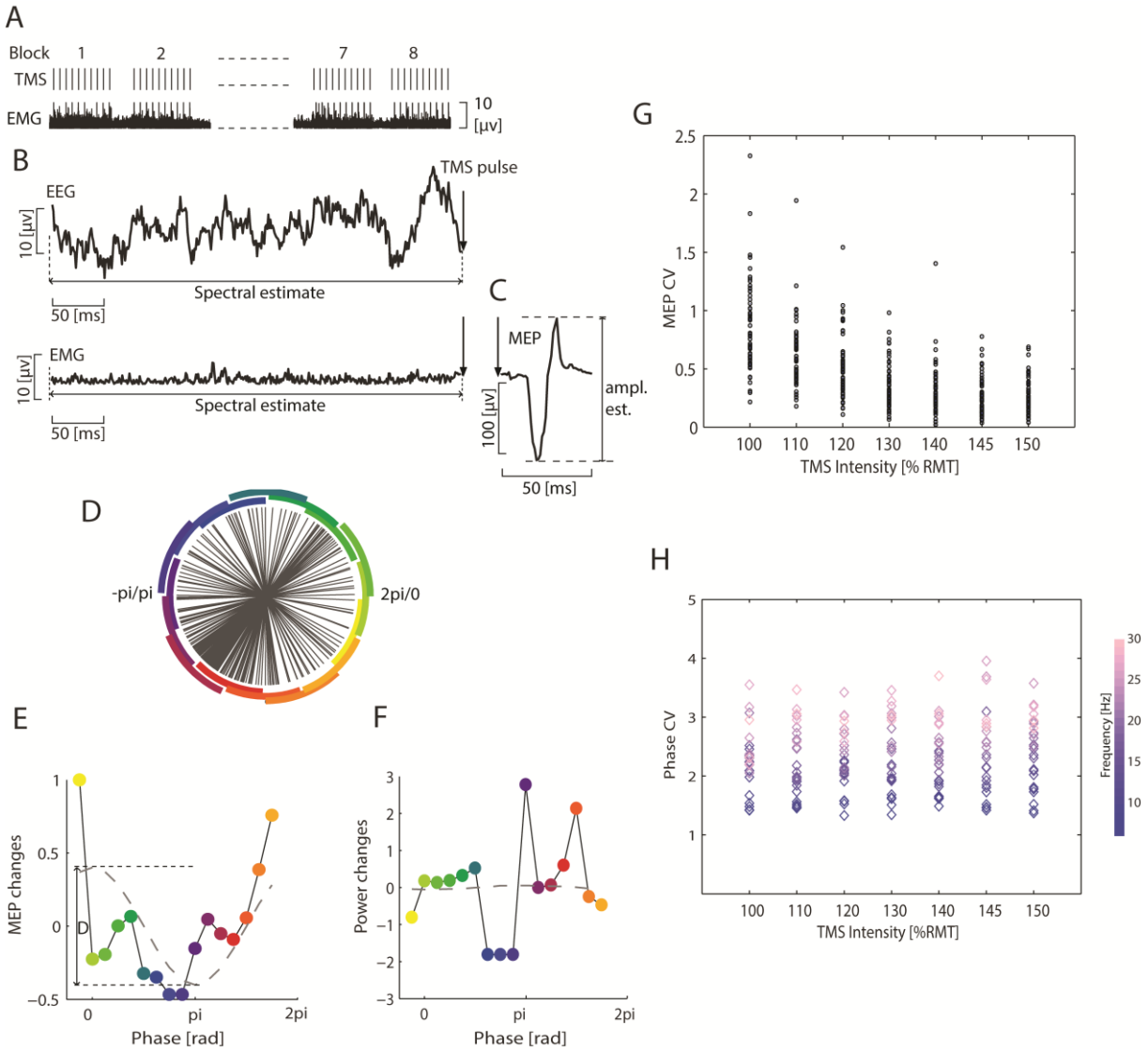

Figure 1 Experimental design, example data of pre-TMS oscillatory activity (EEG/EMG) and MEP. (A) Experiment consisted of 8 blocks; 10 TMS pulses were applied within each block, with intervals of ~2 s between consecutive pulses. (B) Example of pre-TMS EEG/EMG signals. (C) Response was quantified by the peak-to-peak amplitude of the TMS-evoked motor potential (MEP). (D) Group data of the distribution of the phase after Fourier decomposition of the EEG (C4 channel, 17 Hz; near-threshold intensity). Circle segments illustrate the phase binning, and the colors signify phase in the same way as in E and F. (E) Mean peak-to-peak MEP amplitudes as a function of the pre-TMS phase of the EEG. The dashed line is a least-squares fitted cosine function. The MEP (as a function of phase) modulation was quantified by the fitted cosine function called modulation depth (denoted by the symbol D). (F) Same as (E) but for average EEG power. (G) Coefficient of variation of the MEP amplitude (y-axis) was estimated for each subject (represented by a

circle) and intensity (x-axis). (H) Same as G but for EEG phase; each diamond represents one frequency (between 6 to 30 Hz).

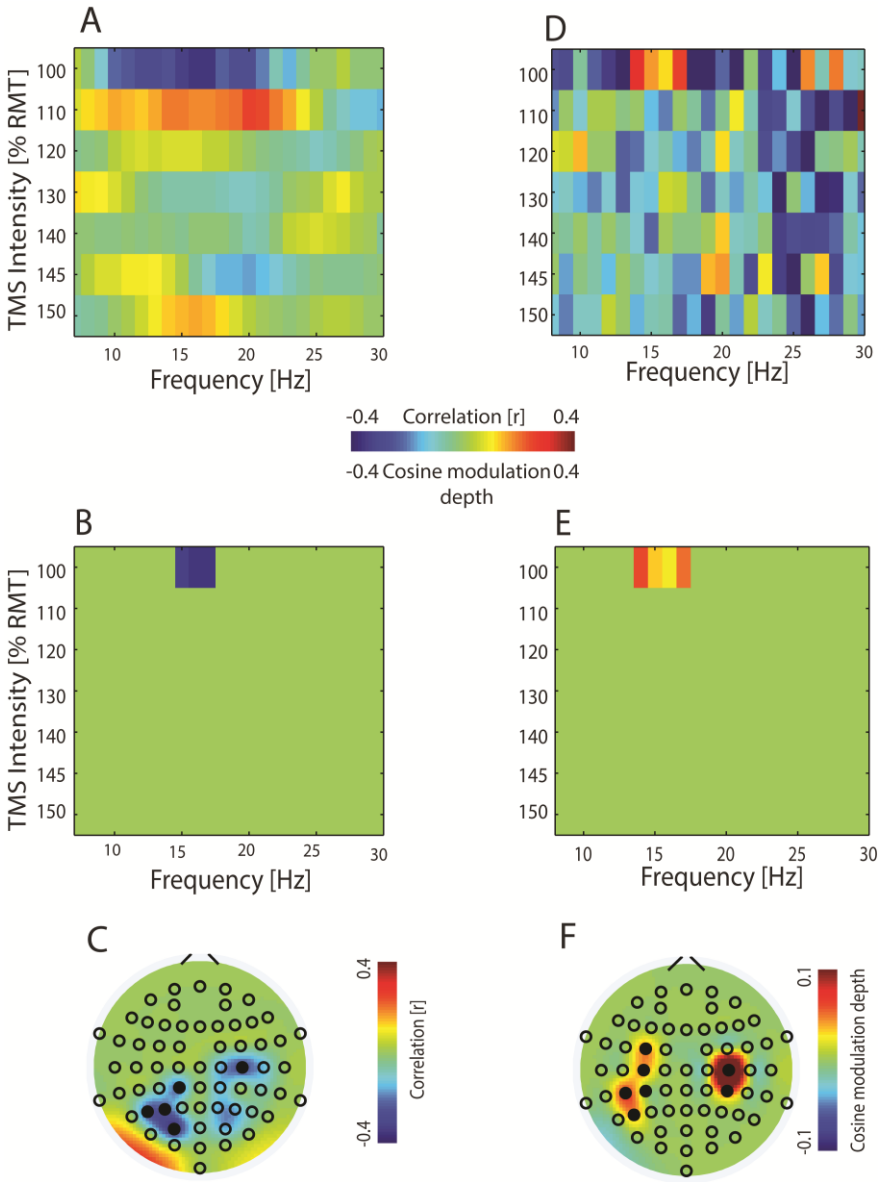

Figure 2 Pre-TMS EEG power and phase predict corticospinal excitability (CSE). (A) Spearman's rank correlation between pre-TMS EEG power and MEP amplitude (group data, right sensorimotor cortex was the site of stimulation). (B) Same as (A) but with statistically significant frequency bands (p≤0.0001). (C) Topographical distribution of the significant frequency band (15-17 Hz) of (B) at near-threshold TMS intensity (100% RMT). (D) Modulation of MEP by pre-TMS EEG phase with the bias for the cosine-fitted function subtracted (group data). (E) Same as (D) but with significant modulation depth (p≤0.001) with respect to the positive bias of the cosine fit. (F) Topographical distribution of the significant frequency band (14-17 Hz) of (E) at near-threshold TMS intensity (100% RMT).

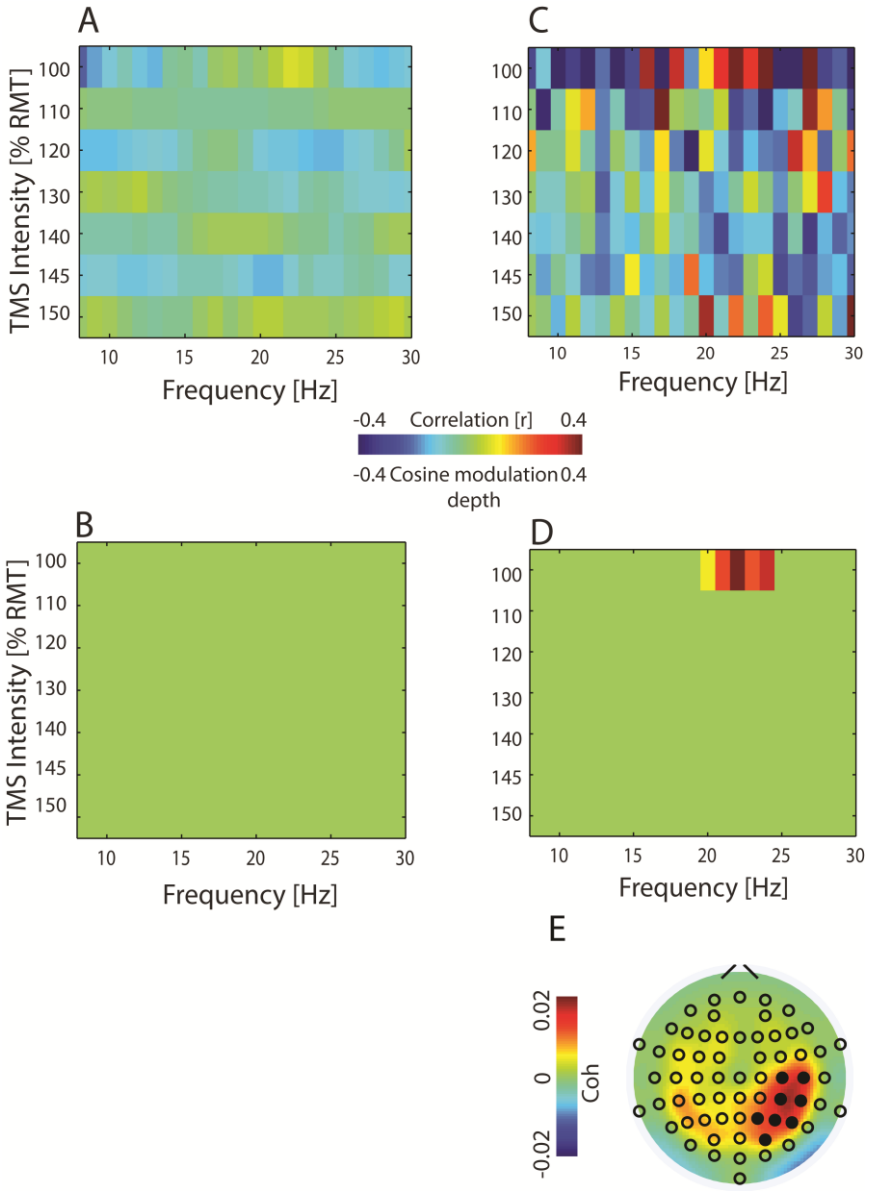

Figure 3 Pre-TMS EMG phase (but not power) predicts CSE. (A) Spearman's rank correlation between pre-TMS EMG power and MEP amplitude. (B) Same as (A)but with no statistically significant frequency band ($p>0.16$). (C) Modulation of MEP by pre-TMS EMG phase with the bias for the cosine-fitted function subtracted (group data). (D) Same as (C) but with significant modulation depth ($p\leq0.001$). (E)The CMC topographical distribution of the significant frequency band (20-24 Hz) of (D) at near-threshold TMS intensity (100% RMT).

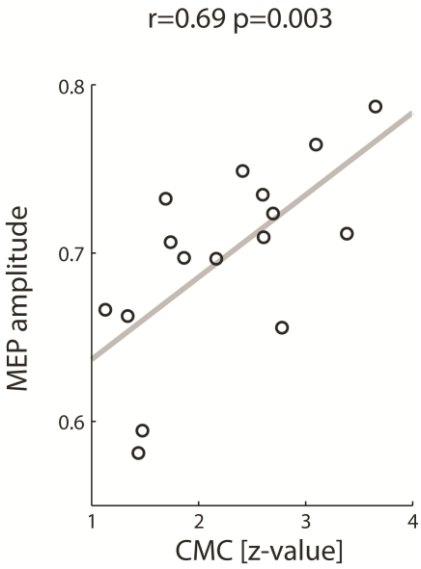

Figure 4 Pre-TMS CMC predicts CSE. Spearman's rank correlation (r=0.63, p=0.0031) between CMC in the 20-24 Hz band and MEP amplitude with the regression line in gray.Each circle represents one phase bin.

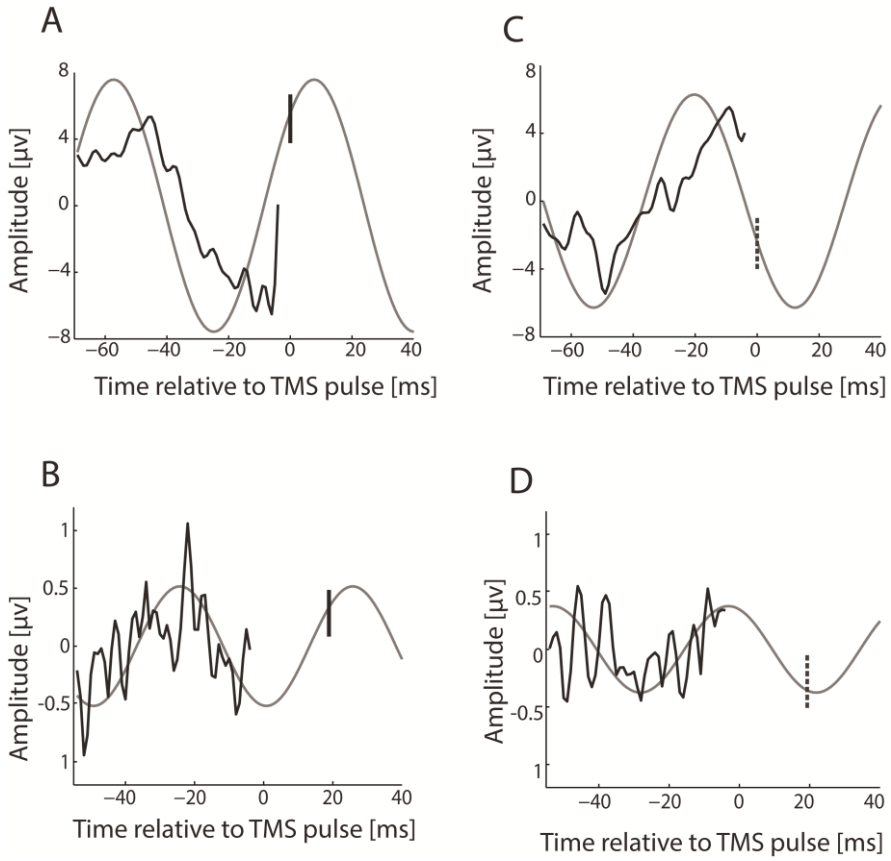

Figure 5 Synaptic input is most effective when it arrives at the rising phase of the cortical and spinal beta rhythm. (A) and (C) Average of the pre-TMS EEG epochs at 17 Hz preceding (A) maximum (vertical solid line) and (C) minimum (vertical dashed line) MEP amplitudes. (B) and (D) Average of the pre-TMS EMG epochs at 22Hz preceding (B) maximum (vertical solid line) and (D) minimum (vertical dashed line) MEP amplitudes. In all figures, the light gray curve is the fitted cosine continued to the moment of TMS-induced synaptic input (vertical line) to the cortex (A) and (C) or spinal cord (B) and (D) to estimate the phase of the respective beta rhythm.

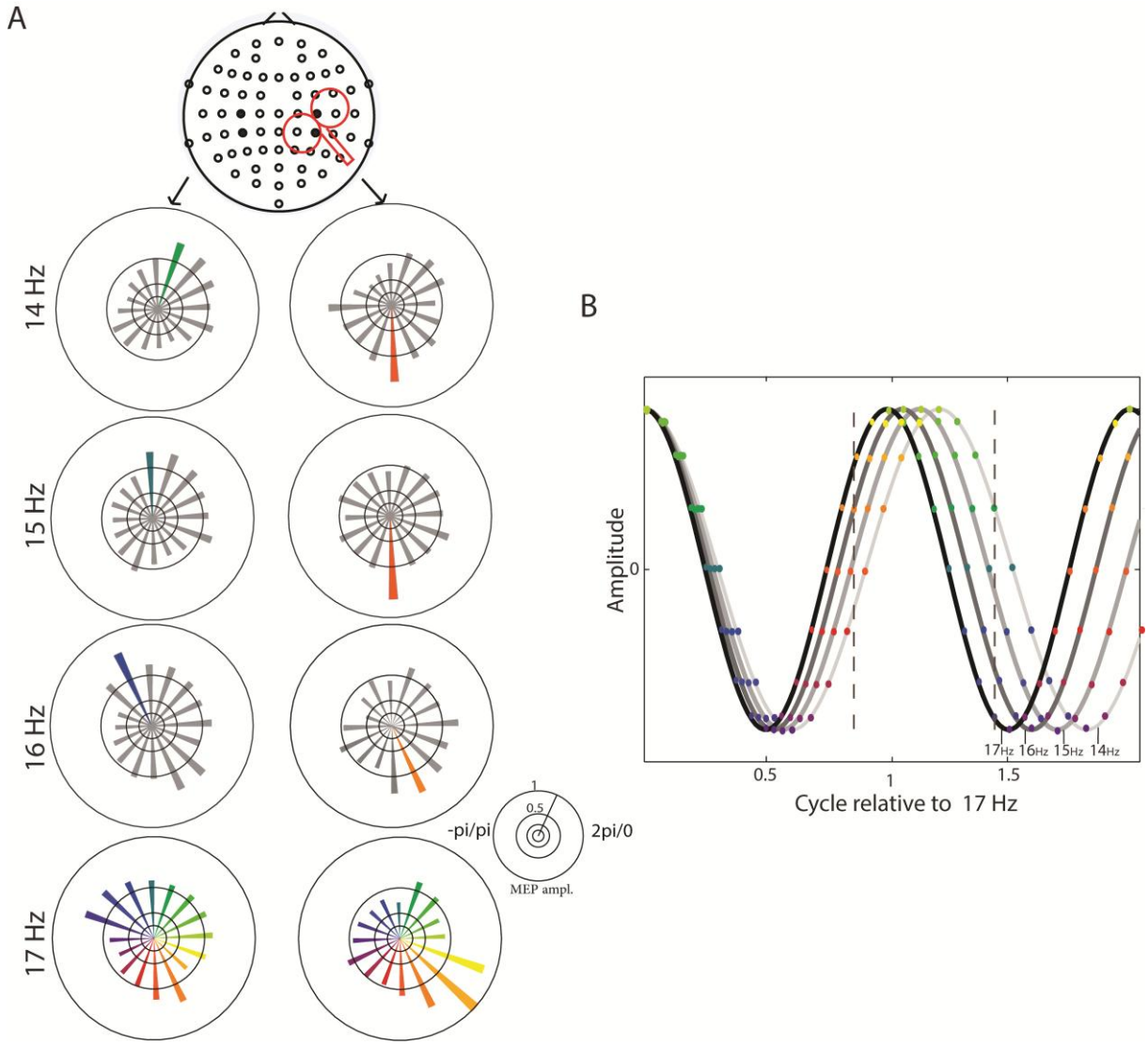

855

856 **Figure 6** The phase bin preceding maximum MEP amplitude was shifted by ~π
857 radian between the left and right hemisphere. (A) Peak-to-peak amplitudes of MEPs
858 (group data) as a function of the pre-TMS phase of the EEG for C3 and CP3 (left)
859 and C4 and CP4 (right). (B) Simulation of the phase-lag from 14 Hz to 17 Hz
860 oscillations starting with a zero phase-lag. The color-coded dots represent the
861 phases according to (A). The spot of maximal MEP (vertical dashed lines) moves
862 along the oscillatory cycle with increasing frequency, for the stimulated (left dashed
863 line) and not stimulated (right dashed line) hemispheres, respectively.

864

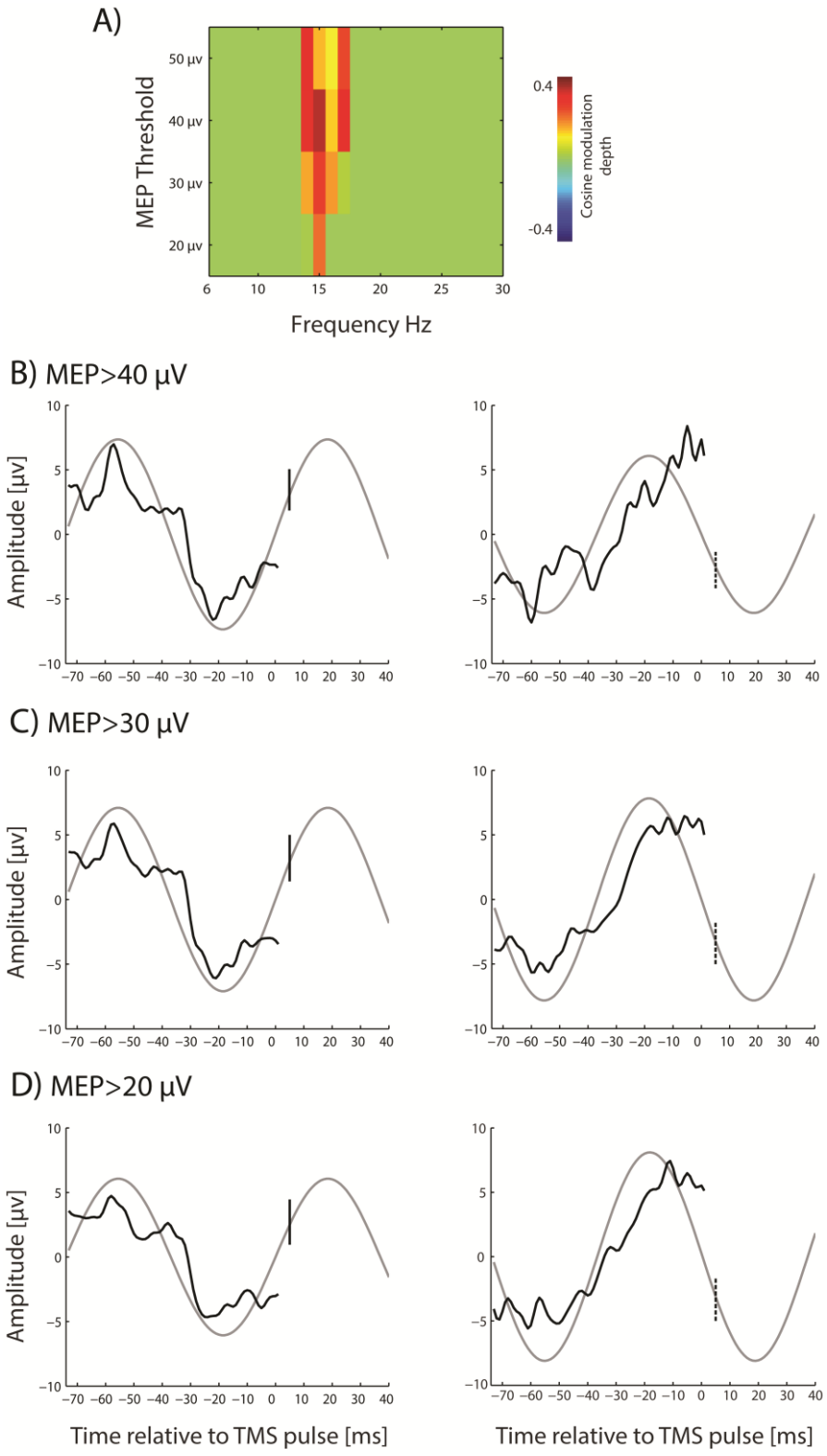

Figure 7 Pre-TMS EEG phase predicts corticospinal excitability for different MEP thresholds. (A) Modulation of MEP by pre-TMS EEG phase (with significant modulation depth ($p \leq 0.001$) with respect to the positive bias of the cosine fit) for different MEP thresholds, i.e., 50 µV, 40 µV, 30 µV, and 20 µV. (B), (C), and (D) Average of the pre-TMS EEG (at 15 Hz) preceding the maximum (left; solid line) and minimum (right; dashed line) MEP amplitude at different MEP thresholds,

872 respectively. A light gray curve is the fitted cosine continued to the time of TMS-
873 induced synaptic input (vertical line) to the cortex.
874

Brain-machine interface feedback shapes cortico-muscular control after stroke

Short title: BMI feedback and cortico-muscular control

Fatemeh Khademi, Georgios Naros, Ali Nicksirat, Dominic Kraus, Alireza Gharabaghi*

Author contributions: A.G. and G.N. designed research; G.N., A.N., and D.K. performed research; F.K. and A.G. analyzed data; F.K. and A.G. wrote the manuscript.

Division of Functional and Restorative Neurosurgery, and Centre for Integrative Neuroscience, Eberhard Karls University Tuebingen, Tuebingen, Germany

*To whom correspondence should be addressed

Professor Alireza Gharabaghi, Division of Functional and Restorative Neurosurgery, Eberhard Karls University Tuebingen, Otfried-Mueller-Str.45, 72076 Tuebingen, Germany. Email address: alireza.gharabaghi@uni-tuebingen.de

Number of pages: 51
Number of Figures: 6
Conflict of interest: None

Acknowledgments

F.K. and D.K. were supported by the Graduate Training Centre of Neuroscience & International Max Planck Research School, Graduate School of Neural Information Processing (F.K.) and Graduate School of Neural and Behavioral Sciences (D.K.), Tuebingen, Germany. A.G. was supported by grants from the Baden-Wuerttemberg Foundation [NEU005] and the German Federal Ministry of Education and Research [BMBF 13GW0119B, IMONAS; 13GW0214B, INSPIRATION]. The authors declare no competing financial interests.

Abstract

Brain-machine interfaces (BMI) are currently investigated as therapeutic tools for motor rehabilitation after stroke. Following neurofeedback principles, limb movements are synchronized to motor-related brain activity to strengthen or restore cortico-muscular control on the basis of Hebbian plasticity. Knowledge about the underlying neural processes remains however vague.

Here, we applied the same BMI intervention in healthy subjects (for one session) and chronic stroke patients with hand paralysis (for 20 sessions) to disentangle intervention-related plasticity from post-stroke reorganization. A robotic orthosis turned sensorimotor beta-band desynchronization (ERD) during kinesthetic motor-imagery (MI) into contingent hand opening. The specificity of the intervention was investigated by studying a control group of healthy subjects who performed the same MI task but received visual feedback only without proprioceptive input via the hand orthosis. We computed cortico-muscular coherence (CMC) with the finger extensors in the course of the interventions and during a motor task performed beforehand and afterward to capture a potential generalization of the effects.

Independent of the feedback modality, ERD was enhanced in the targeted sensorimotor area in a frequency-specific way, i.e., in the feedback frequency band (16-22 Hz). This specific activation pattern was paralleled by CMC increases in the same cortical area and frequency band only when proprioceptive feedback was provided. This enhanced beta-band CMC transferred to the motor task and correlated with task-specific behavioral improvements. Estimation of the phase–frequency relationships indicated an enhancement of the directed coherence (i.e., predominant information flow) from the cortex to the finger extensors. In the patient group, ERD was enhanced in the cortical area targeted by the feedback, i.e. in the ipsilesional sensorimotor cortex, as well. This modulation was, however, not restricted to the

feedback frequency band, but also included the alpha frequency band; the same was true for the induced CMC increases, which covered extended sensorimotor areas of the contralesional hemisphere as well. The directed coherence from cortex to periphery increased, however, in a restricted perilesional area of the affected hemisphere only. Specifically, training-related enhancement of beta-band CMC in the ipsilesional premotor cortex correlated with clinical improvements after the intervention.

BMI feedback increases cortico-muscular control in the healthy and post-stroke brain by enhancing both cortical activity and network connectivity to the periphery when proprioceptive feedback is provided. Activating the motor cortex with MI and closing the loop by robot-assisted natural feedback allows for sensorimotor integration beyond the lesioned corticospinal tract and may, thereby, facilitate neurorehabilitation.

Introduction

Motor rehabilitation can be effective at improving outcome beyond spontaneous neurobiological processes that reach a plateau around six months after stroke. Active movements on the basis of motor learning principles are particularly relevant for recovery (Murphy and Corbett, 2009; Langhorne et al., 2011). Stroke patients are, however, more likely to be severely disabled compared with other conditions (Adamson et al., 2004). Patients with severe arm impairment often fail to show any spontaneous recovery, particularly when the integrity of the corticospinal tract (CST) is compromised beyond a certain threshold (Krakauer and Marshall, 2015; Koch et al., 2015, Hayward et al., 2017; Kim and Winstein, 2017). When active physical practice of the upper extremities was, furthermore, no longer possible in this patient group, the re-learning of movements remains restricted (Doyon and Benali, 2005; Halsband and Lange, 2006). Therefore, motor recovery in severely impaired stroke patients with a long-lasting hand paralysis is limited (Dobkin, 2004; Feigin et al., 2008; Jørgensen et al., 1999).

In these patients, motor-imagery (MI) might be an alternative for physical practice (Boe et al., 2014; Halsband and Lange, 2006) since it activates the sensorimotor system without any overt movement, particularly, when reinforced by feedback (Gao et al., 2011; Szameitat et al., 2012; Vukelić and Gharabaghi, 2015a; Bauer et al., 2015; Naros et al., 2016). Neurofeedback of MI-related brain-states with brain-computer/brain-machine interfaces (BCI/BMI) is therefore being explored as an experimental training to improve the motor outcome of stroke rehabilitation (Sitaram et al., 2017). Controlled trials applied this intervention in addition to standard rehabilitation training, i.e., as a priming intervention before physiotherapy and demonstrated that MI with contingent feedback resulted in larger improvement than

interventions that provided no (Pichiorri et al., 2015) or random feedback(Ramos-Murguialday et al., 2013; Frolov et al., 2017). However, neurofeedback interventions have not achieved clinical benefits beyond those of dose-matched robot-assisted therapy yet (Ang et al., 2010, 2014), which has, in turn, provided only little additional benefit over dose-matched classical physiotherapy so far (Kwakkel et al., 2008; Lo et al., 2010; Klamroth-Marganska et al., 2014). In this context, current neurofeedback interventions resemble (if applied contingently to MI) other priming interventions such as transcranial electrical (Allmann et al., 2016) or magnetic brain stimulation techniques (Volz et al., 2016) that increase (as compared to sham stimulation) the general responsiveness of the brain for the subsequent active practice. These approaches may, thereby, improve the motor outcome of patients who can participate in standard physiotherapy.

For severely impaired stroke patients, however, which lack upper limb function and are not able to engage their hand in useful physical training, the BMI intervention needs to provide more specific effects beyond the practice of primed physiotherapy to be beneficial (Naros and Gharabaghi, 2015). Importantly, recovery from paralysis after stroke would necessitate a result of plasticity along the neuroaxis the re-establishment of functionally relevant motor network interactions, e.g., mediated via the up-regulation of descending pathways other than the lesioned CST (McMorland et al., 2015). For this purpose, BMI technology may be used in conjunction with commercially available rehabilitation devices for the arm (Brauchle et al., 2015) or hand (Naros and Gharabaghi, 2015), to synchronize robot-assisted movements of the paralyzed limb to motor-related brain activity; such an approach can be assumed to strengthen or restore cortico-muscular control via alternate pathways on the basis of Hebbian plasticity (Hebb, 1949). Empirical support for this hypothesis is, however,still missing.

In this study, we applied in both healthy subjects and chronic stroke patients with hand paralysis the same BMI intervention providing feedback via a robotic orthosis to disentangle intervention-related plasticity from post-stroke reorganization. The findings indicate that BMI feedback increases cortico-muscular control in the healthy and post-stroke condition by enhancing both cortical activity and behaviorally relevant network connectivity to the periphery beyond the lesioned corticospinal tract.

Materials and Methods

Experimental design

The study had been approved by the ethics committee of the University of Tuebingen Faculty of Medicine and conformed to the standards set by the latest version of the Declaration of Helsinki. All participants gave their written informed consent before participation.

We applied the same BMI intervention in healthy subjects (for one session) and chronic stroke patients with hand paralysis (for 20 sessions). A robotic orthosis turned sensorimotor beta-band desynchronization (ERD) during kinesthetic motor-imagery (MI) into contingent hand opening. The specificity of the intervention was investigated by studying a control group of healthy subjects who performed the same MI task but received visual feedback only.

Subjects

We recruited twenty-seven right-handed healthy subjects (mean age, 27.30 ± 4.38 years, range 19-37 years, 22 males) with no history of psychiatric or neurological disorder. The Edinburgh handedness inventory (Oldfield, 1971) was used to confirm right-handedness. Fifteen subjects participated in the intervention with proprioceptive

feedback (brain-machine interface, BMI), and twelve subjects participated in the control condition with visual feedback (brain-computer interface, BCI). For the BMI group, changes of corticospinal excitability at rest have been reported elsewhere (Kraus et al., 2016).

Patients

Eight right-handed patients (mean age, 57 ± 11 years, range 34-68 years, 7 males) participated in the same BMI intervention with proprioceptive feedback like the healthy subjects. They were, moreover, part of a larger study on BMI-assisted neurorehabilitation of the upper extremity in severely affected chronic stroke patients. Clinical details of this group of patients have previously been reported and are cited here accordingly (Belardinelli et al., 2017; Grimm et al., 2016): The patients were in the chronic phase after stroke (70 ± 34 months) and presented with a severe and persistent hemiparesis of the left side due to a right hemispheric lesion. All patients had a left-hand paralysis and were unable to extend their fingers. The upper extremity Fugl-Meyer-Assessment (UE-FMA) was evaluated before and after the four-week intervention, respectively. The UE-FMA score for this group of patients was 16.23 ± 6.79 (range 6.80-28.60). These patients participated in 20-sessions of proprioceptive BMI-feedback intervention (four-week rehabilitation period, i.e., one session per day). They have been reported previously with respect to increases in corticospinal connectivity after the intervention (Belardinelli et al., 2017). The underlying neural processes and their impact on actual motor improvements remained, however, unclear and necessitated a secondary analysis. The present study evaluated, therefore, the motor-network changes in the course of the intervention in relation to subsequent behavioral gains.

The data acquisition methods applied in this study have been described in detail in our previous work and are cited here where appropriate (Kraus et al., 2016):

Electromyography (EMG)

We used Ag/AgCIAmbuNeuroline 720 wet gel surface electrodes (Ambu GmbH, Bad Nauheim, Germany) to record electromyography (EMG) activity from the left Extensor Digitorum Communis (EDC) muscle (Kraus et al., 2016). Two electrodes were placed 2 cm apart from each other on the muscle belly. EMG was band-passed filtered between 0.16 Hz (1st order with 6 dB/octave) and 1 kHz (Butterworth 5th order with 30 dB/Octave) recorded with 5 kHz sampling rate and downsampled to 1 kHz (BrainAmpExG amplifier with an antialiasing filter).

Electroencephalography (EEG)

To record electroencephalography (EEG) signals, we used Ag/AgCl electrodes (BrainCap for TMS, Brain Products GmbH, Gilching, Germany) and BrainVision software with DC amplifiers and an antialiasing filter (BrainAmp, Brainproducts GmbH, Germany). A 32-channel EEG setup,which complied with the international 10–20 system, was used (FP1, FP2, F3, Fz, F4, FT7, FC5, FC3, FC1, FC2, FC4, FC6, FT8, C5, C3, C1, Cz, C2, C4, C6, TP7, CP5, CP3, CP1, CPz, CP2, CP4, CP6, TP9, P3, P4, and POz with FCz as reference). We kept the impedances at all electrodes below 10 kΩ. After EEG signals were band-pass filtered between 0.16 Hz (first-order with 6 dB/Octave) and 1 kHz (Butterworth fifth-order with 30 dB/octave), they were recorded with a 5kHz sampling rate and downsampled to 1 kHz. Later, EEG signals were transferred to the BCI2000 software (Schalk et al., 2004) for online analysis and offline storage. Every effort was made to remove the potential sources of ambient noise from the experimental environment (Kraus et al., 2016).

Experimental conditions

Fig. 1A represents the schematic illustration of the experimental design. The experiment started with anisometric motor task (5 minutes), which was followed by the intervention (40 minutes) and another isometric motor task (5 minutes).

The intervention consisted of 15 runs. Each run lasted approximately 2.5 minutes and included 11 trials. Each trial started with a 6 s *rest* phase which was followed by a 2 s *preparation* phase and a 6 s *move* phase, i.e., kinesthetic motor imagery (Fig. 1B). The audio taped cues of a female voice: ‘relax', ‘left hand,' and 'go' were used to initiate the *rest*, *preparation*, and *move* phases, respectively. All subjects were instructed to keep their muscles relaxed during the intervention. During the *move* phase, the subjects were instructed to perform kinesthetic motor imagery, i.e. to imagine the feeling of opening their left hand, i.e., finger extension, from a first-person perspective. During the *move* phase, the passive opening of the left hand (proprioceptive group) and changing the color of the cross on a screen (visual group) was initiated by the BCI2000 software after detection of motor imagery-related ERD in the beta-band (16–22 Hz; Gharabaghi et al., 2014). This feedback was contingent, i.e. the participants were rewarded with robotic opening of the hand (proprioceptive group) or color change on a screen (visual group), when the predefined brain state (i.e. beta-ERD) was achieved and sustained; whenever the respective ERD was insufficient, the robotic movement ceased but could be restarted to continue when the ERD threshold was reached again. Importantly, the robotic hand *opening* was synchronized to the respective motor imagery-related brain activation, whereas the robotic hand *closing* occurred after the relax command automatically and independent of the respective brain state, (Kraus et al., 2016) The feedback frequency band was selected on the basis of previous work in our group on beta-

band oscillatory circuits in the extended motor network (Khademi et al., unpublished observation).

ERD was analyzed over the right surface EEG channels FC4, C4, and CP4 (Fig. 1B) during the *move* phase (McFarland et al., 2000). ERD detection was performed with an adaptive linear classifier (Gharabaghi et al., 2014; Kraus et al., 2016). The spectral power was computed with an autoregressive model order of 16 (McFarland and Wolpaw, 2008), fitted to the last 500 ms of the signal and updated every 40 ms. To avoid a noisy control signal for the orthosis, five consecutive 40 ms epochs (i.e., 200 ms) had to be classified as ERD positive (negative) in order to start (stop) feedback (Bauer and Gharabaghi, 2015a, 2017; Vukelić and Gharabaghi, 2015a, 2015b).

Before and after the intervention, an isometric motor task was performed by the subject. This task has been described in detail elsewhere and is cited here accordingly (Naros et al., 2016): During the isometric motor task, the fingers of the subject were connected to the robotic orthosis via small magnets which were attached to the finger tips. Thereby, the fingers could not move and the applied forces were translated into cursor movements on a screen instead. There, a horizontal target bar, which oscillated vertically with a frequency of 0.1 Hz, was presented about 150 cm in front of the subject. The subject had to control the vertical position of a simultaneously presented cursor via the force of the fingers (digit II–V), Fig. 1C. This task consisted of 15 trials (10 s each) per run (2 runs). Each trial had one *flexion* (5 s) and *extension* (5 s) phase, i.e., downward and upward direction of the cursor, respectively (Fig 1C).

EEG/EMG analysis

Data were analyzed offline using MATLAB (The MathWorks, Inc., Natick, Massachusetts, United States) and the FieldTrip open source MATLAB toolbox (http://fieldtrip. fcdonders.nl/; MathWorks). This included bandpass filtering (finite impulse response) between 2 Hz and 46 Hz, linear detrending, and visualocular/muscular artifact rejection.

Assessing intervention-related cortical and corticomuscular modulation

We analyzed EEG spectral modulation and EEG-EMG corticomuscular coherence (CMC) during the BMI and BCI interventions. The raw EEG and EMG signals were cut into epochs of 1 s (for CMC and 500 ms for ERD) before feedback onset. We studied epochs with at least 500 ms continuous MI-related ERD below the predefined threshold (see above); this resulted on average in 93 ± 27 epochs per subject. To capture the evolution of EEG oscillations in the course of the intervention, epochs were divided into 10 subgroups, yielding on average 9 ± 3 epochs per subgroup.

To quantify the evolution of ERD, the data epochs from the rest phase of the intervention were chosen as baseline with epochs of 500 ms length with a floating window and no overlapping. The epochs were randomly downsampled so that the number of rest phase epochs and the number of MI-related epochs were the same; they were divided into 10 subgroups to estimate the power spectrum. A Hann window was applied on each epoch to attenuate edge effects (Nuttall, 1981). The power spectral density (PSD) of each epoch was calculated frequency-wise from 2 to 46 Hz in steps of 1 Hz using Fast Fourier Transform (FFT). Later, the average of estimated PSD for each subgroup was estimated. For the CMC estimation see the following section.

Assessing motor task-related corticomuscular modulation

We studied the synchronous oscillatory activity between EEG and EMG of the EDC muscle by analyzing CMC. To estimate CMC, each trial of the motor task (10 s) was divided into ten non-overlapping time-windows (1 s) denoted by F1-F5 and E1-E5 during flexion and extension, respectively. Epochs from each interval were visually inspected for ocular/muscular artifacts, yielding on average of 26 ± 4 epochs per interval and subject. Finally, the EMG signals were rectified.

CMC was estimated as the cross-spectral density matrix frequency between EEG and EMG channels (Schulz et al., 2014). This was calculated frequency-wise using the multi-taper method (9 tapers; with 1 s signal width) over the frequency range from 2 to 46 Hz in steps of 1 Hz. We, then, obtained the magnitude of the coherence values by normalizing the magnitudes of the summed cross-spectral density matrix for each frequency to the corresponding power values at that frequency (Schulz et al., 2014). Further, we neither found changes in EEG or EMG spectral power between conditions (BMI vs. BCI) nor a correlation of EEG or EMG spectral power with the difference in CMC strength values in the course of the intervention in healthy and stroke subjects. We therefore could exclude that CMC modulation was confounded by amplitude changes of neuronal oscillations (von Carlowitz-Ghori et al., 2015), which were shown to affect the estimation of CMC (Bayraktaroglu et al., 2013) as they relate to the signal-to-noise ratio (Nikulin et al., 2011).

Assessing behavioral gains

The difference between the cursor movements on a screen controlled by the subject and the oscillating horizontal target bar resulted in the error rate during the motor task; i.e., area under the curve (AUC). Reduction of this error rate was defined as an improved motor performance (Fig.1D).

$$Performance = -\frac{Error_{post} - Error_{pre}}{Error_{pre}} * 100$$

Assessing the relationships between intervention-related, motor task-related corticomuscular modulation, and behavioral gain

We used Spearman's rank correlation to evaluate the relationship between CMC magnitude during the intervention (CMC [intervention]) and during the motor task (CMC [motor task]), and CMC [motor task] and motor performance across subjects. The statistically significant clusters of the previous analyses (see above) were chosen for this estimation. Specifically, the maximum CMC value of EEG channels from the respective cluster was subtracted from the median value of them for each subject individually to compensate for variability. Per subject, one pair of CMC [intervention]/CMC [motor task] was used for further analysis.

Assessing the phase-frequency relationships of corticomuscular modulation

The phase-frequency relationships of CMC were estimated frequency-wise (every 1 Hz). Specifically, the phase was estimated by taking the argument from the estimated EEG-EMG cross-spectrum (Witham et al., 2011), see statistical section.

Patient data

Data analysis for the group of patients was identical to the approaches described above for the group of healthy subjects. Since the patient group performed 20 intervention sessions (instead of one session by each healthy subject); the session were evaluated individually yielding 20 different data sets for ERD and CMC modulation per patient. We averaged the data of sessions 3 to 20 of each patient and compared it to baseline (session 1 and 2), to compensate for the day-to-day performance variability in the course of the 4 week training. The resulting

physiological changes were then compared to the motor improvement assessed by the UE-FMA.

$$Improvement = \frac{UEFMA_{post} - UEFMA_{pre}}{UEFMA_{pre}} * 100$$

Statistical analysis

Testing significance of ERD and CMC modulation

We used a nonparametric randomization test with 1000 repetitions to test the modulation of ERD/CMC magnitude in the course of the intervention. The null hypothesis was that observed increase in ERD/CMC magnitude was not related to the intervention. Therefore, ERD/CMC from begining and end of the intervention, 1st to the 9th ± 1 subgroup (see above), were exchangeable, consqquently the pre- and post-motor task CMC values.

For the CMC estimation, we estimated Z-statistic of the coherence difference prior to the nonparametric statistical test (Maris et al., 2007); since the artifact rejection led an unequal degree of freedoms (d.f.) for each group of epochs (e.g., 474 ± 72 d.f. for motor-task).

We performed the cluster-based randomization test for each frequency band of interest. The frequency bands were selected to cover the feedback frequency band of the intervention (16-22 Hz) and the neighboring frequency bands with the same bandwidth (9-15 Hz, 23-29 Hz, and 30-36 Hz) for balanced statistical comparisons. When the maximum of t-statistic (paired t-test; ERD) or Z-statistic (CMC) exceeded the threshold $p<0.05$, adjacent EEG channels were clustered in the same set (Maris et al., 2007). Cluster-level statistics were, then, conducted by taking an average of the t-statistics. The maximum of the cluster-level statistics was used for later comparisons in case multiple clusters were observed. The p-value to reject

the null hypothesis was the proportion of cluster-based randomizations that resulted in a larger test statistics than the observed one (without randomization).

Testing significance of ERD and CMC modulation in the patients

For the stroke patients, the randomization test was applied for each EEG channel. And, similar approach as explained in the section above was conducted. The null hypothesis was that the observed cortical and corticospinal modulations were not the effects of intervention so that the baseline sessions could be exchanged with the following sessions.

Testing significance of the behavioral gains

Three-way ANOVA was performed for three main factors of *group* (two levels: proprioceptive vs. visual), *condition* (two levels: pre- versus post-isometric motor task), and *time* (ten levels: ten different intervals of the motor task). For each interval of interest, two-way ANOVA were performed for the two main factors of *group* (two levels) and *condition* (two levels).

Testing significance of the relationships estimated with Spearman's rank correlation

We tested the significance of the relationship between intervention-related and motor task-related CMCs, and motor task-related CMCs and improved performance across subjects. Our null hypothesis was that they were not correlated. Therefore, independent and dependent variables were exchangable, i.e., intervention-related CMCs versus motor task-related CMCs and motor task-related CMCs versus performance.. For this purpose, we shuffled the independent variable versus dependent variable with 1000 repetitions. At each repetition, we calculated Spearman's rank correlation. The p-value to reject the null hypothesis was the proportion of randomizations that resulted in a larger test statistics than the observed one (without randomization).

Testing significance of phase-frequency relationships

We calculated the mean of the estimated CMC phase for each frequency across subjects, yielding one phase-frequency spectrum. We, then, fitted a line to the phase-frequency plot using a linear regression (i.e., over a range of frequencies with significant CMC). The regression slope was significantly different from zero if $p<0.05$.

Results

Healthy subjects learned to modulate motor imagery (MI)-related sensorimotor ERD over the feedback frequency range (16-22 Hz) independent of the feedback modality. ERD and CMC changes in the course of the intervention were frequency-specific and restricted to the right hemisphere, i.e. ipsilateral to the side of feedback channels, and overlapped in the primary sensorimotor and premotor cortex (Fig. 2). Specifically, a cluster-based randomization test (1000 repetitions) revealed significant ERD modulation over the frequency range of 16-22 Hz for the proprioceptive (Fig. 2A; EEG channels FC2, C2, C4, Cp2, and CP4; $p=0.017$) and visual (Fig. 2B; EEG channels C2, C4, C6, CPz, CP2, CP4, CP6, and P4; $p=0.004$) groups.The CMC changes were specific for the same frequency range (16-22 Hz), but occurred in the proprioceptive group only (Fig. 2A; EEG channels: FC2, FC6, C2, C4, C6, CP2, CP4, CP6,and P4; $p=0.014$, cluster-based randomization test, 1000 repetition).

This increase in CMC magnitude (16-22 Hz) in the course of the MI intervention was also observed in the motor task (MT) after the intervention (Fig. 3; cluster-based randomization test, 1000 repetitions). The topography of the MT-related CMC modulation was restricted to the right hemisphere, i.e. ipsilateral to the side of feedback channels, and projected to the primary sensorimotor and premotor cortex. In the proprioceptive group, MT-related increase in CMC magnitude occurred at movement intervals reflecting transitions between finger flexion (16-22 Hz,

p=0.002; and 23-29 Hz, p=0.002) and extension (16-22 Hz, p=0.007; and 23-29 Hz, p=0.006). In the visual group, this increase occurred during finger extension independent of the transition intervals (23-29 Hz, p=0.007; and 30-36 Hz, p<0.0001).

In the proprioceptive group, the increase of CMC magnitude correlated significantly (Fig. 4A; r=0.56 p=0.0015; Spearman's rank correlation, randomization test, 1000 repetitions) between the MI-related finger extension (Fig. 2A, 16-22 Hz) and the MT-related finger extension (Fig. 3A, 16-22 Hz).

The MT-related error rate increased around the transition interval from flexion (denoted by F) to extension (denoted by E) for the proprioceptive and visual groups. When comparing the motor tasks before (Fig. 4B) and after (Fig. 4C) the intervention, a three-way ANOVA (full model) showed a significant effect for the main factors of condition ($F(1,500)=38.62$, $p<0.0001$) and time ($F(9,500)=145.2$, $p<0.0001$) but not group ($F(1,500)=0.96$, $p=0.33$). Furthermore, a significant interaction was observed for group by condition ($F(1,500)=4.39$, $p=0.04$) but not for group by time ($F(9,500)=1.33$, $p=0.22$), condition by time ($F(9,500)=0.79$, $p=0.62$), or group by time by condition ($F(9, 500)=0.21$, $p=0.99$). However, the interaction model of the three main factors, i.e. group by condition by time, showed a significant interaction ($F(9,530)=12.44$, $p<0.0001$). In a next step, a two-way ANOVA was performed for each time interval, separately. Thereby, we found a significant difference (Fig. 4D) for the main factor condition ($F(1,50)=6.69$, $p=0.01$) for the time interval with maximum error rate (marked by E1 in Fig.4B and 4C), but not for group ($F(1,50)=0.19$, $p=0.67$, ANOVA) or group by condition ($F(1,50)=1.81$, $p=0.18$). Post-hoc test ($p<0.05$, Bonferroni corrected for number of groups yielding $p<0.025$) showed a significant decrease in error rate for the proprioceptive (Post versus Pre, $t(28)=-2.87$, $p=0.008$, unpaired Student t-test) but not visual group ($t(22)=-0.86$, $p=0.40$, unpaired Student t-test).

This improved performance in the proprioceptive group correlated with the increase in CMC magnitude (Fig. 4E) in the same movement interval (E1) for 16-22 Hz, ($r=0.74$, $p<0.0001$, Spearman's rank correlation, randomization test, 1000 repetitions), but not 23-29 Hz ($r=0.11$ $p=0.70$, Spearman's rank correlation).

Finally, the intervention led to a significant change in the phase-frequency relationship (in the feedback channels) in the course of the intervention (Fig. 5A, middle column), which persisted in the motor task after the intervention (Fig. 5A, right column). This phase-frequency relationship showed consistently a negative slope significantly different from zero (F-statistic, $p<0.05$) indicating a direction of interaction from cortex to muscle. The respective cortical topography included extended sensorimotor and premotor areas ipsilateral to the side of feedback (EEG channels: F4, FC2, FC4, FC6, Cz, C2, C4, C6, CPz, CP2, CP4, and CP6; F-statistic, $p<0.05$), which persisted during the post-intervention motor task (EEG channels: FC2, FC4, Cz, C2, C4, C6, CPz, CP2, CP4, CP6, P4, CP1, P3, and POz; F-statistic, $p<0.05$). The average phase delays of the phase-frequency relationship were 33.5 ± 10.12 ms and 25.16 ± 7.45 ms for the intervention and post-MT, respectively.

Stroke patients learned modulating motor imagery (MI)-related sensorimotor ERD over the feedback frequency range (16-22 Hz) and channels (FC4, C4, and CP4; $p<0.001$, randomization test, 1000 repetitions; Fig. 6A, left column). An increase in ERD magnitude was also observed over the frequency range of 9-15 Hz ($p<0.001$ randomization test, 1000 repetitions). These ERD changes were restricted to the ipsilesional right hemisphere. The changes in CMC magnitude, however, were bilateral (Fig. 6A, right column). Specifically, ipsilesional premotor CMC increased in the beta-band (16-22 Hz), whereas contralesional CMC of extended sensorimotor, premotor and parietal areas increased in the alpha- and beta-band (9-15 Hz and 16-22 Hz; $p<0.001$ randomization test, 1000 repetitions).

In the patient group, the increase in CMC magnitude of ipsilesional premotor cortex (F4, FC2, and FC4) correlated significantly with the improvement of the UE-FMA score after the intervention period (Fig. 6B; r=0.71 p=0.02; Spearman's rank correlation; randomization test, 1000 repetitions).

Finally, also in the patient group the intervention led to a significant change in the phase-frequency relationship in the course of the intervention (Fig. 6C). The phase-frequency relationship in the end of the intervention showed a negative slope significantly different from zero (F-statistic, $p<0.05$) indicating an enhanced direction of interaction from cortex to muscle. The respective cortical topography included premotor (FC4), somatosensory (CP4), and parietal (P4) channels ipsilateral to the side of feedback(F-statistic, $p<0.05$). The average phase delays of the phase-frequency relationship during the intervention were 23.75 ± 12.32 ms and 26.55 ± 7.09 for the ipsi- and contralesional hemisphere, respectively.

Discussion

The present study indicates that BMI feedback induces plasticity along the neuroaxis by enhancing functionally relevant corticospinal interactions via the up-regulation of alternate descending pathways beyond the primary corticospinal tract. This effect occurred in both the healthy and post-stroke condition and correlated with subsequent motor improvements. Healthy subjects and stroke patients differed, however, with regard to the cortical topography and involved frequency spectrum of the cortico-motor connectivity pattern.

Neural processes related to brain-machine interface feedback

Healthy subjects learned to enhance ERD in the targeted sensorimotor area in a frequency-specific way, i.e., in the feedback frequency band (16-22 Hz), irrespective of the provided feedback modality (proprioceptive or visual). This was not surprising,

given that sensorimotor oscillations are modulated by thalamo-cortical and cortico-cortical interactions (Thut and Miniussi, 2009; Jensen and Mazaheri, 2010) and do, therefore, not necessarily dependent on proprioceptive input. However, only when proprioceptive feedback was provided, this specific activation pattern was paralleled by CMC increases as well. They occurred in the same cortical area and frequency band as the ERD modulation, thereby, suggesting interacting processes (figure 2A). Since MI-related ERD has been shown to reduce intracortical inhibition (Takemi et al., 2013), it may serve as the pre-synaptic input for an excitatory drive via proprioceptive input (Kraus et al., 2016). This is in accordance with previous studies that paired specific brain states with peripheral (Mrachacz-Kersting et al., 2012, 2016), cortical (Kraus et al., 2016b) or combined stimulation (Gharabaghi et al., 2014; Royter and Gharabaghi, 2016) to increase corticospinal excitability. We speculate that the kinesthetic MI that was applied in the present study has modulated the susceptibility of an extended cortical motor network to the provided natural proprioceptive input and would thereby fulfill the requirements of Hebbian-stimulation (Hebb, 1949).

Recently, the same BMI intervention was studied by transcranial magnetic stimulation (TMS) and motor evoked potentials (MEP) applying refined TMS protocols (Kraus and Gharabaghi, 2015, 2016a; Mathew et al., 2016). This evaluation provided a link between the ERD modulation and the changed connectivity to the periphery (Kraus et al., 2016a). Specifically, the largest MEP gains were found in those cortical areas that were most strongly modulated by the intervention (Kraus et al., 2016a). Furthermore, this topographic specificity was paralleled by a correlation between the ERD changes and the increased connectivity to the periphery, i.e., the largest MEP gains were observed in the subjects with the strongest ERD modulation range (Kraus et al., 2016a). The direct dependency of ERD strength and CMC

magnitude is thereby in accordance with the *gating by inhibition* framework (Jensen and Mazaheri, 2010)

Beta-band corticomuscular coherence and motor performance

The present study complements and extends these previous findings; it suggests- consistent with the *communication through coherence* hypothesis (Fries, 2005) - synchronized neural activity at cortical and spinal level in the feedback frequency range as the underlying neural mechanism of the BMI induced effects. The cognitive demands of the feedback task alone could not account for this phenomenon since the control intervention with visual feedback only did not lead to these connectivity changes (figure 2B).

Furthermore, we demonstrated that this enhanced beta-band CMC during the MI task with dynamic movement feedback transferred to the subsequent isometric motor task. It occurred during the transition intervals between flexion and extension and in a broader beta frequency band (16-22 Hz, 23-29 Hz), which may be related to elevated attentional demands (Murthy and Fetz, 1992; Kristeva-Feige et al., 2002). The magnitude of beta-band CMC during the BMI and the motor tasks correlated with each other (figure 4A) and with motor performance (figure 4E). The motor task-related correlation between beta-band CMC and performance is a known phenomenon and reflects its proposed role in effective corticospinal interactions (Baker et al., 1999; Kristeva et al., 2007).Moreover, motor learning has been shown to both increase pre existing (Houweling et al., 2010) and develop new beta-band CMC (Mendez-Balbuena et al., 2011).

Notably, the improved motor performance in our study revealed task-specificity by occurring during the initiation of finger extension only (E1 interval, figure 4D), i.e., the very movement that was reinforced during the preceding BMI task. Moreover, this specific improvement of motor performance correlated with the feedback frequency

only (16-22 Hz) and not with the higher beta-band (23-29 Hz) that changed as well. Together these observations suggest a link between sensorimotor processing during the BMI task and the following motor-task related beta-band CMC; this relationship implies the generation of the later independence of memory traces induced by the former (Omlor et al., 2011). A similar mechanism has been described for the primary motor cortex in association with the preceding motor experience (Chouinard et al., 2005; Nowak et al., 2005; Berner et al., 2007; Loh et al., 2010) and for beta-band CMC during steady force following a dynamic force task (Omlor et al., 2011). Along these lines, beta-band CMC has been suggested to serve as the major *functional corticospinal gateway* for efficient integration and transmission of sensorimotor information (Omlor et al., 2011; Aumann and Prut, 2015). The present findings suggest BMI feedback as a mean to enhance this process.

The estimation of the phase–frequency relationships indicated, moreover, an enhancement of the directed coherence (i.e., predominant information flow) from the cortex to the finger extensors (Halliday et al., 1998; Mima et al., 2000; Witham et al., 2011) in the course of the intervention and thereafter (figure 5A). This is, to the best of our knowledge, the first observation of shaping the CMC directionality by an intervention. Importantly, this phenomenon occurred in an extended sensorimotor area beyond the primary motor cortex (figure 5B). This indicates the functionally relevant engagement of an extended motor network for task performance and provides, thereby, the rationale for the application of this technique in patients with a lesioned primary CST. These observations are in line with earlier studies (He et al., 1993; Kombos et al., 1999; Teitti et al., 2008; Schmidt et al., 2013; Kraus and Gharabaghi, 2016), which indicated that corticospinal connections are not limited to the primary motor cortex but may originate from different regions of the sensorimotor system. The phase delays estimated in this study are consistent with a range of

conduction times and may thereby reflect the involvement of both direct and indirect (e.g., cortico-rubro-spinal, cortico-reticulo-spinal) pathways.

Post-stroke reorganization related to brain-machine interface feedback

The rationale for patients selection in this study has been reported previously (Belardinelli et al., 2017): To detect common processes underlying the intervention and potential factors relevant for functional restoration, the patients were unified as far as possible. This ensured that the detected CMC changes were attributable to the BMI feedback. The patients were specifically selected on the basis of their clinical symptoms and not on the basis of their lesion location. The impaired transmission along the efferent pathway in the corticospinal tract was the common factor in all of them. This is due to the fact that the recruitment of cortical areas during motor performance (Ward et al., 2007; Ward et al., 2006) and motor function (Stinear et al., 2012; Stinear et al., 2007) depends on corticospinal integrity post-stroke (von Carlowitz-Ghori et al., 2014). Our patients therefore had a similar severity level of motor impairment, i.e., a persistent hand paralysis in the chronic stage after stroke. They were, moreover, all right-handers and had their lesion in the right, non-dominant hemisphere. Although other factors such as lesion type, volume and location, age or time since stroke differed between the patients, none of these properties influenced the motor gains or post-intervention CMC changes as reported previously (Belardinelli et al., 2017).

Since the patients were unable to voluntary extend their fingers, performing this movement with robotic assistance and contingent to the respective MI allowed both activating and physiologically monitoring the related neural circuitry on a moment-to-moment basis. We report that the BMI intervention resembled in stroke patients the neurophysiological processes observed in healthy subjects: Operant conditioning of ERD in the cortical area targeted by the feedback; an increase of the

CMC magnitude in the course of the intervention; enhancement of the directed coherence from the cortex to the finger extensors.

Stroke patients differed, however, with regard to the cortical topography and involved frequency spectrum of the cortico-motor connectivity pattern from healthy subjects. Both ERD and CMC changes were not restricted to the feedback frequency in the beta band, but included the alpha frequency band as well. Consistently, cortical networks in the oscillatory alpha and beta band have been related to both BMI control (Buch et al., 2012, Vukelic et al., 2014, Bauer et al., 2015; Vukelic and Gharabaghi, 2015a,b) and post-stroke recovery (Dubovik et al., 2012; Westlake et al., 2012; Nicolo et al., 2015). Moreover, work in healthy subjects indicated that cortical oscillations in the alpha range are important for the selection of task-relevant cortical areas via the functional coupling of distant cortical regions (Başar et al., 1997; Palva and Palva, 2011; Pineda, 2005), as well as for suppression of task-irrelevant areas by inhibition (Jensen and Mazaheri, 2010; Klimeschet al., 2007). Furthermore, CMC in the alpha range has been shown to correlate with corticospinal excitability (Schulz et al., 2014), movement discontinuities (Gross et al., 2002) and transitions in force output with a time delay from muscle to cortex indicating afferent interactions (Mehrkanoon et al., 2014). One might speculate that the patients in our study relied in comparison to healthy subjects on a different mode of sensorimotor processing during integration of sensory reafference into the motor command to ensure maintenance of a stable output (Witham et al., 2011).

The cortical CMC topography of the patients group was, moreover, characterized by the extended bihemispheric involvement in the course of the intervention (figure 6A).Having in mind that not all post-stroke neuronal reorganization relates to functional restoration, CMC may nonetheless serve as a measure to detect functionally relevant efferent drive (Braun et al., 2007; Gerloff et

al., 2006a;b; Rossiter et al., 2013) and neural plasticity (von Carlowitz-Ghori et al., 2014; Belardinelli et al., 2017). Therefore, our observation of increased influence of non-primary motor areas over the finger extensors in the course of the intervention complements earlier reports of widespread changes of brain activity in patients with more severe impairment (Brown, 2008; Gerloff et al., 2006b; Serrien et al., 2004; Ward et al., 2003, Volz et al., 2015; Diekhoff-Krebset al., 2017, Belardinelli et al., 2017).

Furthermore, experimental work indicates the motor control system to maintain a variability of representations so that it can adapt to unpredictable changes (Peters et al., 2017); similarly, the descending corticospinal connectivity is known to be malleable (Brus-Ramer et al., 2007; Mosberger et al., 2017). In this context, our findings indicate that the amount of synchronization between cortical and spinal cord activity (Brown et al., 1998; Mima and Hallett, 1999; Salenius and Hari, 2003) during the execution of a (robot-assisted) movement will represent the task-relevant recruitment of the available corticospinal output after stroke and the corresponding motor network representation. This view is supported by cross-sectional and longitudinal structural (Koch et al., 2015) and functional magnetic resonance imaging (Grefkes and Fink, 2011, 2014) studies in stroke patients: Specifically, in chronic stroke patients damage to the descending output fibers from one region of the cortical motor system was compensated by activity in areas that retain corticofugal outputs, e.g., from secondary motor areas such as the dorsal premotor cortex (Newton et al., 2006; Riley et al., 2011; Schulz et al., 2012, 2015a,b; Potter-Baker et al., 2016).

Our findings support the observation that the contralesional hemisphere can act as a source of coherent descending cortical drive to functionally relevant muscles after stroke (Rossiter et al., 2013). Moreover, we provide empirical support that BMI

feedback may serve as a technique to enhance this connectivity. The directed coherence from cortex to periphery increased, however, in a restricted perilesional area of the affected hemisphere only. Specifically, training-related enhancement of beta-band CMC in the ipsilesional premotor cortex correlated with clinical improvements after the intervention. Future approached may directly address this biomarker by applying CMC feedback (von Carlowitz_Ghori et al., 2015) between this specific area and the targeted muscles. A shift of cortico-muscular coherence anteriorly and medially from the ipsilesional primary motor cortex has already been described in chronic stroke patients (Mima et al., 2001). This has led to the development of interventions that specifically target premotor areas with brain stimulation (Cunningham et al., 2015; Sankarasubramanian et al., 2017). Furthermore, inhibition of the dorsal premotor cortices in either hemisphere with magnetic stimulation disrupted motor performance in chronic stroke patients, but not in control subjects (Johansen-Berg et al., 2002; Fridman et al., 2004; Lotze et al., 2006), thereby implicating that these regions contribute to post-stroke motor recovery (Belardinelli et al., 2017).

Our findings are in accordance with recent work that applied *in vivo* two-photon calcium imaging in mice to longitudinally monitor the activity of corticospinal neuron populations across learning (Peters et al., 2017). This study revealed that corticospinal activity changed with time to create novel relationships between activity and movement, thereby, suggesting the corticospinal output itself (and not only intercortical circuits) to be plastic. Our results complement this work by demonstrating that learning related plastic reorganization of corticospinal out may be induced not only within the motor cortex but on a more distributed network level as well.

Limitations and future perspectives

Direct comparisons between the healthy subject and patient groups have to be made with caution due to apparent differences with regard to age, dose of intervention and motor evaluation. Bearing this in mind the BMI-related similarities are, however, remarkable. Specifically, the enhancement of cortico-muscular control seems to be a robust BMI-related phenomenon across groups. Future work may apply a dose-matched intervention in age-matched healthy subjects to better delineate physiological patterns related specifically to post-stroke reorganization. Moreover, source analysis may help to better describe possible generators of CMC beyond the primary motor cortex. Direct comparisons with magnetic resonance imaging metrics may, furthermore, allow a better understanding how structural determinants of connections interrelate with task-related functional connectivity measures (Koch et al., 2015).

The present study intended to elucidate neurophysiological mechanisms related to BMI feedback and not its impact on motor outcome improvement after stroke. This would have necessitated a controlled study design. The observed correlation of ipsilesional premotor beta-band CMC with clinical improvement might therefore be influenced by non-specific factors in the course of the training program.Previous BMI/BCI studies in stroke rehabilitation with a controlled designindicate,however, the importance of contingent feedback to achieve clinical benefits (Ramos-Murguialday et al., 2013; Pichiorri et al., 2015; Frolov et al., 2017). Here, we extended these observations by demonstrating – albeit in healthy subjects – that this feedback needed to be proprioceptive to enhance cortico-muscular control; the according pattern of CMC modulation, enhancement of directed coherence from cortex to finger extensors and corresponding motor improvements observed in healthy subjects was then replicated in stroke patients undergoing the same BMI

intervention. This provides empirical support for the consistency of the finding across different populations but needs to be replicated in controlled studies with larger patient cohorts and longer follow-up periods.Future work on patients with hand paralysis may, furthermore, consider capturing objectively, e.g., by sensors, even minimal motor improvements not detectable by clinical scores as well to better relate physiological changes to specific behavioral gains.

Conclusion

Operant conditioning of cortical oscillations with proprioceptive feedback enhances both cortical activity and behaviorally relevant connectivity to the periphery. This enhanced cortico-muscular control can be induced in the healthy and post-stroke brain. Thereby, activating the motor cortex with MI and closing the loop by robot-assisted natural feedback allows for sensorimotor integration beyond the lesioned corticospinal tract. This may facilitate neurorehabilitation in the absence of volitional muscle control.

References

Adamson J, Beswick A, Ebrahim S. Is stroke the most common cause of disability? J Stroke Cerebrovasc Dis 2004; 13:171-7.

Allman C, Amadi U, Winkler AM, Wilkins L, Filippini N, Kischka U, Stagg CJ, Johansen-Berg H. Ipsilesional anodal tDCS enhances the functional benefits of rehabilitation in patients after stroke. Sci Transl Med 2016; 8:330re1.

Ang KK, Guan C, Phua KS, Wang C, Zhou L, Tang KY, Ephraim Joseph GJ, Kuah CW, Chua KS. Brain-computer interface-based robotic end effector system for wrist and hand rehabilitation: results of a three-armed randomized controlled trial for chronic stroke. Front Neuroeng 2014; 7:30.

Ang KK, Guan C, Chua KS, Ang BT, Kuah C, Wang C, Phua KS, Chin ZY, Zhang H. Clinical study of neurorehabilitation in stroke using EEG-based motor imagery brain-computer interface with robotic feedback. Conf Proc IEEE Eng Med Biol Soc 2010; 2010:5549-52.

Aumann TD, Prut Y. Do sensorimotor β-oscillations maintain muscle synergy representations in primary motor cortex? Trends Neurosci 2015; 38:77-85.

Baker SN, Philbin N, Spinks R, Pinches EM, Wolpert DM, MacManus DG, Pauluis Q, Lemon RN. Multiple single unit recording in the cortex of monkeys using independently moveable microelectrodes. J Neurosci Methods 1999; 94:5-17.

Baker SN, Olivier E, Lemon RN. Coherent oscillations in monkey motor cortex and hand muscle EMG show task-dependent modulation. J Physiol 1997; 501:225-41.

Başar E, Schürmann M, Başar-Eroglu C, Karakaş S. Alpha oscillations in brain functioning: an integrative theory. Int J Psychophysiol. 1997; 26:5-29.

Bauer R, Fels M, Vukelić M, Ziemann U, Gharabaghi A. Bridging the gap between motor imagery and motor execution with a brain-robot interface. Neuroimage 2015; 108:319-27.

Bauer R, Gharabaghi A. Constraints and Adaptation of Closed-Loop Neuroprosthetics for Functional Restoration. Front Neurosci 2017;11:111.

Bayraktaroglu Z, von Carlowitz-Ghori K, Curio G, Nikulin VV. It is not all about phase: amplitude dynamics in corticomuscular interactions. Neuroimage 2013; 64:496-504.

Belardinelli P, Laer L, Ortiz E, Braun C, Gharabaghi A. Plasticity of premotor cortico-muscular coherence in severely impaired stroke patients with hand paralysis. Neuroimage Clin 2017; 14:726-33.

Berner J, Schönfeldt-Lecuona C, Nowak DA. Sensorimotor memory for fingertip forces during object lifting: the role of the primary motor cortex. Neuropsychologia 2007; 45:1931-8.

Boe S, Gionfriddo A, Kraeutner S, Tremblay A, Little G, Bardouille T. Laterality of brain activity during motor imagery is modulated by the provision of source level neurofeedback. Neuroimage 2014; 101:159-67.

Brauchle D, Vukelić M, Bauer R, Gharabaghi A. Brain state-dependent robotic reaching movement with a multi-joint arm exoskeleton: combining brain-machine interfacing and robotic rehabilitation. Front Hum Neurosci 2015; 9:564.

Braun C, Staudt M, Schmitt C, Preissl H, Birbaumer N, Gerloff C. Crossed cortico-spinal motor control after capsular stroke. Eur J Neurosci 2007; 25:2935-45.

Brown JA, Lutsep HL, Weinand M, Cramer SC. Motor cortex stimulation for the enhancement of recovery from stroke: a prospective, multicenter safety study. Neurosurgery 2008; 62 Suppl 2:853-62.

Brown P, Salenius S, Rothwell JC, Hari R. Cortical correlate of the Piper rhythm in humans. J Neurophysiol 1998; 80:2911-7.

Brus-Ramer M, Carmel JB, Chakrabarty S, Martin JH. Electrical stimulation of spared corticospinal axons augments connections with ipsilateral spinal motor circuits after injury. J Neurosci. 2007; 27:13793–801.

Buch ER, Modir Shanechi A, Fourkas AD, Weber C, Birbaumer N, Cohen LG. Parietofrontal integrity determines neural modulation associated with grasping imagery after stroke. Brain. 2012; 135:596-614.

Chouinard PA, Leonard G, Paus T. Role of the primary motor and dorsal premotor cortices in the anticipation of forces during object lifting. J Neurosci 2005; 25:2277-84.

Cunningham DA, Machado A, Janini D, Varnerin N, Bonnett C, Yue G, Jones S, Lowe M, Beall E, Sakaie K, Plow EB. Assessment of inter-hemispheric imbalance using imaging and noninvasive brain stimulation in patients with chronic stroke. Arch Phys Med Rehabil 2015; 96:S94-103.

Diekhoff-Krebs S, Pool EM, Sarfeld AS, Rehme AK, Eickhoff SB, Fink GR, Grefkes C. Interindividual differences in motor network connectivity and behavioral response to iTBS in stroke patients. Neuroimage Clin 2014;15:559-71.

Dobkin BH, Firestine A, West M, Saremi K, Woods R. Ankle dorsiflexion as an fMRI paradigm to assay motor control for walking during rehabilitation. Neuroimage 2004; 23:370-81.

Doyon J, Benali H. Reorganization and plasticity in the adult brain during learning of motor skills. Curr Opin Neurobiol. 2005; 15:161-7.

Dubovik S, Pignat JM, Ptak R, Aboulafia T, Allet L, Gillabert N, Magnin C, Albert F, Momjian-Mayor I, Nahum L, Lascano AM, Michel CM, Schnider A, Guggisberg AG. The behavioral significance of coherent resting-state oscillations after stroke. Neuroimage 2012; 61:249-57.

Feigin VL, Barker-Collo S, McNaughton H, Brown P, Kerse N. Long-term neuropsychological and functional outcomes in stroke survivors: current evidence and perspectives for new research. Int J Stroke 2008; 3:33-40.

Fridman EA, Hanakawa T, Chung M, Hummel F, Leiguarda RC, Cohen LG. Reorganization of the human ipsilesional premotor cortex after stroke. Brain 2004; 127:747-58.

Fries P. A mechanism for cognitive dynamics: neuronal communication through neuronal coherence. Trends Cogn Sci 2005; 9:474-80.

Frolov AA, Mokienko O, Lyukmanov R, Biryukova E, Kotov S, Turbina L, Nadareyshvily G, Bushkova Y. Post-stroke Rehabilitation Training with a Motor-Imagery-Based Brain-Computer Interface (BCI)-Controlled Hand Exoskeleton: A Randomized Controlled Multicenter Trial. Front Neurosci 2017;11:400.

Gao Q, Duan X, Chen H. Evaluation of effective connectivity of motor areas during motor imagery and execution using conditional Granger causality. Neuroimage 2011; 54:1280-8.

Gerloff C, Braun C, Staudt M, Hegner YL, Dichgans J, Krägeloh-Mann I. Coherent corticomuscular oscillations originate from primary motor cortex: evidence from patients with early brain lesions. Hum Brain Mapp 2006; 27:789-98.

Gerloff C, Bushara K, Sailer A, Wassermann EM, Chen R, Matsuoka T, Waldvogel D, Wittenberg GF, Ishii K, Cohen LG, Hallett M. Multimodal imaging of brain reorganization in motor areas of the contralesional hemisphere of well recovered patients after capsular stroke. Brain 2006; 129:791-808.

Gharabaghi A., Kraus D., Leão MT, Spüler M, Walter A, Bogdan, M., Rosenstiel W, Naros G, Ziemann U. Coupling brain–machine interfaces with cortical stimulation for brain-state dependent stimulation: enhancing motor cortex excitability for neurorehabilitation. Front Hum Neurosci 2014; 8:122.

Grefkes C, Fink GR. Connectivity-based approaches in stroke and recovery of function. Lancet Neurol 2014; 13:206-16.

Grefkes C, Fink GR. Reorganization of cerebral networks after stroke: new insights from neuroimaging with connectivity approaches. Brain 2011; 134:1264-76.

Grimm F. Naros G. Gharabaghi A.Compensation or restoration: closed-loop feedback of movement quality for assisted reach-to-grasp exercises with a multijoint arm exoskeleton. Front Neurosci 2016; 10.

Cárdenas-Morales L, Volz LJ, Michely J, Rehme AK, Pool EM, Nettekoven C, Eickhoff SB, Fink GR, Grefkes C. Network connectivity and individual responses to brain stimulation in the human motor system. Cereb Cortex 2014; 24:1697-707.

Gross J, Timmermann L, Kujala J, Dirks M, Schmitz F, Salmelin R, Schnitzler A. The neural basis of intermittent motor control in humans. Proc Natl Acad Sci USA 2002; 99:2299-302.

Halliday DM, Conway BA, Farmer SF, Rosenberg JR. Using electroencephalography to study functional coupling between cortical activity and electromyograms during voluntary contractions in humans. Neurosci Lett 1998; 241:5-8.

Halsband U, Lange RK. Motor learning in man: a review of functional and clinical studies. J Physiol Paris 2006; 99:414-24.

Hayward KS, Brauer SG, Ruddy KL, Lloyd D, Carson RG. Repetitive reaching training combined with transcranial Random Noise Stimulation in stroke survivors with chronic and severe arm paresis is feasible: a pilot, triple-blind, randomised case series. J Neuroeng Rehabil 2017;14:46.

He SQ, Dum RP, Strick PL. Topographic organization of corticospinal projections from the frontal lobe: motor areas on the lateral surface of the hemisphere. J Neurosci 1993;13:952-80.

Hebb DO. The Organization of Behavior: A Neuropsychological Theory. New 629 York:Wiley 1949.

Houweling S, van Dijk BW, Beek PJ, Daffertshofer A. Cortico-spinal synchronization reflects changes in performance when learning a complex bimanual task. Neuroimage 2010; 49:3269-75.

Jensen O, Mazaheri A. Shaping functional architecture by oscillatory alpha activity: gating by inhibition. Front Hum Neurosci 2010; 4:186.

Johansen-Berg H, Dawes H, Guy C, Smith SM, Wade DT, Matthews PM. Correlation between motor improvements and altered fMRI activity after rehabilitative therapy. Brain 2002; 125:2731-42.

Jørgensen HS, Reith J, Nakayama H, Kammersgaard LP, Raaschou HO, Olsen TS. What determines good recovery in patients with the most severe strokes? The Copenhagen Stroke Study. Stroke. 1999; 30:2008-12.

Kim B, Winstein C. Can Neurological Biomarkers of Brain Impairment Be Used to Predict Poststroke Motor Recovery? A Systematic Review. Neurorehabil Neural Repair 2017; 31:3-24.

Klimesch W, Sauseng P, Hanslmayr S, Gruber W, Freunberger R. Event-related phase reorganization may explain evoked neural dynamics. Neurosci Biobehav Rev. 2007; 31:1003-16.

Klamroth-Marganska V, Blanco J, Campen K, Curt A, Dietz V, Ettlin T, Felder M, Fellinghauer B, Guidali M, Kollmar A, Luft A, Nef T, Schuster-Amft C, Stahel W, Riener R. Three-dimensional, task-specific robot therapy of the arm after stroke: a multicentre, parallel-group randomised trial. Lancet Neurol 2014; 13:159-66.

Koch MW, Greenfield J, Javizian O, Deighton S, Wall W, Metz LM. The natural history of early versus late disability accumulation in primary progressive MS. J Neurol Neurosurg Psychiatry 2015; 86:615-21.

Kombos T, Suess O, Kern BC, Funk T, Hoell T, Kopetsch O, Brock M. Comparison between monopolar and bipolar electrical stimulation of the motor cortex. Acta Neurochir (Wien) 1999;141:1295-301.

Krakauer JW, Marshall RS. The proportional recovery rule for stroke revisited. Ann Neurol 2015; 78:845-7.

Kraus D, Gharabaghi A. Projecting Navigated TMS Sites on the Gyral Anatomy Decreases Inter-subject Variability of Cortical Motor Maps. Brain Stimul 2015; 8:831-7.

Kraus D, Gharabaghi A. Neuromuscular Plasticity: Disentangling Stable and Variable Motor Maps in the Human Sensorimotor Cortex. Neural Plast 2016; 2016:7365609.

Kraus D, Naros G, Bauer R, Leão MT, Ziemann U, Gharabaghi A. Brain-robot interface driven plasticity: Distributed modulation of corticospinal excitability. Neuroimage 2016a;125:522-532.

Kraus D, Naros G, Bauer R, Khademi F, Leão MT, Ziemann U, Gharabaghi A. Brain State-Dependent Transcranial Magnetic Closed-Loop Stimulation Controlled by Sensorimotor Desynchronization Induces Robust Increase of Corticospinal Excitability. Brain Stimul 2016b; 9:415-424.

Kristeva R, Patino L, Omlor W. Beta-range cortical motor spectral power and corticomuscular coherence as a mechanism for effective corticospinal interaction during steady-state motor output. Neuroimage 2007; 36:785-92.

Kristeva-Feige R, Fritsch C, Timmer J, Lücking CH.Effects of attention and precision of exerted force on beta range EEG-EMG synchronization during a maintained motor contraction task. Clin Neurophysiol 2002; 113:124-31.

Kwakkel G, Meskers CG, van Wegen EE, Lankhorst GJ, Geurts AC, van Kuijk AA, Lindeman E, Visser-Meily A, de Vlugt E, Arendzen JH. Impact of early applied upper limb stimulation: the EXPLICIT-stroke programme design. BMC Neurol 2008; 8:49.

Langhorne P, Bernhardt J, Kwakkel G. Stroke rehabilitation. Lancet 2011; 377:1693-702.

Loh MN, Kirsch L, Rothwell JC, Lemon RN, Davare M. Information about the weight of grasped objects from vision and internal models interacts within the primary motor cortex. J Neurosci 2010; 30:6984-90.

Lo AC, Guarino PD, Richards LG, Haselkorn JK, Wittenberg GF, Federman DG, Ringer RJ, Wagner TH, Krebs HI, Volpe BT, Bever CT Jr, Bravata DM, Duncan PW, Corn BH, Maffucci AD, Nadeau SE, Conroy SS, Powell JM,

Huang GD, Peduzzi P. Robot-assisted therapy for long-term upper-limb impairment after stroke. N Engl J Med 2010; 362:1772-83.

Lotze M, Markert J, Sauseng P, Hoppe J, Plewnia C, Gerloff C. The role of multiple contralesional motor areas for complex hand movements after internal capsular lesion. J Neurosci 2006; 26:6096-102.

Maris E, Schoffelen JM, Fries P. Nonparametric statistical testing of coherence differences. J Neurosci Methods 2007; 163:161-75.

Mathew J, Kübler A, Bauer R, Gharabaghi A. Probing Corticospinal Recruitment Patterns and Functional Synergies with Transcranial Magnetic Stimulation. Front Cell Neurosci 2016; 10:175.

McFarland DJ and Wolpaw JR.Sensorimotor rhythm-based brain–computer interface (BCI): feature selection by regression improves performance IEEE Trans. Neural Syst. Rehabil Eng 2005; 13 372–9

McMorland AJ, Runnalls KD, Byblow WD. A neuroanatomical framework for upper limb synergies after stroke. Front Hum Neurosci. 201; 9:82.

Mehrkanoon S, Breakspear M, Boonstra TW. The reorganization of corticomuscular coherence during a transition between sensorimotor states. Neuroimage 2014; 100:692-702.

Mendez-Balbuena I, Huethe F, Schulte-Mönting J, Leonhart R, Manjarrez E, Kristeva R. Corticomuscular coherence reflects interindividual differences in the state of the corticomuscular network during low-level static and dynamic forces. Cereb Cortex 2012; 22:628-38.

Mima T, Hallett M. Electroencephalographic analysis of cortico-muscular coherence: reference effect, volume conduction and generator mechanism. Clin Neurophysiol 1999;110:1892-9.

Mima T, Toma K, Koshy B, Hallett M. Coherence between cortical and muscular activities after subcortical stroke. Stroke 2001; 32:2597-601.

Mima T, Matsuoka T, Hallett M. Functional coupling of human right and left cortical motor areas demonstrated with partial coherence analysis. Neurosci Lett 2000; 287:93-6.

Mosberger AC, Miehlbradt JC, Bjelopoljak N, Schneider MP, Wahl AS, Ineichen BV, Gullo M, Schwab ME. Axotomized Corticospinal Neurons Increase Supra-Lesional Innervation and Remain Crucial for Skilled Reaching after Bilateral Pyramidotomy. Cereb Cortex 2017;

Mrachacz-Kersting N, Kristensen SR, Niazi IK, Farina D. Precise temporal association between cortical potentials evoked by motor imagination and afference induces cortical plasticity. J Physiol 2012; 590:1669-82.

Mrachacz-Kersting N, Jiang N, Stevenson AJ, Niazi IK, Kostic V, Pavlovic A, Radovanovic S, Djuric-Jovicic M, Agosta F, Dremstrup K, Farina D. Efficient

neuroplasticity induction in chronic stroke patients by an associative brain-computer interface.J Neurophysiol 2016; 115:1410-21.

Murphy TH, Corbett D. Plasticity during stroke recovery: from synapse to behaviour. Nat Rev Neurosci 2009; 10:861-72.

Murthy VN, Fetz EE. Coherent 25- to 35-Hz oscillations in the sensorimotor cortex of awake behaving monkeys. Proc Natl Acad Sci USA 1992; 89:5670-4.

Naros G, Gharabaghi A. Reinforcement learning of self-regulated β-oscillations for motor restoration in chronic stroke. Front Hum Neurosci 2015; 9:391.

Naros G, Naros I, Grimm F, Ziemann U, Gharabaghi A. Reinforcement learning of self-regulated sensorimotor β-oscillations improves motor performance. Neuroimage. 2016; 134:142-152.

Newton JM, Ward NS, Parker GJ, Deichmann R, Alexander DC, Friston KJ, Frackowiak RS.Non-invasive mapping of corticofugal fibres from multiple motor areas--relevance to stroke recovery. Brain 2006; 129:1844-58.

Nicolo P, Rizk S, Magnin C, Pietro MD, Schnider A, Guggisberg AG.Coherent neural oscillations predict future motor and language improvement after stroke. Brain 2015; 138:3048-60.

Nikulin VV, Nolte G, Curio G.A novel method for reliable and fast extraction of neuronal EEG/MEG oscillations on the basis of spatio-spectral decomposition. Neuroimage 2011; 55:1528-35.

Nowak DA, Voss M, Huang YZ, Wolpert DM, Rothwell JC.High-frequency repetitive transcranial magnetic stimulation over the hand area of the primary motor cortex disturbs predictive grip force scaling. Eur J Neurosci 2005; 22:2392-6.

Nuttall A. Some windows with very good sidelobe behavior. IEEE Trans Acoust 1981;29:84–91.

Oldfield RC. The assessment and analysis of handedness: the Edinburgh inventory. Neuropsychologia 1971; 9:97–113.

Omlor W, Patino L, Mendez-Balbuena I, Schulte-Moenting J, Kristeva R. Corticospinal beta-range coherence is highly dependent on the pre-stationary motor state. J Neurosci2011; 31:8037-45.

Palva S, Palva JM. Functional roles of alpha-band phase synchronization in local and large-scale cortical networks. Front Psychol 2011; 2:204.

Peters S, Wadden KP, Hayward KS, Neva JL, Auriat AM, Boyd LA. A structural motor network correlates with motor function and not impairment post stroke. Neurosci Lett 2017; 658:155-160.

Pichiorri F, Morone G, Petti M, Toppi J, Pisotta I, Molinari M, Paolucci S, Inghilleri M, Astolfi L, Cincotti F, Mattia D. Brain-computer interface boosts motor imagery practice during stroke recovery. Ann Neurol 2015; 77:851-65.

Pineda JA. The functional significance of mu rhythms: translating "seeing" and "hearing" into "doing". Brain Res Brain Res Rev 2005; 50:57-68.

Potter-Baker KA, Varnerin NM, Cunningham DA, Roelle SM, Sankarasubramanian V, Bonnett CE, Machado AG, Conforto AB, Sakaie K, Plow EB. Influence of Corticospinal Tracts from Higher Order Motor Cortices on Recruitment Curve Properties in Stroke. Front Neurosci 2016; 10:79.

Ramos-Murguialday A, Broetz D, Rea M, Läer L, Yilmaz O, Brasil FL, Liberati G, Curado MR, Garcia-Cossio E, Vyziotis A, Cho W, Agostini M, Soares E, Soekadar S, Caria A, Cohen LG, Birbaumer N. Brain-machine interface in chronic stroke rehabilitation: a controlled study. Ann Neurol 2013; 74:100-8.

Riley JD, Le V, Der-Yeghiaian L, See J, Newton JM, Ward NS, Cramer SC. Anatomy of stroke injury predicts gains from therapy. Stroke 2011; 42:421-6.

Rossiter HE, Worthen SF, Witton C, Hall SD, Furlong PL. Gamma oscillatory amplitude encodes stimulus intensity in primary somatosensory cortex. Front Hum Neurosci 2013; 7:362.

Royter V, Gharabaghi A. Brain State-Dependent Closed-Loop Modulation of Paired Associative Stimulation Controlled by Sensorimotor Desynchronization. Front Cell Neurosci 2016;10:115.

Salenius S, Hari R. Synchronous cortical oscillatory activity during motor action. Curr Opin Neurobiol 2003;13:678-84.

Sankarasubramanian V, Machado AG, Conforto AB, Potter-Baker KA, Cunningham DA, Varnerin NM, Wang X, Sakaie K, Plow EB. Inhibition versus facilitation of contralesional motor cortices in stroke: Deriving a model to tailor brain stimulation. Clin Neurophysiol 2017;1 28:892-902.

Schalk G, McFarland DJ, Hinterberger, T, BirbaumerN,Wolpaw JR. BCI2000: a general-purposebrain–computerinterface (BCI) system. IEEE Trans Biomed Eng 2004; 51:1034–43.

Schulz R, Park CH, Boudrias MH, Gerloff C, Hummel FC, Ward NS.Assessing the integrity of corticospinal pathways from primary and secondary cortical motor areas after stroke.Stroke 2012; 43:2248-51.

Schulz H, Ubelacker T, Keil J, Müller N, Weisz N. Now I am ready-now i am not: The influence of pre-TMS oscillations and corticomuscular coherence on motor-evoked potentials. Cereb Cortex 2014; 24:1708-19.

Schulz R, Koch P, Zimerman M, Wessel M, Bönstrup M, Thomalla G, Cheng B, Gerloff C, Hummel FC. Parietofrontal motor pathways and their association with motor function after stroke. Brain 2015a; 138:1949-60.

Schulz R, Braass H, Liuzzi G, Hoerniss V, Lechner P, Gerloff C, Hummel FC.White matter integrity of premotor-motor connections is associated with motor output in chronic stroke patients. Neuroimage Clin 2015b; 7:82-6.

Schmidt S, Fleischmann R, Bathe-Peters R, Irlbacher K, Brandt SA. Evolution of premotor cortical excitability after cathodal inhibition of the primary motor

cortex: a sham-controlled serial navigated TMS study. PLoS One 2013; 8:e57425.

Serrien DJ, Strens LH, Cassidy MJ, Thompson AJ, Brown P. Functional significance of the ipsilateral hemisphere during movement of the affected hand after stroke. Exp Neurol 2004; 190:425-32.

Sitaram R, Ros T, Stoeckel L, Haller S, Scharnowski F, Lewis-Peacock J, Weiskopf N, Blefari ML, Rana M, Oblak E, Birbaumer N, Sulzer J. Closed-loop brain training: the science of neurofeedback. Nat Rev Neurosci 2017; 18:86-100.

Stinear CM, Barber PA, Smale PR, Coxon JP, Fleming MK, Byblow WD. Functional potential in chronic stroke patients depends on corticospinal tract integrity. Brain 2007; 130:170-80.

Stinear CM, Barber PA, Petoe M, Anwar S, Byblow WD. The PREP algorithm predicts potential for upper limb recovery after stroke. Brain 2012; 135:2527-35.

Szameitat AJ, McNamara A, Shen S, Sterr A. Neural activation and functional connectivity during motor imagery of bimanual everyday actions. PLoS One 2012; 7:e38506.

Takemi M, Masakado Y, Liu M, Ushiba J. Event-related desynchronization reflects downregulation of intracortical inhibition in human primary motor cortex. J Neurophysiol 2013;110:1158-66.

Teitti S, Määttä S, Säisänen L, Könönen M, Vanninen R, Hannula H, Mervaala E, Karhu J. Non-primary motor areas in the human frontal lobe are connected directly to hand muscles. Neuroimage 2008; 40:1243-50.

Thut G, Miniussi C. New insights into rhythmic brain activity from TMS-EEG studies. Trends Cogn Sci 2009;13:182-9.

Volz LJ, Eickhoff SB, Pool EM, Fink GR, Grefkes C. Differential modulation of motor network connectivity during movements of the upper and lower limbs. Neuroimage. 2015; 119:44-53.

Volz LJ, Rehme AK, Michely J, Nettekoven C, Eickhoff SB, Fink GR, Grefkes C. Shaping Early Reorganization of Neural Networks Promotes Motor Function after Stroke. Cereb Cortex 2016; 26:2882-94.

von Carlowitz-Ghori K, Bayraktaroglu Z, Hohlefeld FU, Losch F, Curio G, Nikulin VV.Corticomuscular coherence in acute and chronic stroke. Clin Neurophysiol 2014; 125:1182-91.

von Carlowitz-Ghori K, Bayraktaroglu Z, Waterstraat G, Curio G, Nikulin VV. Voluntary control of corticomuscular coherence through neurofeedback: a proof-of-principle study in healthy subjects. Neuroscience 2015; 290:243-54.

Vukelić M, Gharabaghi A. Oscillatory entrainment of the motor cortical network during motor imagery is modulated by the feedback modality. Neuroimage. 2015a;111:1-11.

Vukelić M, Gharabaghi A. Self-regulation of circumscribed brain activity modulates spatially selective and frequency specific connectivity of distributed resting state networks. Front Behav Neurosci. 2015b; 9:181.

Vukelić M, Bauer R, Naros G, Naros I, Braun C, Gharabaghi A. Lateralized alpha-band cortical networks regulate volitional modulation of beta-band sensorimotor oscillations. Neuroimage 2014; 87:147-53.

Ward NS, Frackowiak RS. Age-related changes in the neural correlates of motor performance. Brain 2003; 126:873-88.

Ward NS, Newton JM, Swayne OB, Lee L, Thompson AJ, Greenwood RJ, Rothwell JC, Frackowiak RS. Motor system activation after subcortical stroke depends on corticospinal system integrity. Brain 2006;129:809-19.

Ward NS, Newton JMv , Swayne OB, Lee L, Frackowiak RS, Thompson AJ, Greenwood RJ, Rothwell JC. The relationship between brain activity and peak grip force is modulated by corticospinal system integrity after subcortical stroke. Eur J Neurosci 2007; 25:1865-73.

Westlake KP, Hinkley LB, Bucci M, Guggisberg AG, Byl N, Findlay AM, Henry RG, Nagarajan SS. Resting state α-band functional connectivity and recovery after stroke. Exp Neurol 2012; 237:160-9.

Witham CL, Riddle CN, Baker MR, Baker SN. Contributions of descending and ascending pathways to corticomuscular coherence in humans. J Physiol 2011; 589:3789-800.

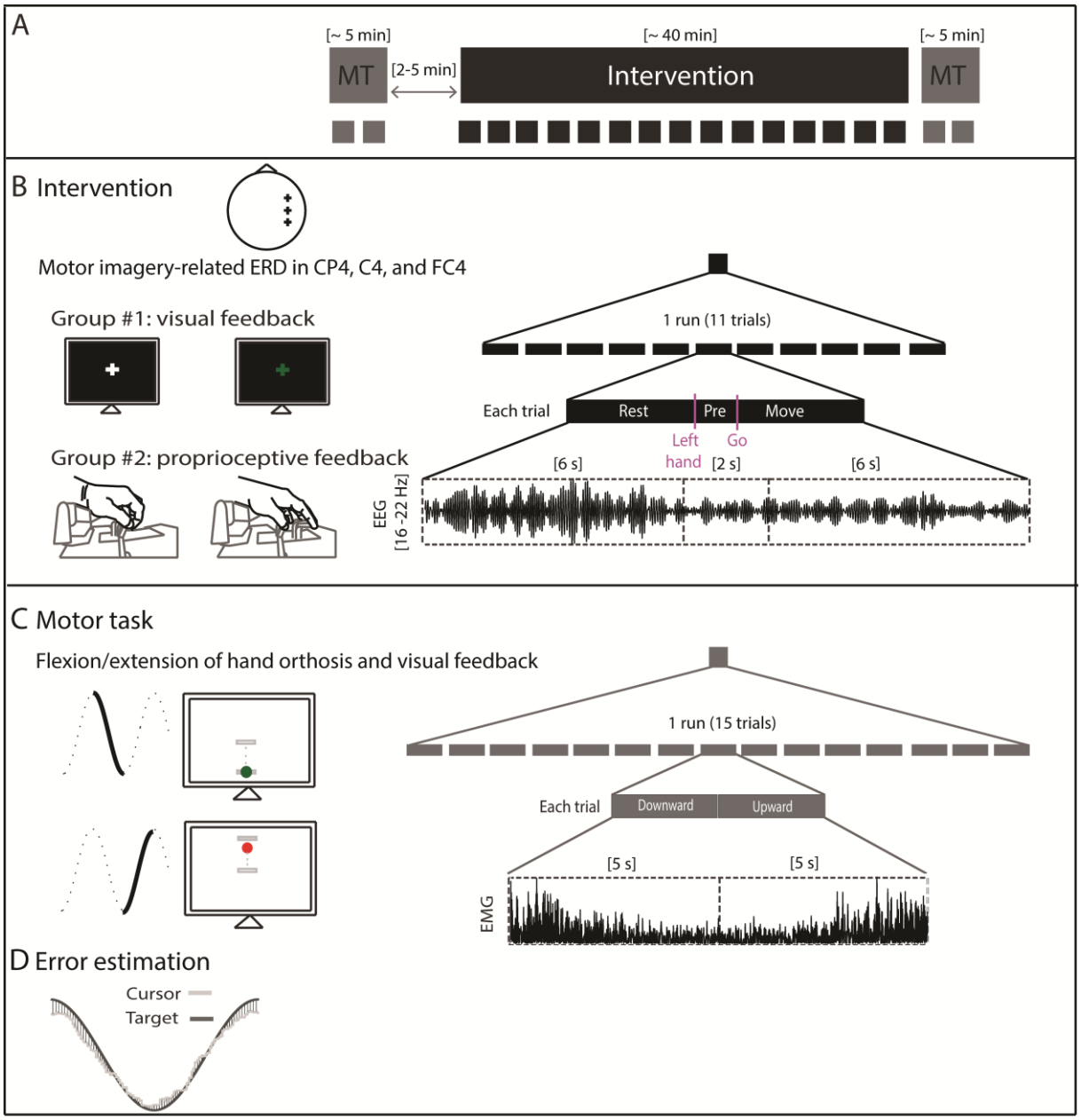

Figure 1 Experimental design and example data.(**A**) Schematic illustration of the experimental design and timeline. (**B**)Participants (healthy subjects and patients) underwent a neurofeedback intervention of modulating beta-activity (16-22 Hz) in circumscribed premotor and sensorimotor regions (marked by '+' on the topography) of the right (i.e. ipsilesional in stroke patients) hemisphere by kinesthetic motor imagery (MI). Healthy participants participated in an intervention session (~40 minutes) receiving feedback which was contingent to their MI-associated brain activity in a parallel-group design with one of two different modalities: (I) visual feedback with a brain–computer interface (BCI; n=12) or (II) proprioceptive feedback with a brain–machine interface (BMI; n=15) orthosis attached to the left hand. In a subsequent study with stroke patients (n=8), proprioceptive BMI-feedback was

applied to the paralyzed left hand in 20 sessions the course of four weeks. (**C**)Healthy subjects performed a motor task (~5 minutes) before (pre-MT) and after (post-MT) the intervention. An oscillating target (0.1 Hz) was presented to the subjects on a screen. The subject was instructed to follow the target by a cursor which was controlled by isometric flexion and extension of the left hand that was attached to a hand orthosis. (**D**) Motor performance was defined as the difference between target and actual force applied to the hand orthosis which was paralleled by a deviation between the target and the actual oscillation on the screen, i.e. the closer the target and the actual oscillation, the better the performance.

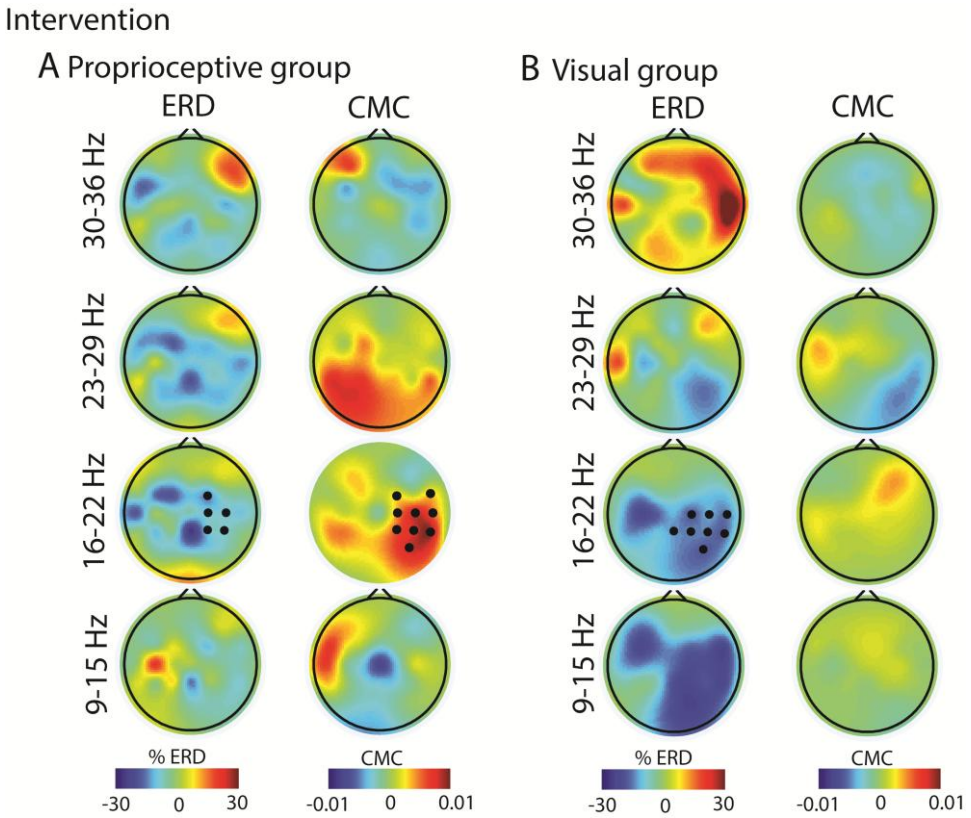

Figure 2 Modulation of motor imagery-related event-related desynchronization (ERD) and corticomuscular coherence (CMC).(**A**)Group data of the proprioceptive group in healthy subjects. Black circles indicate clusters with statistically significant modulation (nonparametric randomization test) in the course of the intervention (the contrast between end and start, see methods). Cortical topographies are presented for the feedback frequency band (16-22 Hz) and the neighboring bands (9-15 Hz, 23-29 Hz, and 30-36 Hz). (**B**) same as **A** but for the visual group.

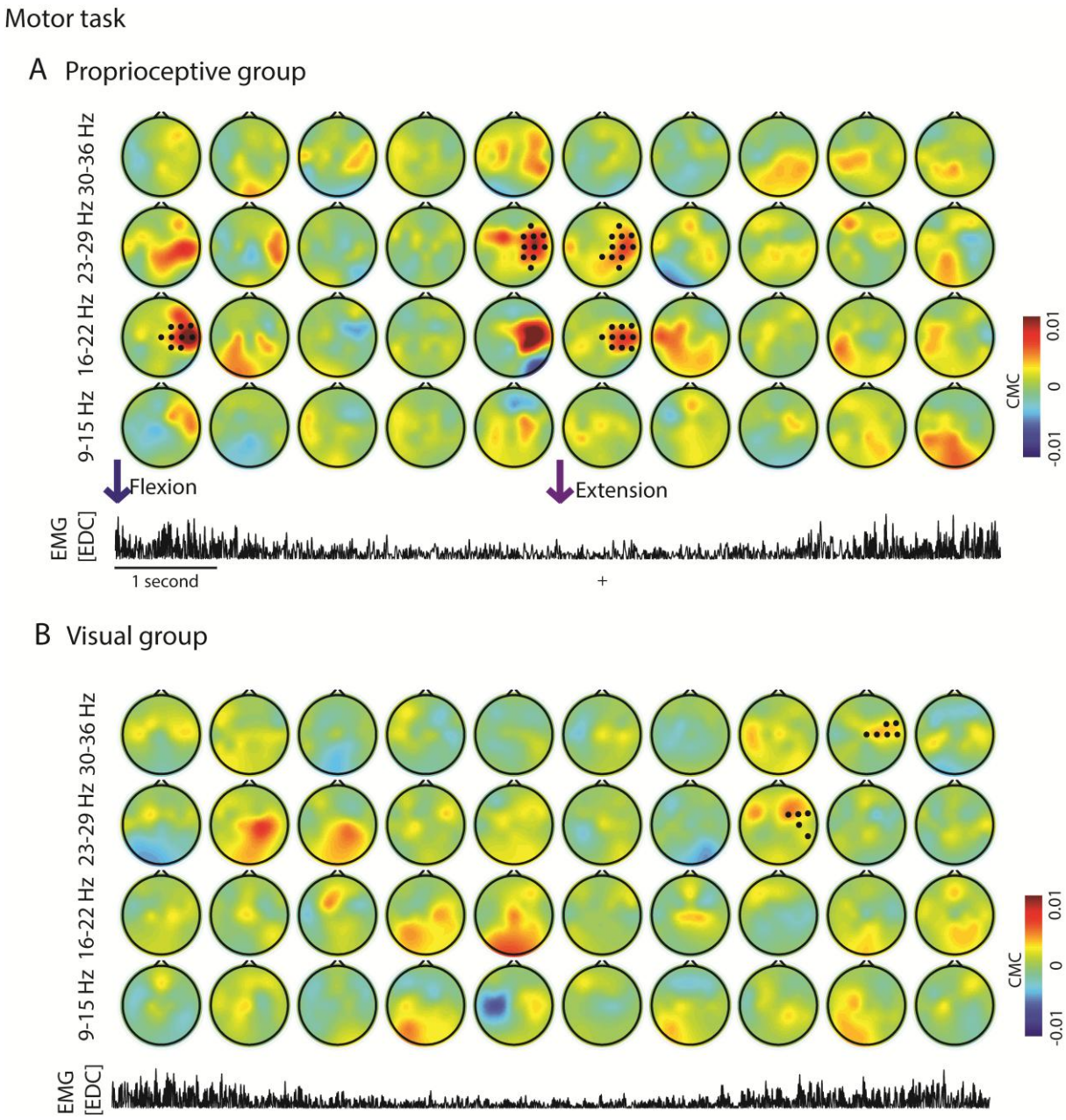

Figure 3 Modulation of motor task-related corticomuscular coherence (CMC).(**A**)Group data of the proprioceptive group in healthy subjects. Black circles indicate clusters with statistically significant modulation (nonparametric cluster-based randomization test) in the course of the experiment (the contrast between post-MT vs. pre-MT). Cortical topographies are presented across the motor task in 1-second intervals, i.e. during flexion (F1-F5) and extension (E1-E5), for the feedback frequency band (16-22 Hz) and the neighboring bands (9-15 Hz, 23-29 Hz, and 30-36 Hz). Transitions of the motor task are marked with arrows (blue: *flexion to extension*; purple: *extension to flexion*). The grand-average of the EMG of the EDC

muscle across all subjects is plotted below the topographies. (**B**) same as **A** but for the visual group.

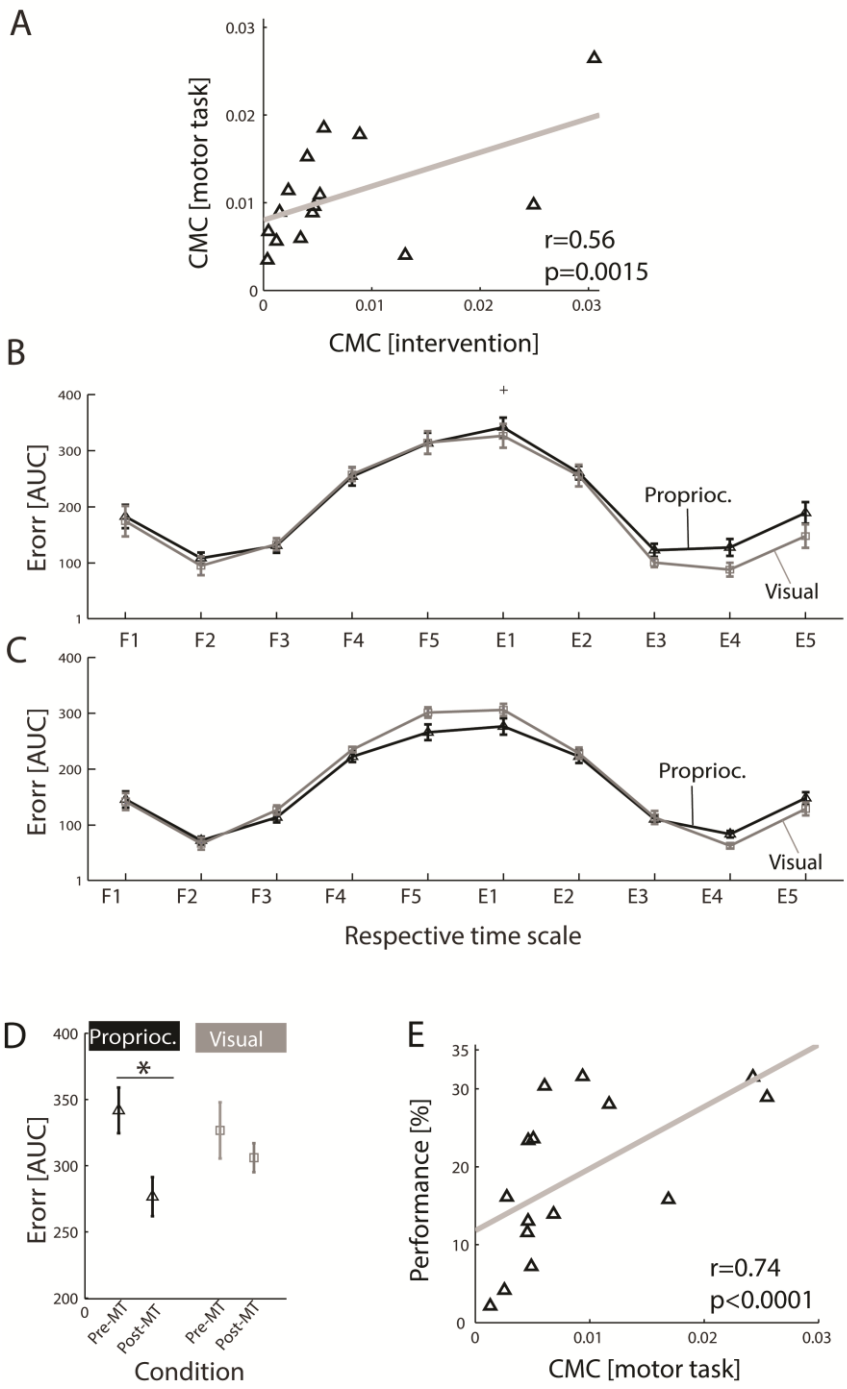

Figure 4 Modulation of corticomuscular coherence (CMC) correlates with behavioral gains.(**A**)Group data of the proprioceptive group in healthy subjects. The increase of CMC (16-22 Hz) in the course of the intervention correlates with the (post vs. pre) CMC increase (16-22 Hz) during the *flexion to extension* transition of the motor task (r=0.56, p=0.0015, Spearman's rank correlation, randomization test); each triangle represents one subject. The regression line is represented in gray.(**B**)Error estimation (mean and standard error) across the motor task (pre-intervention) in 1-second intervals, i.e. during flexion (F1-F5) and extension (E1-E5). E1 represents the

interval with the maximum error (i.e. the transition from *flexion to extension*). (**C**) Same as **B** but for the post-intervention motor task. (**D**) The proprioceptive group showed a statistically significant decrease of error ($t(28)=-2.87$, $p=0.008$, unpaired t-test, potshot test after performing ANOVA) during the motor task (i.e. improved performance) for the interval with the maximum error (i.e., E1). (**E**)That improved performance correlated significantly with the increase in CMC magnitude (16-22 Hz; $r=0.74$ $p<0.0001$, Spearman's rank correlation, randomization test). Each triangle represents one subject. The regression line is represented in gray.

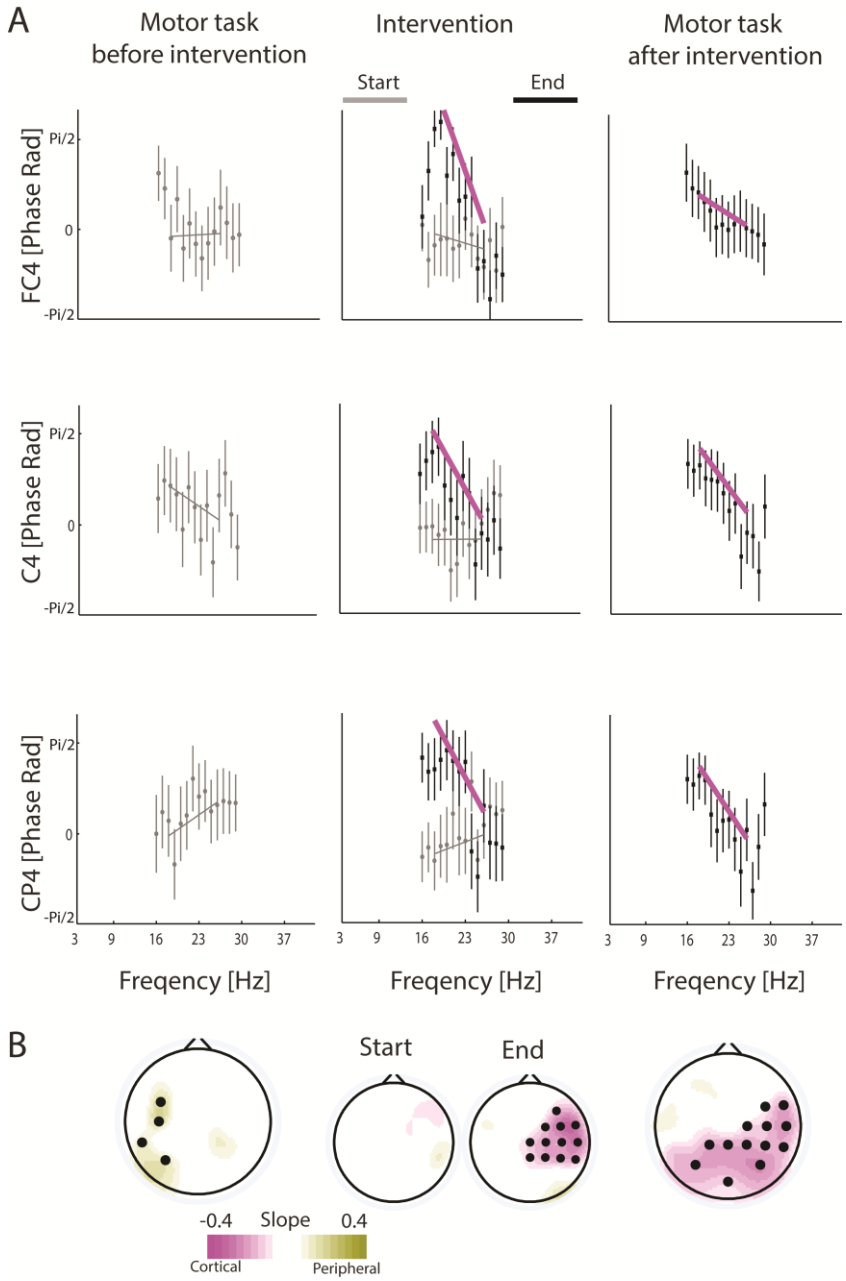

Figure 5 Changed directionality of corticomuscular coherence (CMC). (**A**) Phase-frequency plots of healthy subjects in the proprioceptive group (mean and standard error) for the EEG feedback channels (FC4, C4, and CP4) and frequencies with significant CMC modulation. Left and right columns represent the motor task-related finding before (gray) and after (black) the intervention, respectively. The middle column represents the intervention-related findings at the start (gray) and end (black) of the intervention, respectively. The regression slopes for the frequency band between 18-26 Hz are represented by lines; this frequency band was determined by a change of the sign of the regression slope. Regression slopes significantly different from zero are indicated by magenta. (**B**) Topographies of the respective regression slopes. Magenta and yellow colors indicate the directionality of information flow from

cortex to the periphery and from peripheral to the cortex, respectively. Black circles represent the EEG channels which have a regression slope that is significantly different from zero.

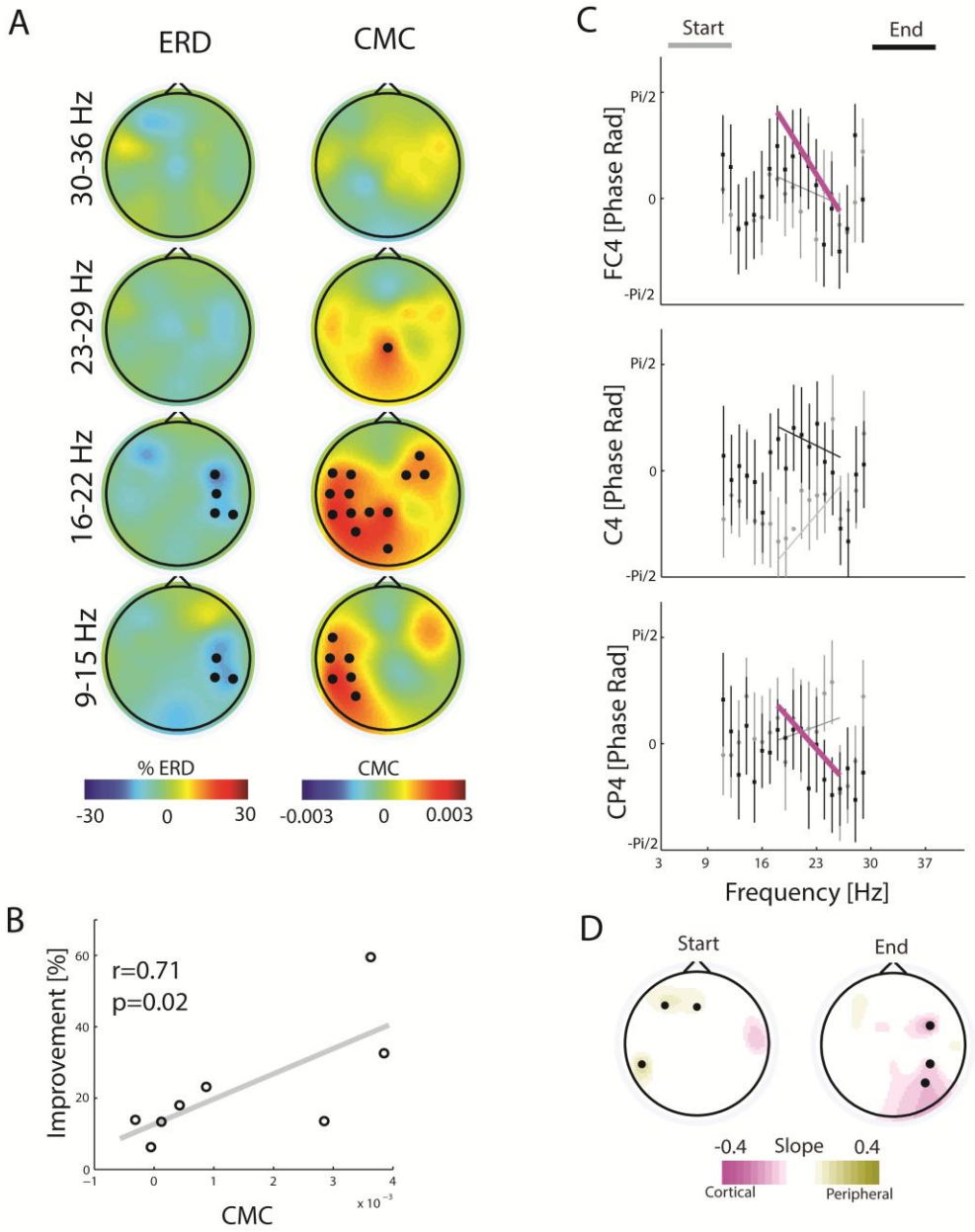

Figure 6 Modulation of corticomuscular coherence (CMC) correlates with motor improvement in stroke patients. (**A**)Modulation of motor imagery-related event-related desynchronization (ERD) and corticomuscular coherence (CMC).Group data of stroke patients with proprioceptive BMI-feedback. Black circles indicate clusters with statistically significant modulation (randomization test) in the course of the intervention (the contrast between end and start, see methods). Cortical topographies are presented for the feedback frequency band (16-22 Hz) and the neighboring bands (9-15 Hz, 23-29 Hz, and 30-36 Hz). (**B**) The relationship between improvement in the Fugl-Meyer-Assessment score and the CMC modulation (16-22 Hz; F4, FC2, and FC4 channels). Each circle represents one patient. The regression line is represented in gray (r=0.71 p=0.02 Spearsman's rank correlation,

randomization test). (**C**) Phase-frequency plots (mean and standard error) for the EEG feedback channels (FC4, C4, and CP4) and frequencies with significant CMC modulation at the start (gray) and end (black) of the intervention, respectively. The regression slopes for the frequency band between 18-26 Hz are represented by lines; this frequency band was determined by a change of the sign of the regression slope. Regression slopes significantly different from zero are indicated by magenta. (**D**) Topographies of the respective regression slopes. Magenta and yellow colors indicate the directionality of information flow from cortex to the periphery and from peripheral to the cortex, respectively. Black circles represent the EEG channels which have a regression slope that is significantly different from zero.

Brain Stimulation 9 (2016) 415–424

Contents lists available at ScienceDirect

Brain Stimulation

journal homepage: www.brainstimjrnl.com

Brain State-Dependent Transcranial Magnetic Closed-Loop Stimulation Controlled by Sensorimotor Desynchronization Induces Robust Increase of Corticospinal Excitability

Dominic Kraus [a], Georgios Naros [a], Robert Bauer [a], Fatemeh Khademi [a], Maria Teresa Leão [a], Ulf Ziemann [b], Alireza Gharabaghi [a,*]

[a] Division of Functional and Restorative Neurosurgery, and Centre for Integrative Neuroscience, Eberhard Karls University, Tuebingen, Germany
[b] Department of Neurology and Stroke, and Hertie Institute for Clinical Brain Research, Eberhard Karls University, Tuebingen, Germany

ARTICLE INFO

Article history:
Received 27 July 2015
Received in revised form 1 February 2016
Accepted 10 February 2016
Available online 16 February 2016

Keywords:
Event-related desynchronization
Motor cortex plasticity
Sensorimotor rhythm
Beta-band
Brain–computer interface
Brain state-dependent stimulation
Closed-loop stimulation

ABSTRACT

Background: Desynchronization of sensorimotor rhythmic activity increases instantaneous corticospinal excitability, as indexed by amplitudes of motor-evoked potentials (MEP) elicited by transcranial magnetic stimulation (TMS). The accumulative effect of cortical stimulation in conjunction with sensorimotor desynchronization is, however, unclear.
Objective: The aim of this study was to investigate the effects of repetitive pairing event-related desynchronization (ERD) with TMS of the precentral gyrus on corticospinal excitability.
Methods: Closed-loop single-pulse TMS was controlled by beta-band (16–22 Hz) ERD during motor-imagery of finger extension and applied within a brain–computer interface environment in eleven healthy subjects. The same number and pattern of stimuli were applied in a control group of eleven subjects during rest, i.e. independent of ERD. To probe for plasticity resistant to depotentiation, stimulation protocols were followed by a depotentiation task.
Results: Brain state-dependent application of approximately 300 TMS pulses during beta-ERD resulted in a significant increase of corticospinal excitability. By contrast, the identical stimulation pattern applied independent of beta-ERD in the control experiment resulted in a decrease of corticospinal excitability. These effects persisted beyond the period of stimulation and the depotentiation task.
Conclusion: These results could be instrumental in developing new therapeutic approaches such as the application of closed-loop stimulation in the context of neurorehabilitation.

Introduction

For the induction of motor cortex (M1) plasticity, different transcranial magnetic stimulation (TMS) protocols are available [1,2], e.g. application of stimuli with a fixed frequency (rTMS), patterned theta burst stimulation (TBS) and associative pairing of peripheral and cortical stimulation (PAS), to name a few. One common feature of all of these protocols is that they can modulate corticospinal excitability measured by changes in motor-evoked potential (MEP) amplitude that outlast the stimulation itself. Although significant efforts have already been made to describe the stimulation effects during different conditions [2], e.g. stimulation at rest or during a task, reports on their dependency on the actual oscillatory brain state remain sparse.

The activity of the sensorimotor rhythm (SMR) is indicative of the brain's responsiveness to an excitatory drive and reflects the current excitatory state [3,4] with high and low sensorimotor activity, suggesting an inhibitory and excitatory brain state, respectively, caused by thalamo-cortical and cortico-cortical interdependences [5,6]. Oscillatory variations between these brain states may at least partly account for the large trial-to-trial variance of MEP amplitude induced by TMS [7–9]. The MEP amplitude was recently shown to increase during up-states of slow oscillation sleep waves [10]. Moreover, the MEP amplitude increases with the event-related desynchronization (ERD) of sensorimotor rhythms [11,12].

Sensorimotor ERD in both α- and β-frequency bands occurs during actual, imagined and observed movements with a highly correlated pattern. However, these frequency bands serve distinct functional mechanisms [13–15]. While α-activity gates

* Corresponding author. Tel.: +49 7071 29 83550; fax: +49 7071 29 25104.
E-mail address: alireza.gharabaghi@uni-tuebingen.de (A. Gharabaghi).

1935-861X/
http://dx.doi.org/10.1016/j.brs.2016.02.007

information by inhibiting task-irrelevant regions [6], β-activity mediates the disinhibition of the sensorimotor cortex and the coherent interaction with the muscles [14–19]. These differences become particularly relevant when applying neurofeedback interventions which aim at operant learning of specific brain states for novel therapeutic purposes. Bearing the restoration of corticospinal connectivity in mind [19], we chose ERD of the β-band as the physiological marker for our intervention [20].

However, the extent to which repetitive pairing of stimulation with ERD would lead to a lasting change of corticospinal excitability remains unclear. This challenge is related to the strong influence of prior muscle activity on stimulation effects and the large intertrial variability in spontaneous and movement-related brain activity [9,21–23].

Neurofeedback devices could constitute a viable solution to overcome such unpredictability of intrinsic brain states. The power changes in oscillatory activity during motor imagery are known to mimic the spectral activation patterns during an actual movement, i.e. sensorimotor ERD [24]. Contingent feedback of theses brain states using a brain–computer interface (BCI)-based technique can help subjects to repeatedly activate the targeted oscillatory patterns without performing actual movements [25–27].

We used a brain–computer interface environment in conjunction with kinesthetic motor imagery to pair TMS of the precentral gyrus with event-related desynchronization (ERD) in the β-band (16–22 Hz), and tested for increases in corticospinal excitability, indexed by MEP amplitude, that were resistant to a depotentiation motor task following the stimulation protocol [28]. Results were compared to a control experiment in which the same number and pattern of stimuli were applied during rest, i.e. independent of ERD.

Materials and methods

Subjects

Seventeen different healthy subjects (mean age, 26.4 ± 3.4 years, range 21–35 years, 10 male) with no contraindications to TMS [29] and no history of psychiatric or neurological disease were recruited for this study. Five subjects participated in both experiments; in these cases, we ensured that there was a pause of at least five days between the sessions to avoid carry-over effects. The study comprised a total of 22 sessions, i.e. 11 subjects/sessions for Experiment 1 and 11 subjects/sessions for Experiment 2. Right-handedness was confirmed by the Edinburgh handedness inventory [30]. All subjects gave their written informed consent prior to participation in the study, which had been approved by our local ethics committee. The study was carried out in accordance with the latest version of the Declaration of Helsinki.

Recordings

Electromyography (EMG)

We used Ag/AgCI AmbuNeuroline 720 wet gel surface electrodes (Ambu GmbH, Germany) to record electromyography (EMG) activity from the left Extensor Digitorum Communis (EDC) muscle during the intervention. We placed two electrodes on the muscle belly 2 cm apart from each other. After filtering between 0.16 Hz and 1 kHz, EMG was recorded with 5 kHz sampling rate and downsampled to 1 kHz by the BrainAmp Amplifier. To determine plastic changes (see below) we applied the integrated 6 channel EMG device of the eXimia Navigated Brain Stimulation (NBS) system (Nexstim Inc., Finland) with 3 kHz sampling rate and band-pass filter of 10–500 Hz before and after the intervention.

Electroencephalography (EEG)

Throughout the experiment, Ag/AgCl electrodes and BrainVision software with DC amplifiers and an antialiasing filter (BrainAmp, Brainproducts GmbH, Germany) were used to record electroencephalography (EEG) signals in a 32 channel setup that complied with the international 10–20 system (Fp1, Fp2, F3, Fz, F4, FT7, FC5, FC3, FC1, FC2, FC4, FC6, FT8, C5, C3, C1, Cz, C2, C4, C6, TP7, CP5, CP3, CP1, CPz, CP2, CP4, CP6, TP8, P3, P4, POz with FCz as reference). For each experiment, impedances at all electrodes were set below 10 kΩ. Following digitization at 1 kHz rate, high-pass filtering with 0.16 Hz and low-pass filtering with 1000 Hz, the EEG signals were transferred for online analysis to BCI2000 software, where they were later stored offline [31]. Since ambient noise could influence electrophysiological recordings, we made every effort to remove its potential sources from the experimental environment by turning off mobile phones, unplugging superfluous power supplies and computers, etc. The effect of this procedure on, for example the 50 Hz line noise, was verified online.

The aim of the EEG data analysis was to register the differential information contents between experimental conditions, i.e. enhanced ERD during the motor imagery condition. We were also interested in the contingency of TMS with beta-ERD during the intervention and the topographic distribution of the beta-band modulation. We therefore examined the EEG differences between experiments (i.e. Experiment 1–Experiment 2).

TMS protocol

We used a navigated TMS stimulator (eXimia®, Nexstim, Helsinki, Finland) with a biphasic current waveform connected to a figure-8 eXimia Focal Bipulse Coil (5 cm mean winding diameter) to determine MEP stimulus–response curves (SRC) before and after the intervention, as well as to stimulate during the intervention (Fig. 1). Prior to the experiment, a 3-tesla Siemens TIM Trio MRI system (Siemens AG, Germany) was used to obtain anatomical T1 weighted magnetic resonance imaging (MRI) sequences for each participant. Images were loaded into the eXimia NBS system for coregistration with the participant's head. Subjects were seated in a comfortable reclining chair. The representation of the left EDC in the right M1 was determined for each subject prior to the onset of the first experiment. As initial intensity, we used 40% of maximum stimulator output and the anatomically defined 'hand knob' of M1. Whenever the initial stimulator output did not suffice to elicit MEPs, we increased output in steps of 5%. We ensured that the orientation of the coil remained perpendicular to the central sulcus and defined the coil site that consistently elicited the largest MEPs as our stimulation site. Having determined this 'hotspot', we varied the orientation of the coil in steps of roughly 10° around the original orientation to ascertain which orientation elicited the largest MEP at this site. The optimal coil orientation and location remained constant throughout the session. We then determined the resting motor threshold (RMT) by the relative frequency method, i.e. by detecting the minimum stimulus intensity (closest 2% of maximum stimulator output (MSO)) that resulted in MEPs >50 μV in the peak-to-peak amplitude in at least 5 out of 10 consecutive trials [32]. We calculated the RMT and the MEP stimulus–response curve to determine corticospinal excitability at baseline (prior to intervention) and after the intervention. The estimated electrical field of the NBS system at the 'hotspot' in a depth of ~22 mm [33,34] was then used to determine the intensities for the MEP stimulus–response curve. The initial intensity was set at 60% RMT and increased in steps of 10 V/m. Ten MEPs were recorded for each intensity step. We next acquired a cortical map representation at 110% RMT and with evenly distributed stimuli until MEP could no longer be evoked in the investigated muscle. During the mapping procedure, a visual grid

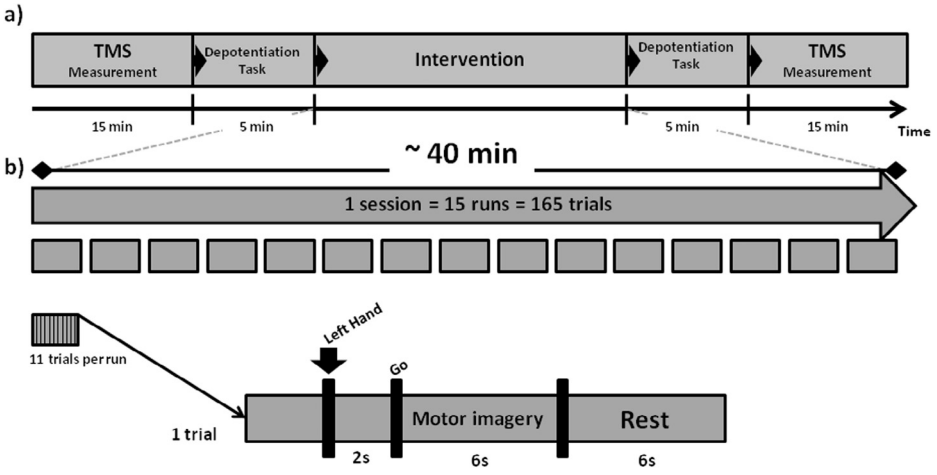

Figure 1. Experimental design and temporal structure of the study.

($5 \times 5 \times 5$ mm) which was predefined in the navigation software was used for guidance. The actual navigation coordinates of each stimulus were then used for data analysis, resulting in a spacing of approximately 3 mm. Finally, these spots were interpolated and sampled on a $1 \times 1 \times 1$ mm grid for visualization to close the gap between stimulation sites and then projected onto the gyral anatomy to decrease the variability of the cortical motor maps following a procedure recently described in detail elsewhere [35]. Approximately 100 stimuli were applied during this ~15-minute mapping procedure. Subjects were requested to keep their muscles relaxed for the duration of all TMS measurements. We inspected the EMG data during offline analysis, discarding any trials containing muscle preactivation. Less than 1% of all trials were rejected due to contamination by muscle activity.

Depotentiation of fragile stimulation effects

To identify stimulation effects that persisted despite voluntary muscle contraction, participants were asked to perform a depotentiation task [28,36]. This task consisted of a bar drifting rhythmically up and down on a computer screen. Subjects were requested to match the bar with a ball on the screen. This ball was controlled by a hand orthosis (Amadeo®, Tyromotion GmbH, Austria) attached to the subject's hand. Subjects were instructed to extend the fingers in the hand orthosis to initiate an upward movement of the ball and to flex the fingers to move the ball downwards on the screen accordingly. When matched with the moving bar, the ball on the screen turned from red to green. This depotentiation task, which lasted for five minutes, was performed twice during the experiment (Fig. 1): (a) after the first TMS mapping to rule out potential effects on the TMS measurements per se [36] since 150 stimuli had already been shown to induce transient changes of corticospinal excitability [37], and (b) following the intervention to identify robust changes of corticospinal excitability [28].

Experimental condition

An outline of the experiment is provided in Fig. 1. The intervention lasted for approximately 40 min and consisted of 15 runs. Each run took approximately 2.5 min and contained 11 trials. A preparation phase of 2 s marked the onset of each trial. This was followed by a 6 s motor imagery phase and a 6 s rest phase. The auditory cues 'left hand' and 'go' – presented by a recorded female voice – marked the onset of the preparation and imagery phases. In all trials, subjects performed the same kinesthetic motor imagery task during the motor imagery phase. They were instructed to imagine and to sense the opening of their left hand from a first person perspective without actually moving it. To prevent active movement, the hand was attached to an immobile hand orthosis throughout the experiment. The motor imagery feedback consisted of a red cross in the middle of a computer screen. During the motor imagery phase, this cross changed to green whenever ERD was detected. In the rest phases, the subjects were asked to count backwards from ten without paying any attention to their left hand.

Experiment 1: TMS during sensorimotor desynchronization (n = 11)

A biphasic single TMS pulse was used to stimulate the EDC 'hotspot' of the right M1 with 110% RMT. Whenever event-related desynchronization (ERD) was observed in the β-band (16–22 Hz) during the motor imagery phase, the BCI2000 software triggered cortical stimulation [38]. If ERD was sustained or reestablished after the first stimulus, more than one TMS pulse was applied during the motor imagery phase (Fig. 2a). The minimum interstimulus interval was set at 500 ms. ERD detection was confined to electrodes FC4, C4 and CP4 over the right sensorimotor area [39]. Once ERD disappeared, stimulation ceased. We used a linear classifier of 9 features consisting of three 2-Hz frequency bins (16–22 Hz) and three channels (FC4, C4, and CP4) to detect decreases in sensorimotor rhythm (SMR) power in the β-band. An autoregressive model, with a model order of 16 and based on the Burg Algorithm, was used to estimate frequency power [40]. Five consecutive 40 ms epochs had to be classified as ERD-positive before stimulation could be initiated. This ensured that stimulation occurred during prolonged sessions of ERD only (Fig. 2). Prior to the experiment, a desynchronization task, consisting of three motor imagery training runs without stimulation, was performed for calibration to account for each subject's ability for desynchronization. Following this calibration session, an individual desynchronization threshold, described in detail elsewhere [41], was implemented for the intervention. This threshold balanced challenge and motivation of the participant and preserved the specificity of the feedback, i.e. stimulation was not provided until subjects attained consistent ERD. Stimulation did not occur in instances where the threshold was not met due to event-related synchronization (ERS) or when the ERD was not consistent, i.e. not long and/or strong enough. The ERD threshold ensured that each subject received the same task-related demand and that this remained constant in each subject throughout the intervention. We discarded the first 50 ms after each pulse and used a modified Burg

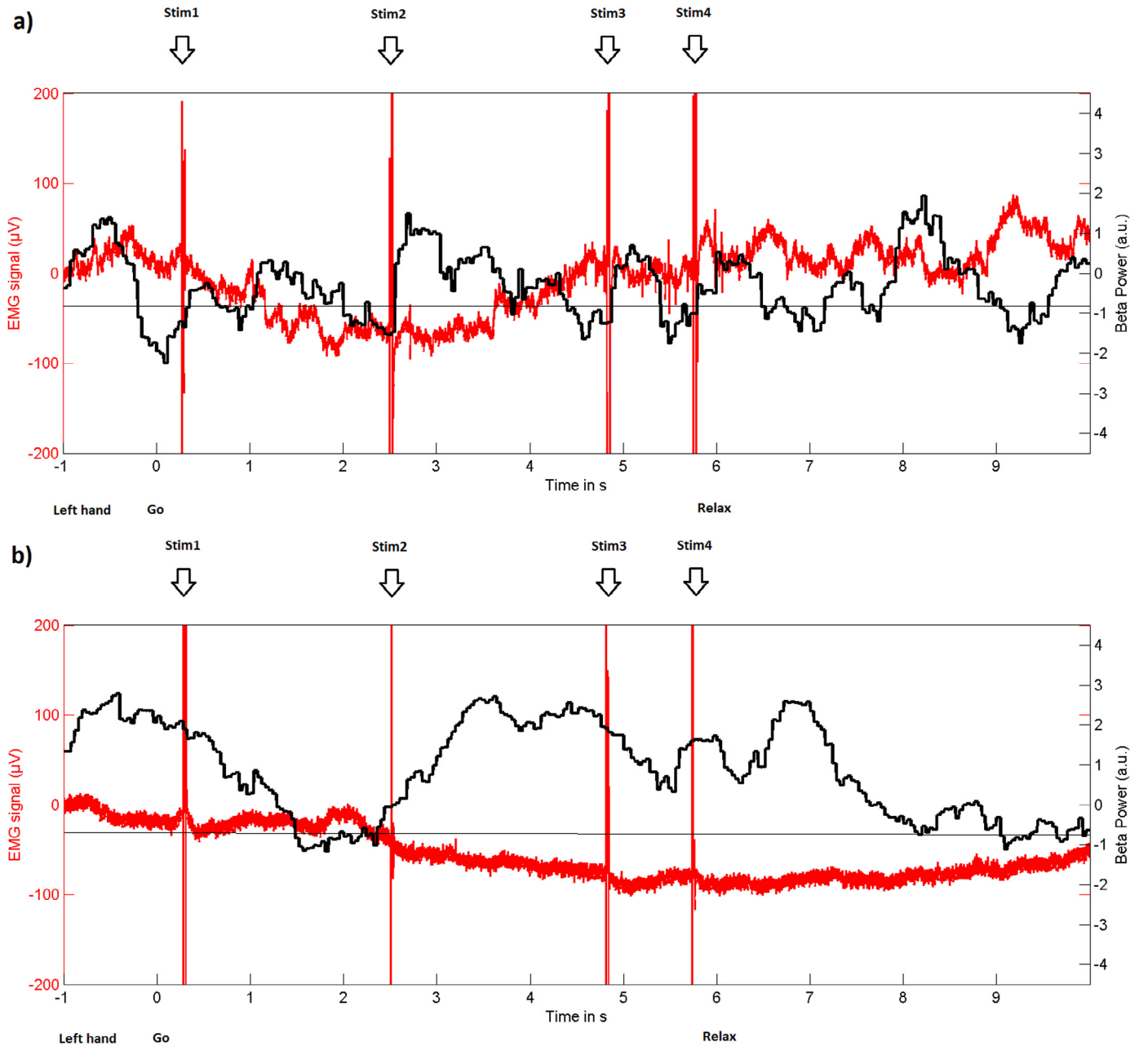

Figure 2. Exemplary single trial raw data of EMG recordings (red) of the EDC muscle (in µV, left y-axis) and the online classifier output (black, ß-power, in arbitrary units, right y-axis) of Experiment 1 (a) and 2 (b). Please note that, in the closed-loop feedback condition (a), motor imagery-related ERD frequently reaches the predefined threshold during the movement imagination phase (6s after "go" signal). Moreover, TMS is applied during these ERD phases only. In the control condition (b), the same number and pattern of stimuli are applied independent of the brain state. (For interpretation of the references to color in this figure legend, the reader is referred to the web version of this article.)

algorithm for segmented data in the online analysis to interpolate the gap [42]. This ensured that the EEG signal in the β-range was not contaminated by the TMS artifact.

Experiment 2: TMS in rest without sensorimotor desynchronization (n = 11)

In this control experiment, cortical stimulation was not triggered by ERD. The stimulation intensity relative to RMT, the amount of stimuli and the sequential pattern of cortical stimulation pulses in this experiment were recorded from Experiment 1 and were therefore identical in both experiments (Fig. 2b). This ensured that the same number and pattern of cortical stimuli were applied in Experiments 1 and 2, but independent of the ongoing brain activity in the latter. In Experiment 2, subjects were instructed not to perform motor imagery and to maintain muscle relaxation throughout the intervention.

Data analysis

Matlab R2010b (Mathworks) with custom built code and SPSS V21 (IBM) were used to analyze the data.

Resting motor threshold and map parameters

Using the coil coordinates acquired by the navigation system [35], we projected all stimulation points of the cortical map onto the

cortex along the coil axis in the direction of the magnetic field. The resulting map area (with responses above 50 μV) was obtained for each pre- and post-measurement. We then calculated the following parameters: Mean MEP of the map, number of active grid cells (Map area) and center of gravity (CoG). A repeated measures ANOVA (rmANOVA) was performed for changes in map parameters (Mean MEP, Area and CoG) and RMT for the within-subject effect of Time (pre-, post-) and the between-subject effect of Experiment (Experiment 1, Experiment 2).

Changes in MEP amplitude and area under the MEP curve

rmANOVA with Time and Intensity as within-subject effect and Experiment as between-subject effect were performed on the binned data (Bins: 71–90% RMT, 91–110% RMT, 111–130% RMT, 131–160% RMT) for MEP peak-to-peak amplitude and MEP area. When violation of sphericity was observed, a Greenhouse–Geisser correction was performed. Post-hoc testing was carried out as described below for the parameters of the stimulus response curve.

We fitted a three parameter Boltzmann sigmoidal function to the pre- and post-intervention MEP SRC of all subjects. Peak-to-peak amplitude was calculated using Equation 1 [43–45] and the area under the MEP curve was derived from Equation 2. A Huber weighted least square method, which compensated for outliers and heteroscedasticity, was used to perform a robust fit, i.e. the further it moved away from the curve in each fitting iteration step, the further the response decreased linearly in weight [46].

$$MEP(S) = MEPmax/(1+\exp(k(S_{50}-S))) \quad (1)$$

$$MEP\ Area(S) = MEPmax\ area/(1+\exp(m(Sarea_{50}-S))) \quad (2)$$

In Equations 1 and 2, MEP(S) represents the mean peak-to-peak MEP and the MEP Area(S) stands for the mean area under the MEP curve elicited by a stimulus S normalized to the RMT stimulation intensity. The saturation amplitude of the peak-to-peak MEP amplitude and the MEP area are represented by MEPmax and MEPmax area. S50 and Sarea50 stand for the stimulation intensity required to gain 50% of the maximum response, while k and m are the slope parameters of MEP(S) and the MEP Area(S), respectively, representing the recruitment gain in the corticospinal pathway [35] or trans-synaptic excitability [47].

This resulted in one mean stimulus response curve for all subjects under the pre and post conditions. We calculated a 95% confidence for each curve parameter, as well as for the actual curves. We then calculated the 95% confidence interval of the differences between the means of the pre- and post-intervention curve parameters. This resulted in a confidence interval for the change between pre and post condition similar to a paired sample t-test. The method described by Altmann and Bland [48] was used to calculate P-values for the differences in MEPmax, MEPmax area, S50, Sarea50, k and m. These were then Bonferroni-corrected for multiple comparisons ($\alpha = 0.004$).

Electrophysiological analysis

Differences in EMG-trace and event-related desynchronization were assessed for statistical significance using a mixed permutation approach, allowing us to account for the five subjects who took part in both experimental conditions. All tests were run for 10,000 repetitions.

Results

The average number of stimuli applied per subject was 304.2 ± 82.3 in both experiments. An overlaid plot of rectified EMG enabled us to directly compare the background activity of both experiments. The whole trial period, i.e. the –2s to 8s epoch relative to the Go-cue, was detrended, rectified and baselined to zero. The grand median activity within this epoch was 3.15 μV (range of 0–9.93 μV) for Experiment 1 and 2.46 μV (range of 0–7.95 μV) for Experiment 2. There was no significant difference in the median activity of these two experiments ($Z = 0.178$, $p > 0.859$). Furthermore, statistical analysis for every time-point (i.e. millisecond-wise) revealed no evidence for significant differences (at 5% alpha error) between Exp. 1 and 2 during the feedback period when the stimulation was applied. These findings indicate that the differences in corticospinal excitability between conditions were not related to different EMG activity in the experiments.

EEG time–frequency analysis illustrated the differential information contents between imagery and rest in Experiment 1 (motor imagery) and Experiment 2 (control), with enhanced ERD in the former (Fig. 3a). Stimulus-averaged EEG time–frequency analysis revealed contingency of TMS pulses to preceding beta-ERD in Experiment 1 but not in Experiment 2 (Fig. 3b). Evaluation of EEG topography of beta-power showed distributed MI-related ERD with a particular focus over contralateral sensorimotor areas in Experiment 1 in contrast to Experiment 2 (Exp.1–Exp.2) (Fig. 3c).

MEP mapping

The rmANOVA revealed a significant effect of Time × Experiment on the mean MEP of the cortical map ($F_{1, 20} = 12.33$; $p = 0.002$) but not on Map area or CoG. A post-hoc paired sample t-test between pre and post mean MEP of the cortical map revealed a significant increase in Experiment 1 ($p = 0.0113$) and a decreasing trend in Experiment 2 ($p = 0.0748$). Fig. 4 shows the topographic changes in the cortical TMS maps, revealing consistent MEP increases and decreases in comparison to baseline for Experiments 1 and 2, respectively. The MEP increases in Experiment 1 were distributed and covered large parts of the pre- and postcentral gyrus, while small parts of the precentral gyrus showed MEP increases in Experiment 2 as well. There were no significant effects of Time or Experiment on any of the other MEP map measurements (Table 1). Measures of goodness of fit supported the Boltzmann sigmoidal function and the validity of subsequent statistical analysis: The pre/post goodness of fit was computed for the MEP amplitude and the

Table 1
Summary of RMT and map parameters before and after the intervention (Mean ± SD). CoG in individual MRI coordinates with reference to the lower right corner. *indicates significant change post vs. pre ($p < 0.05$).

Measure	RMT (% MSO)	Mean MEP (μV)	Map area (mm^3)	CoG anterior–posterior (mm)	CoG lateral–medial (mm)
Pre					
Experiment 1	45.9 ± 9.2	147.8 ± 46.5	2260.4 ± 1556	110.2 ± 8	54.5 ± 8.5
Experiment 2	43.9 ± 7.5	220.5 ± 102.1	1734.5 ± 856.7	116.1 ± 26	54.2 ± 10.1
Post					
Experiment 1	47.5 ± 9.6	212.2 ± 103.2*	2872.7 ± 1510.7	109.5 ± 7.8	54.3 ± 8.8
Experiment 2	44 ± 8.6	170.9 ± 67.2	1513.7 ± 881	114 ± 24.8	56.3 ± 5.2

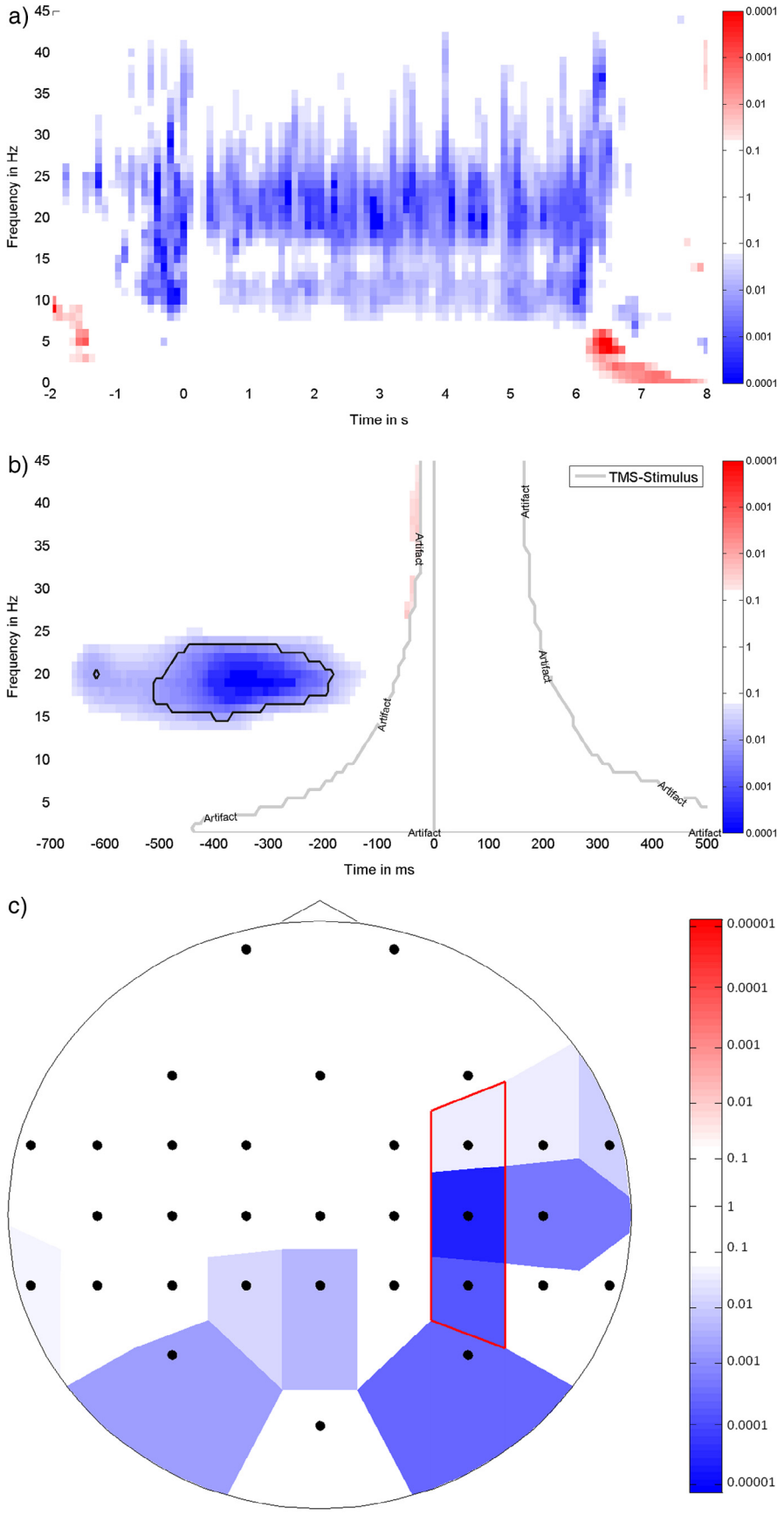
a)
Frequency in Hz
Time in s
b)
Frequency in Hz
Time in ms
TMS-Stimulus
Artifact
c)

Figure 3. (a) EEG time–frequency analysis shows evidence for stronger desynchronization during the feedback period relative to rest for the feedback channels (i.e. FC4, C4 and CP4), contrasting Experiment 1 with Experiment 2 (Exp.1–Exp.2). (b) Stimulus-locked EEG time–frequency analysis shows frequency-contingency of TMS pulses in Experiment 1 in comparison to Experiment 2 (Exp.1–Exp.2), based on the spatial average of all channels. The black line delineates areas with desynchronization at the $p < 0.01$ level, indicating significant desynchronization in the 16–22 Hz range around 700–200 ms before the TMS-pulse. The gray trace indicates the time–frequency response of the TMS-artifact. All plots present the log10 of the p-value in a color-coded fashion, with blue and red colors showing relative desynchronization and synchronization, respectively. (c) Evaluation of EEG topography of beta-power (16–22 Hz) in the 500 ms period before the GO-cue and with TMS artifact rejection (–5 ms to +20 ms around the pulse) revealed distributed MI-related ERD in comparison to the rest period baseline with a particular focus over contralateral sensorimotor areas in Experiment 1 in contrast to Experiment 2 (Exp.1–Exp.2) with the strongest ERD projecting to C4 at the $p < 0.0001$ level. The red trace around FC4, C4 and CP4 highlights the channels used for on-line classification. Colored areas indicate ERD of at least $p < 0.05$ level.

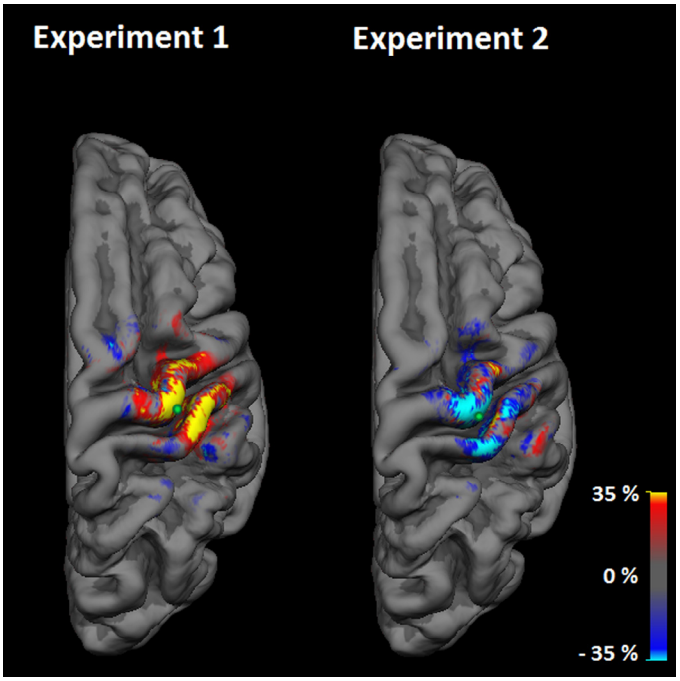

Figure 4. Topographic changes in cortical TMS maps pre- versus post-intervention on the group level. Color bar indicates percentage increases in MEP size (red/yellow) and decreases in MEP size (blue/turquoise); the green dot represents the stimulation spot where the stimulus response curve was acquired.

MEP area of Experiment 1. This resulted in values of $r^2 = 0.95/0.94$ and $r^2 = 0.97/0.98$. For the MEP amplitude and the MEP area of Experiments 2, the pre/post goodness of fit values were $r^2 = 0.99/0.99$ and $r^2 = 0.98/0.99$, respectively.

MEP stimulus–response curves

rmANOVA after Greenhouse-Geisser correction revealed a significant effect of Experiment for the MEP area ($F_{1,\ 42} = 14.95$; $p < 0.001$), a significant effect of Intensity for both MEP peak-to-peak amplitude ($F_{2.1,\ 88.3} = 183.22$; $p < 0.001$) and MEP area ($F_{1.51,\ 63.55} = 194.65$; $p < 0.001$), an interaction of Experiment × Intensity for MEP peak-to-peak amplitude ($F_{2.1,\ 88.3} = 4.7$; $p = 0.01$) and MEP area ($F_{1.51,\ 63.55} = 15.9$; $p < 0.001$), as well as an interaction for Time × Intensity for the MEP peak-to-peak amplitude ($F_{1.54,\ 64.55} = 5.68$; $p = 0.01$) and the MEP area ($F_{1.175,\ 49.4} = 6.81$; $p = 0.009$). In addition, the interaction Experiment × Time was significant for the MEP peak-to-peak amplitude ($F_{1,\ 42} = 4.15$; $p = 0.048$) and the MEP area ($F_{1,\ 42} = 4.98$; $p = 0.031$). The empirical data and the Boltzmann fit of the mean MEP stimulus–response curve (Fig. 5a + c) and the area under the MEP curve (Fig. 5b + d) for pre- and post-intervention are presented for Experiment 1 (Fig. 5a + b) and Experiment 2 (Fig. 5c + d), respectively. There is a significant increase in corticospinal excitability between 110% and 130% of RMT in the stimulus response curve of Experiment 1, which is reflected in decreases of both S50 and Sarea50 and in increases of both slopes k and m.

Experiment 1: TMS with sensorimotor desynchronization

In comparison to baseline, significant alterations were observed in the Boltzmann parameters S50, Sarea50, k and m, but not in MEPmax amplitude, MEPmax area (Fig. 5a + b), or RMT following the intervention (pre: 45.9 ± 9.2% MSO; post: 47.5 ± 9.6% MSO).

The slopes k and m increased to 149.1% ($p = 0.0008$) and 149.3% ($p = 0.0003$) of the baseline value, respectively. S50 and Sarea50 decreased to 91.2% ($p < 0.0001$) and 89.7% ($p = 0.0002$) of the baseline value, respectively (Fig. 6a). The MEP increase in the steep part of the SRC correlated positively with the applied number of ERD triggered stimuli ($rho = 0.82$; $p = 0.004$).

Experiment 2: TMS without sensorimotor desynchronization

TMS applied during rest led to a significant decrease in MEPmax to 84.4% of baseline value ($p < 0.0001$) and to 87% of baseline value ($p = 0.0015$) in MEPmax area (Fig. 5b). Changes were not significant in S50, Sarea50, k and m or RMT (pre: 43.9 ± 7.5% MSO; post: 44 ± 8.6% MSO) (Fig. 5c + d, Fig. 6b). There was no correlation of the SRC with the applied number of stimuli.

Discussion

In the present study, we tested whether closed-loop single-pulse cortical stimulation triggered by motor imagery-related ß-ERD could induce a robust increase in corticospinal excitability. We chose kinesthetic motor imagery because this task activates similar neuronal correlates to those during motor execution [49–52], increases corticospinal excitability [53–56] and decreases short intracortical inhibition (SICI) [57] in a muscle- and time-specific way [55]. However, to the best of our knowledge, previous cortical stimulation studies revealed an increase of corticospinal excitability *during* specific brain states only [11,12] and did not show any robust changes *following* a brain state-dependent intervention.

A stable LTP-like increase in corticospinal excitability has been shown only in studies using peripheral stimulation with either passive movement or electrical stimulation of the peroneal nerve timed to the peak negativity of the movement-related cortical potential during motor imagery [58,59]. Interestingly, these studies showed no increase of corticospinal excitability when motor imagery was performed without additional input, i.e. peripheral stimulation. Bearing this in mind, we reasoned that such additional input could also be provided at the cortical level. We therefore conducted a pairing study in which TMS pulses were applied during ERD. The motor-imagery related power modulations resulted in distributed ERD of non-primary motor areas, e.g. temporo-parietal and precuneus area, as well; the most relevant modulation however occurred over contralateral sensorimotor areas with the strongest ERD projecting to C4, i.e. the hand knob area of the motor cortex which was used for online decoding and targeted by TMS. We hypothesized that such an approach could stimulate the cortico-cortical connections to pyramidal neurons during depolarization, albeit the

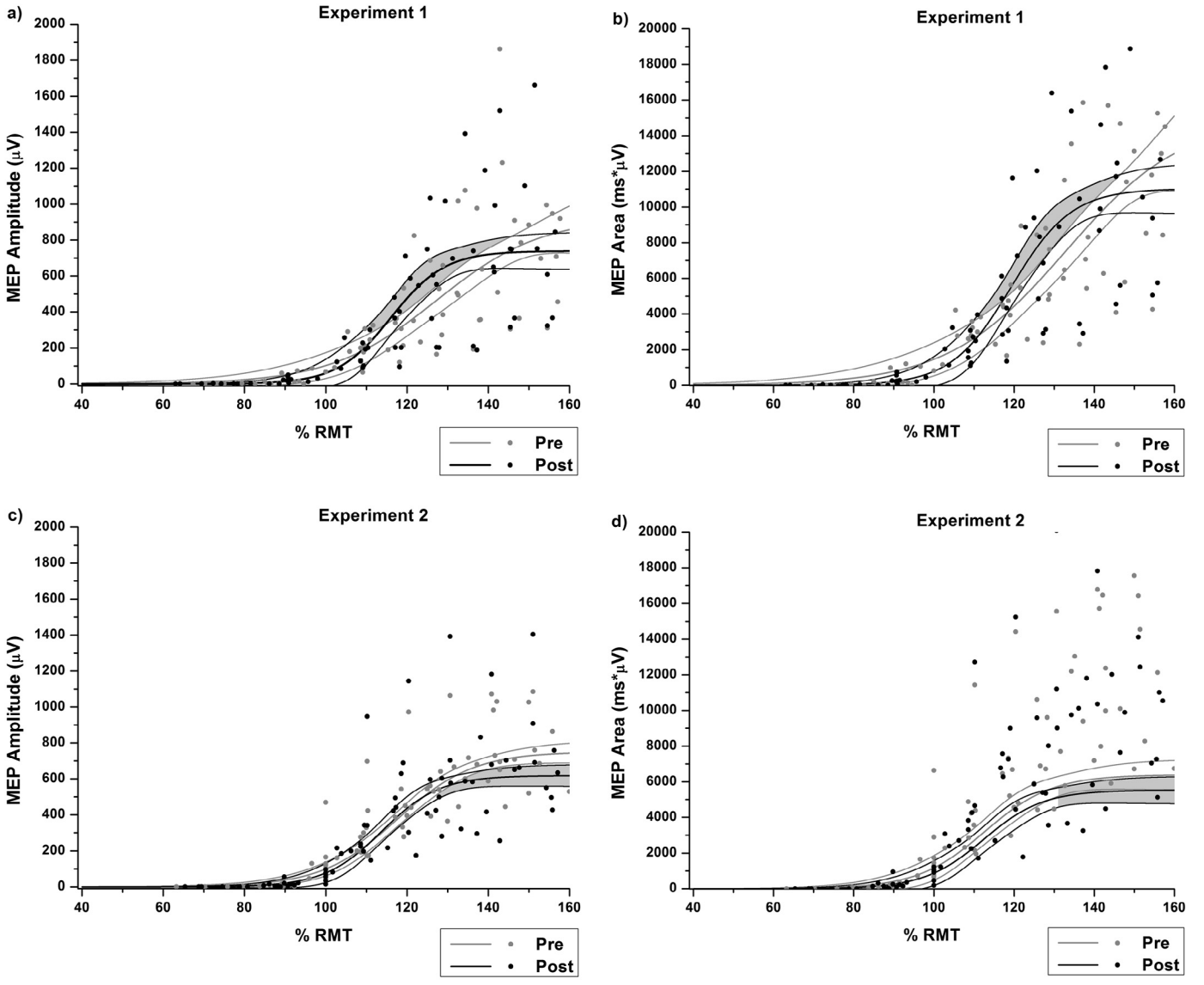

Figure 5. Empirical data (dots) and Boltzmann fit (lines) of (a,c) the mean MEP stimulus–response curves (in μV) and (b,d) the area under the MEP curve (in μV × ms) for pre-intervention (gray) and post-intervention (black) for Experiment 1 (a,b) and Experiment 2 (c,d), respectively. Each Boltzmann curve is paralleled by thin lines running above/below it and indicating the respective 95% confidence intervals. Shaded areas indicate significant differences between pre vs. post curves.

exact mechanisms of both TMS and ERD still require clarification. Our approach modulated the corticospinal excitability without relevant muscle contraction by decreasing intracortical inhibition via motor imagery-related ERD [12], using ERD as presynaptic input for a Hebbian-like stimulation protocol [60].

The results of the present study indicate that stimulation during the β-ERD brain state presents an appropriate target for closed-loop approaches aiming at an increase of motor cortex excitability. These findings are in accordance with previous TMS studies which showed an inverse correlation of MEP amplitude with β-band power [11] and an inverse correlation of intracortical inhibition with the ERD level during motor imagery [12]. A decrease of intracortical inhibition, in turn, was shown to enhance the effectiveness of α-motor neuron recruitment, i.e. the corticospinal excitability [61,62].

To further clarify the neurophysiological mechanisms of the increases observed in corticospinal excitability and indexed by significant changes of the peak-to-peak stimulus–response curve, we analyzed changes of the area under the MEP curve. This enabled us to disentangle whether the observed increase in MEP peak-to-peak amplitude was mediated by more synchronous firing of the stimulated neuronal population, repetitive discharges of motor neurons or by the recruitment of additional neurons [63,64]. The detected increase in peak-to-peak MEP amplitudes was paralleled by a significant increase in the respective area under the MEP curve, a finding that supports the concept that the increase in corticospinal excitability is the result of the recruitment of additional neurons [65,66]. Moreover, repetitive discharges of motor neurons cannot explain our findings (restricted to the steep part of the stimulus response curve), since such phenomena have been reported for the saturation level and during additional pre-activation of the muscle only [64]. Since the MEP changes in the present study were observed during rest (pre- and post-intervention), conventional explanations, i.e. relating them to the background muscle activity [43], a higher recruitment gain [43] or trans-synaptic excitability of the corticospinal pathway during movement [46] are not applicable either. The increase in corticospinal excitability between 110% and 130% of RMT in the stimulus response curve of our intervention, reflected in decreases of both S50 and Sarea50 and in

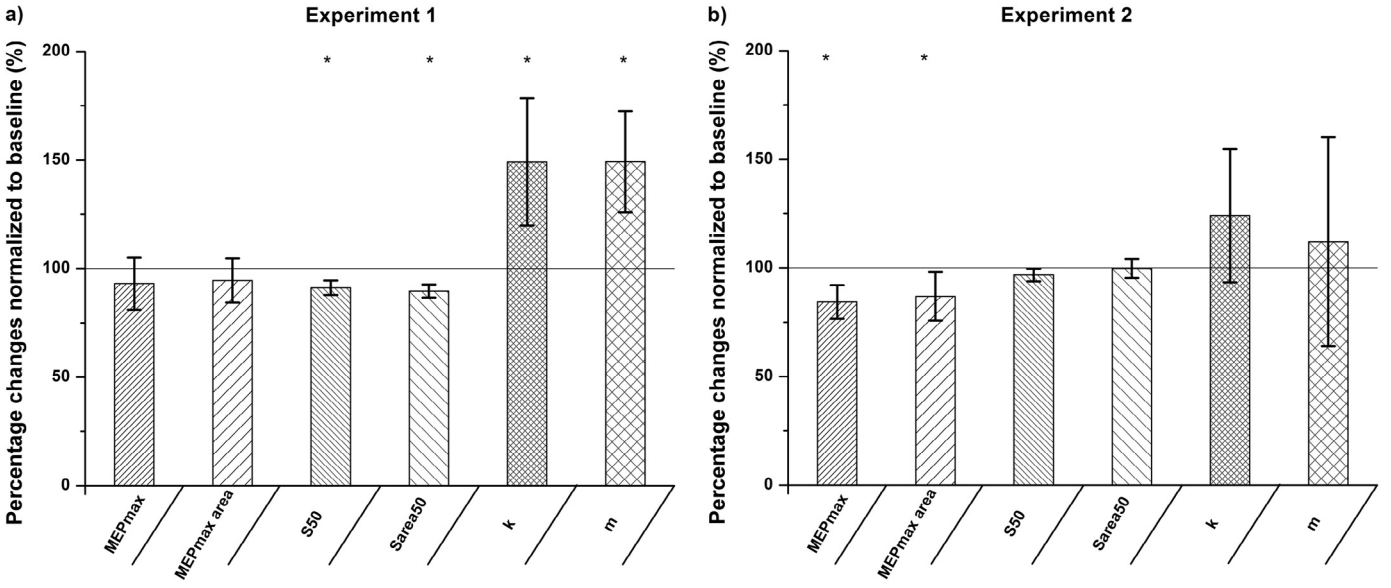

Figure 6. Cumulative overview of the stimulus response curve parameter (MEPmax, S50, k) and the area under the MEP curve parameters (MEPmax area, Sarea50, m) investigated for Experiment 1 (a) and Experiment 2 (b). Deviations from normalized baseline, i.e. comparisons of post-intervention compared to pre-intervention findings, are shown as percentage changes. Significant changes are indicated by asterisks (Bonferroni corrected, $p < 0.004$). The error bars indicate 95% confidence intervals.

increases of both slopes k and m, is therefore most likely due to the additional recruitment of higher threshold corticospinal neurons [67–69]. The correlation detected between the increased corticospinal excitability and the number of ERD triggered stimuli suggests a dose-effect for this intervention. This question needs to be addressed in detail in future studies.

Single-pulse stimulation at rest (as applied in Experiment 2) increased the slope parameters k and m as well, albeit not significantly. However, like in standard low-frequency TMS protocols [68,70] or traditional inhibiting PAS protocols [68,71], this intervention decreased MEPmax and the MEPmax area. When pairing the same pattern and number of stimuli with the brain state (as applied in our β-ERD-triggered stimulation paradigm, Experiment 1) the decreasing effect of single-pulse stimulation on the plateau of the stimulus response curve dissolved, thus highlighting the importance of the brain state on the induced effects on corticospinal excitability.

In future studies, some of the limitations of the present study need to be addressed: We applied the identical sequential pattern and number of cortical stimuli during both interventions by recording them during the ERD experiment and applying them several days later during the non-ERD experiment. This might introduce order effects (although this is improbable due to the wash out period between the interventions) and could be avoided by randomizing Experiments 1 and 2 and waiving the matching of the stimulation patterns. More relevantly, future experiments may consider adding a control attention task to the experimental setup to ensure that different vigilance levels do not influence the observed effects. Alternatively, a control experiment with the same task but asynchronous delivery of pulses or with varying levels of ERD might be considered in future.

In conclusion, we showed that TMS of the motor cortex during β-ERD increased corticospinal excitability that persisted beyond the period of stimulation and the depotentiation task. These findings may be instrumental in developing new closed-loop interventions based on the oscillatory brain state to facilitate use-dependent plasticity, e.g. in the context of neurorehabilitation.

Acknowledgement

DK, RB and MTL were supported by the Graduate Training Centre of Neuroscience, International Max Planck Research School for Cognitive and Systems Neuroscience, Tuebingen, Germany. AG was supported by grants from the German Research Council [DFG GH 94/2-1, DFG EC 307] and from the Federal Ministry of Education and Research [BFNT 01GQ0761, BMBF 16SV3783, BMBF 0316064B, BMBF 16SV5824].

References

[1] Ziemann U, Paulus W, Nitsche MA, Pascual-Leone A, Byblow WD, Berardelli A, et al. Consensus: motor cortex plasticity protocols. Brain Stimul 2008;1(3):164–82.
[2] Hoogendam JM, Ramakers GMJ, Di Lazzaro V. Physiology of repetitive transcranial magnetic stimulation of the human brain. Brain Stimul 2010;3(2):95–118.
[3] Salinas E, Thier P. Gain modulation: a major computational principle of the central nervous system. Neuron 2000;27(1):15–21.
[4] Chance FS, Abbott LF, Reyes AD. Gain modulation from background synaptic input. Neuron 2002;35(4):773–82.
[5] Thut G, Miniussi C. New insights into rhythmic brain activity from TMS-EEG studies. Trends Cogn Sci 2009;13(4):182–9.
[6] Jensen O, Mazaheri A. Shaping functional architecture by oscillatory alpha activity: gating by inhibition. Front Hum Neurosci 2010;4:186.
[7] Kiers L, Cros D, Chiappa KH, Fang J. Variability of motor potentials evoked by transcranial magnetic stimulation. Electroencephalogr Clin Neurophysiol 1993;89(6):415–23.
[8] Thickbroom GW, Byrnes ML, Mastaglia FL. A model of the effect of MEP amplitude variation on the accuracy of TMS mapping. Clin Neurophysiol 1999;110(5):941–3.
[9] Darling WG, Wolf SL, Butler AJ. Variability of motor potentials evoked by transcranial magnetic stimulation depends on muscle activation. Exp Brain Res 2006;174(2):376–85.
[10] Bergmann TO, Mölle M, Schmidt MA, Lindner C, Marshall L, Born J, et al. EEG-guided transcranial magnetic stimulation reveals rapid shifts in motor cortical excitability during the human sleep slow oscillation. J Neurosci 2012;32(1):243–53.
[11] Schulz H, Ubelacker T, Keil J, Müller N, Weisz N. Now I am ready–now I am not: the influence of pre-TMS oscillations and corticomuscular coherence on motor-evoked potentials. Cereb Cortex 2013;24(7):1708–19.
[12] Takemi M, Masakado Y, Liu M, Ushiba J. Event-related desynchronization reflects downregulation of intracortical inhibition in human primary motor cortex. J Neurophysiol 2013;110(5):1158–66.

[13] Brinkman L, Stolk A, Dijkerman HC, de Lange FP, Toni I. Distinct roles for alpha- and beta-band oscillations during mental simulation of goal-directed actions. J Neurosci 2014;34(44):14783–92.
[14] Kilavik BE, Zaepffel M, Brovelli A, MacKay WA, Riehle A. The ups and downs of beta oscillations in sensorimotor cortex. Exp Neurol 2013;245(July):15–26.
[15] Van Wijk BCM, Beek PJ, Daffertshofer A. Neural synchrony within the motor system: what have we learned so far? Front Hum Neurosci 2012;6:252.
[16] Kristeva R, Patino L, Omlor W. Beta-range cortical motor spectral power and corticomuscular coherence as a mechanism for effective corticospinal interaction during steady-state motor output. Neuroimage 2007;36(3):785–92.
[17] Mima T, Steger J, Schulman AE, Gerloff C, Hallett M. Electroencephalographic measurement of motor cortex control of muscle activity in humans. Clin Neurophysiol 2000;111(2):326–37.
[18] Aumann TD, Prut Y. Do sensorimotor B-oscillations maintain muscle synergy representations in primary motor cortex? Trends Neurosci 2015;38(2):77–85.
[19] Naros G, Gharabaghi A. Reinforcement learning of self-regulated B-oscillations for motor restoration in chronic stroke. Front Hum Neurosci 2015;9(July):391.
[20] Kraus D, Naros G, Bauer R, Leão MT, Ziemann U, Gharabaghi A. Brain-robot interface driven plasticity: Distributed modulation of corticospinal excitability. Neuroimage 2016;15(125):522–32.
[21] Hess CW, Mills KR, Murray NM. Magnetic stimulation of the human brain: facilitation of motor responses by voluntary contraction of ipsilateral and contralateral muscles with additional observations on an amputee. Neurosci Lett 1986;71(2):235–40.
[22] Di Lazzaro V, Restuccia D, Oliviero A, Profice P, Ferrara L, Insola A, et al. Effects of voluntary contraction on descending volleys evoked by transcranial stimulation in conscious humans. J Physiol 1998a;508(April Pt 2):625–33.
[23] Mitchell WK, Baker MR, Baker SN. Muscle responses to transcranial stimulation in man depend on background oscillatory activity. J Physiol 2007;583(Pt 2):567–79.
[24] Miller KJ, Leuthardt EC, Schalk G, Rao RPN, Anderson NR, Moran DW, et al. Spectral changes in cortical surface potentials during motor movement. J Neurosci 2007;27(9):2424–32.
[25] Wolpaw JR, Birbaumer N, McFarland DJ, Pfurtscheller G, Vaughan TM. Brain-computer interfaces for communication and control. Clin Neurophysiol 2002;113(6):767–91.
[26] Daly JJ, Wolpaw JR. Brain-computer interfaces in neurological rehabilitation. Lancet Neurol 2008;7(11):1032–43.
[27] Jensen O, Bahramisharif A, Oostenveld R, Klanke S, Hadjipapas A, Okazaki YO, et al. Using brain-computer interfaces and brain-state dependent stimulation as tools in cognitive neuroscience. Front Psychol 2011;2:100.
[28] Goldsworthy MR, Müller-Dahlhaus F, Ridding MC, Ziemann U. Resistant against de-depression: LTD-like plasticity in the human motor cortex induced by spaced cTBS. Cerebral Cortex 2014;25:1724–34.
[29] Rossi S, Hallett M, Rossini PM, Pascual-Leone A, The Safety of TMS Consensus Group. Safety, ethical considerations, and application guidelines for the use of transcranial magnetic stimulation in clinical practice and research. Clin Neurophysiol 2009;120(12):2008–39.
[30] Oldfield RC. The assessment and analysis of handedness: the Edinburgh inventory. Neuropsychologia 1971;9(1):97–113.
[31] Schalk G, McFarland DJ, Hinterberger T, Birbaumer N, Wolpaw JR. BCI2000: a general-purpose brain-computer interface (BCI) system. IEEE Trans Biomed Eng 2004;51(6):1034–43.
[32] Groppa S, Oliviero A, Eisen A, Quartarone A, Cohen LG, Mall V, et al. A practical guide to diagnostic transcranial magnetic stimulation: report of an IFCN committee. Clin Neurophysiol 2012;123(5):858–82.
[33] Danner N, Julkunen P, Könönen M, Säisänen L, Nurkkala J, Karhu J. Navigated transcranial magnetic stimulation and computed electric field strength reduce stimulator-dependent differences in the motor threshold. J Neurosci Methods 2008;174(1):116–22.
[34] Danner N, Könönen M, Säisänen L, Laitinen R, Mervaala E, Julkunen P. Effect of individual anatomy on resting motor threshold-computed electric field as a measure of cortical excitability. J Neurosci Methods 2012;203(2):298–304.
[35] Kraus D, Gharabaghi A. Projecting navigated TMS sites on the gyral anatomy decreases inter-subject variability of cortical motor maps. Brain Stimul. 2015;8(4):831–7.
[36] Todd G, Rogasch NC, Flavel SC, Ridding MC. Voluntary movement and repetitive transcranial magnetic stimulation over human motor cortex. J Appl Physiol 2009;106(5):1593–603.
[37] Touge T, Gerschlager W, Brown P, Rothwell JC. Are the after-effects of low-frequency rTMS on motor cortex excitability due to changes in the efficacy of cortical synapses? Clin Neurophysiol 2001;112(11):2138–45.
[38] Gharabaghi A, Kraus D, Leão MT, Spüler M, Walter A, Bogdan M, et al. Coupling brain-machine interfaces with cortical stimulation for brain-state dependent stimulation: enhancing motor cortex excitability for neurorehabilitation. Front Hum Neurosci 2014;8:122.
[39] McFarland DJ, Miner LA, Vaughan TM, Wolpaw JR. Mu and beta rhythm topographies during motor imagery and actual movements. Brain Topogr 2000;12(3):177–86.
[40] McFarland DJ, Wolpaw JR. Sensorimotor rhythm-based brain-computer interface (BCI): model order selection for autoregressive spectral analysis. J Neural Eng 2008;5(2):155–62.
[41] Naros G, Gharabaghi A. Reinforcement learning of self-regulated β-oscillations for motor restoration in chronic stroke. Front Hum Neurosci 2015;9:391.
[42] Walter A, Ramos Murguialday A, Spüler M, Naros G, Leão M-T, Gharabaghi A, et al. Coupling BCI and cortical stimulation for brain-state-dependent stimulation: methods for spectral estimation in the presence of stimulation after-effects. Front Neural Circuits 2012;6:87.
[43] Devanne H, Lavoie BA, Capaday C. Input-output properties and gain changes in the human corticospinal pathway. Exp Brain Res 1997;114(2):329–38.
[44] Houdayer E, Degardin A, Cassim F, Bocquillon P, Derambure P, Devanne H. The effects of low- and high-frequency repetitive TMS on the input/output properties of the human corticospinal pathway. Exp Brain Res 2008;187(2):207–17.
[45] Möller C, Arai N, Lücke J, Ziemann U. Hysteresis effects on the input-output curve of motor evoked potentials. Clin Neurophysiol 2009;120(5):1003–8.
[46] Huber PJ. Robust statistics. Hoboken, NJ: John Wiley & Sons, Inc; 1981.
[47] Ridding MC, Rothwell JC. Stimulus/response curves as a method of measuring motor cortical excitability in man. Electroencephalogr Clin Neurophysiol 1997;105(5):340–4.
[48] Altman DG, Bland JM. How to obtain the P value from a confidence interval. BMJ 2011;343:d2304.
[49] Lotze M, Montoya P, Erb M, Hülsmann E, Flor H, Klose U, et al. Activation of cortical and cerebellar motor areas during executed and imagined hand movements: an fMRI study. J Cogn Neurosci 1999;11(5):491–501.
[50] Neuper C, Scherer R, Reiner M, Pfurtscheller G. Imagery of motor actions: differential effects of kinesthetic and visual-motor mode of imagery in single-trial EEG. Brain Res Cogn Brain Res 2005;25(3):668–77, E.
[51] Pfurtscheller G, Neuper C. Motor imagery activates primary sensorimotor area in humans. Neurosci Lett 1997;239(2–3):65–8.
[52] Kaiser V, Kreilinger A, Müller-Putz GR, Neuper C. First steps toward a motor imagery based stroke BCI: new strategy to set up a classifier. Front Neurosci 2011;5:86.
[53] Ridding MC, Rothwell JC. Afferent input and cortical organisation: a study with magnetic stimulation. Exp Brain Res 1999;126(4):536–44.
[54] Roosink M, Zijdewind I. Corticospinal excitability during observation and imagery of simple and complex hand tasks: implications for motor rehabilitation. Behav Brain Res 2010;213(1):35–41.
[55] Stinear CM, Byblow WD. Modulation of corticospinal excitability and intracortical inhibition during motor imagery is task-dependent. Exp Brain Res 2004;157(3):351–8.
[56] Stinear CM, Byblow WD, Steyvers M, Levin O, Swinnen SP. Kinesthetic, but not visual, motor imagery modulates corticomotor excitability. Exp Brain Res 2006;168(1–2):157–64.
[57] Abbruzzese G, Assini A, Buccolieri A, Marchese R, Trompetto C. Changes of intracortical inhibition during motor imagery in human subjects. Neurosci Lett 1999;263(2–3):113–16.
[58] Xu R, Jiang N, Mrachacz-Kersting N, Lin C, Asin Prieto G, Moreno JC, et al. A closed-loop brain-computer interface triggering an active ankle-foot orthosis for inducing cortical neural plasticity. IEEE Trans Biomed Eng 2014;61(7):2092–101.
[59] Mrachacz-Kersting N, Kristensen SR, Niazi IK, Farina D. Precise temporal association between cortical potentials evoked by motor imagination and afference induces cortical plasticity. J Physiol 2012;590(Pt 7):1669–82.
[60] Hebb DO. The organization of behavior: a neuropsychological theory. New York: Wiley; 1949.
[61] Devanne H, Cohen LG, Kouchtir-Devanne N, Capaday C. Integrated motor cortical control of task-related muscles during pointing in humans. J Neurophysiol 2002;87(6):3006–17.
[62] Kouchtir-Devanne N, Capaday C, Cassim F, Derambure P, Devanne H. Task-dependent changes of motor cortical network excitability during precision grip compared to isolated finger contraction. J Neurophysiol 2012;107(5):1522–9.
[63] Rösler KM, Roth DM, Magistris MR. Trial-to-trial size variability of motor-evoked potentials. A study using the triple stimulation technique. Exp Brain Res 2008;187(1):51–9.
[64] Z'Graggen WJ, Humm AM, Durisch N, Magistris MR, Rösler KM. Repetitive spinal motor neuron discharges following single transcranial magnetic stimuli: a quantitative study. Clin Neurophysiol 2005;116(7):1628–37.
[65] Rösler KM, Petrow E, Mathis J, Arányi Z, Hess CW, Magistris MR. Effect of discharge desynchronization on the size of motor evoked potentials: an analysis. Clin Neurophysiol 2002;113(11):1680–7.
[66] Magistris MR, Rösler KM, Truffert A, Myers JP. Transcranial stimulation excites virtually all motor neurons supplying the target muscle. A demonstration and a method improving the study of motor evoked potentials. Brain 1998;121(March Pt 3):437–50.
[67] Di Lazzaro V, Oliviero A, Profice P, Saturno E, Pilato F, Insola A, et al. Comparison of descending volleys evoked by transcranial magnetic and electric stimulation in conscious humans. Electroencephalogr Clin Neurophysiol 1998b;109(5):397–401.
[68] Di Lazzaro V, Ziemann U, Lemon RN. State of the art: physiology of transcranial motor cortex stimulation. Brain Stimul 2008;1(4):345–62.
[69] Di Lazzaro V, Profice P, Ranieri F, Capone F, Dileone M, Oliviero A, et al. I-wave origin and modulation. Brain Stimul 2012;5(4):512–25.
[70] Di Lazzaro V, Pilato F, Dileone M, Profice P, Oliviero A, Mazzone P, et al. Low-frequency repetitive transcranial magnetic stimulation suppresses specific excitatory circuits in the human motor cortex. J Physiol 2008;586(Pt 18):4481–7.
[71] Di Lazzaro V, Dileone M, Profice P, Pilato F, Oliviero A, Mazzone P, et al. LTD-like plasticity induced by paired associative stimulation: direct evidence in humans. Exp Brain Res 2009;194(4):661–4.

Brain state-dependent stimulation enhances task-specific motor network connectivity

Short title: Task-specific enhancement of motor network connectivity

Fatemeh Khademi, Dominic Kraus, Alireza Gharabaghi*

Author contributions: A.G. designed research; D.K. performed research; F.K. and A.G. analyzed data; F.K. and A.G. wrote the manuscript.

Division of Functional and Restorative Neurosurgery, and Centre for Integrative Neuroscience, Eberhard Karls University Tuebingen, Tuebingen, Germany

*To whom correspondence should be addressed

Professor Alireza Gharabaghi, Division of Functional and Restorative Neurosurgery, Eberhard Karls University Tuebingen, Otfried-Mueller-Str.45, 72076 Tuebingen, Germany. Email address: alireza.gharabaghi@uni-tuebingen.de

Number of pages: 36

Number of Figures: 5

Conflict of interest: None

Acknowledgments

F.K. and D.K. were supported by the Graduate Training Centre of Neuroscience & International Max Planck Research School, Graduate School of Neural Information Processing (F.K.) and Graduate School of Neural and Behavioral Sciences (D.K.), Tuebingen, Germany. A.G. was supported by grants from the Baden-Wuerttemberg Foundation [NEU005] and the German Federal Ministry of Education and Research [BMBF 13GW0119B, IMONAS; 13GW0214B, INSPIRATION]. The authors declare no competing financial interests.

Abstract

Recovery from paralysis after stroke necessitates restoration of motor network connectivity. This requires the re-establishment of functionally relevant network interactions. Standard brain stimulation protocols, however, address plasticity in the resting brain. We investigated a novel stimulation protocol to enhance task-specific motor network interactions.

Sensorimotor event-related desynchronization (ERD) in the beta-band (16-22 Hz) during motor-imagery (MI) of finger extension triggered transcranial magnetic stimulation (TMS) to the respective cortical motor representation within a brain-computer interface environment in eleven healthy subjects. The same number and pattern of stimuli were applied in a control group of eleven subjects during rest, i.e., independent of MI-related ERD.

The application of approximately 300 TMS pulses – when applied state-dependently only -resulted in a significant and frequency-specific (16-22 Hz) enhancement of cortico-spinal and cortico-cortical motor network connectivity in the course of the intervention and thereafter. This network plasticity was task-specific, i.e., occurred in the subsequent motor task only during initiation of finger extension.

Functional enhancement of task-specific network interactions may be achieved when the cortical input is paired with self-regulated intrinsic brain states. These findings are probably mediated via a Hebbian mechanism and are potentially important for developing closed-loop brain stimulation for the treatment of hand paralysis after stroke.

Significance

Recovery from paralysis after stroke necessitates restoration of task-specific motor network interactions. Standard brain stimulation protocols, however, address plasticity in the resting brain.

In this study with healthy subjects, we investigated a novel stimulation protocol that applied intrinsic brain states during motor-imagery of finger extension to trigger transcranial magnetic stimulation to the respective cortical motor representation within a brain-computer interface environment. The state-dependent approach – but not the same number and pattern of stimuli applied during rest - resulted in a significant and frequency-specific enhancement of cortico-spinal and cortico-cortical motor network connectivity in the course of the intervention and thereafter. This network plasticity was task-specific, i.e., occurred in the subsequent motor task only during initiation of finger extension.

Introduction

Neural plasticity at the local and systems level contributes to the reorganization and repair of the lesioned brain (Murphy and Corbett, 2009) and is a largely stimulus-dependent synaptic phenomenon (Small et al., 2013; Dayan and Cohen, 2011). For the induction of plasticity in the human brain, different transcranial magnetic stimulation (TMS) protocols are available, e.g. application of pulses with a fixed frequency (rTMS), patterned theta burst stimulation (TBS) and associative pairing of distinct stimuli (PAS), to name a few (Kraus et al., 2016).

In the motor system, local plasticity is usually captured as the modulation of cortico-spinal excitability that outlasts the stimulation itself-indexed by the motor-evoked potential (MEP) amplitude (Ziemann et al., 2008). The strength of the connectivity between motor cortex and specific muscles can however also be measured by the magnitude of coherence between cortical and muscular activity, i.e. by cortico-muscular coherence (CMC; Schnitzler and Gross, 2005). This measure provides additional motor state-dependent information on the cortical topology, spectral characteristics, and type of interaction between cortex and muscles on a moment-to-moment basis (Mehrkanoon et al., 2014).

Systems-level plasticity is commonly assessed via the strength of connections between spatially distinct cortical regions by identifying motor network nodes with correlated activity, e.g. of the resting blood oxygen-level-dependent (BOLD) signal (Fox and Raichle, 2007). When measuring the magnitude of coherence between nodes within a cortico-cortical oscillatory network, e.g., with electroencephalography (EEG), additional information can be acquired. This approach allows for characterizing motor state-dependent transitions by distinct carrier frequencies which reflect different types of neural processing (Schnitzler and Gross, 2005).

Several TMS protocols have been shown to modify both local and network-level plasticity; rTMS (Bestmann et al., 2003; 2005), PAS (Veniero et al., 2013) and TBS (Nettekoven et al., 2014; Volz et al., 2016) not only modulated the excitability of the stimulated motor cortex but also its connectivity with remote but interconnected brain areas. One common feature of these protocols was their application during rest; the induced local and network-based plasticity were evaluated at rest as well. Resting-state connectivity within the motor system is however only weakly correlated with task-related network connections (Rehme et al., 2013). Functional restoration after brain lesions such as stroke needs, therefore, a more targeted reorganization of connectivity (Small et al., 2013), e.g. via the enhancement of task-specific motor network interactions.

For this purpose, current task-related approaches apply single-pulse TMS concurrently with specific voluntary movements (Bütefisch et al., 2004; Thabit et al., 2010; Bütefisch et al., 2011; Narayana et al., 2014). Even though these activity-dependent interventions have been shown to effectively induce local motor cortex (M1) plasticity, evidence for enhanced network-level connectivity is still missing. Moreover, these protocols depend on voluntary muscle control and are, therefore, not applicable to severely affected patients, e.g., with hand paralysis after stroke. For them, novel plasticity-inducing interventions are required that reestablish both cortico-spinal and motor network connectivity. Activating intrinsic brain states without performing actual movements could constitute a viable solution for state-dependent stimulation that targets functionally specific oscillatory networks (Kraus et al., 2016).

Motor-imagery (MI) is known to mimic actual movements with regard to both spectral activation, e.g., sensorimotor event-related desynchronization (ERD; Pfurtscheller and Neuper, 1997; Miller et al., 2007; 2010), and cortical connectivity

patterns, e.g. interhemispheric coherence (Vukelic et al., 2014; Bauer et al., 2015; Vukelic and Gharabaghi, 2015 a,b). Furthermore, MI-related ERD has been shown to reduce intracortical inhibition (Takemi et al., 2013); it may, therefore, be applied as the pre-synaptic input for an excitatory drive via TMS within a brain-computer interface environment (Gharabaghi et al., 2014; Kraus et al., 2016).

We hypothesized that such a modified PAS protocol (Suppa et al., 2017) would modulate the susceptibility of cortical motor circuits to an external input and thereby fulfill the requirements of Hebbian-stimulation at the network level (Hebb, 1949). Here, we provide empirical support that state-dependent primary motor cortex (M1) stimulation enhanced task-specific motor network connectivity beyond the site of stimulation in a frequency-selective way.

Material and method

Experimental design

Subjects

All subjects gave their written informed consent prior to participation in the study, which had been approved by the local ethics committee. The study was carried out in accordance with the latest version of the Declaration of Helsinki. The current work was part of a larger study on plasticity induction by brain state-dependent TMS. In the group of healthy subjects reported here, we have previously described an increase in cortico-spinal excitability (CSE), indexed by MEP changes, following the same intervention (Kraus et al., 2016). This previous work studied local M1 plasticity of the stimulated sensorimotor cortex *after* the intervention and *at rest*. In the present

secondary analysis, we intended to study task-related network-level plasticity and the underlying intervention-related neurophysiological mechanisms. We, therefore, explored more distributed network changes of functional connectivity (both cortico-cortical and cortico-muscular) *during* the intervention and there after, i.e., *during* an isometric motor task. This allowed us to capture task-related online effects and aftereffects of coherent oscillatory activity. The material and methods of data acquisition applied here are identical to the previous study (Kraus et al., 2016) and are cited accordingly: Seventeen healthy subjects (mean age, 26.4 ± 3.4 years, range 21–35 years, 10 male) with no contraindications to TMS (Rossi et al., 2009) and no history of psychiatric or neurological disease participated. Five subjects took part in both experiments; in these cases, we ensured that there was a pause of at least five days between the sessions to avoid carry-over effects. The study comprised a total of 22 sessions, i.e., 11 subjects/sessions for Experiment 1 and 11 subjects/sessions for Experiment 2 (Kraus et al., 2016). Right-handedness was confirmed by the Edinburgh handedness inventory (Oldfield, 1971)

Electromyography (EMG)

We used Ag/AgCIAmbuNeuroline 720 wet gel surface electrodes (Ambu GmbH, Germany) to record electromyography (EMG) activity from the left Extensor Digitorum Communis (EDC) muscle during the intervention. We placed two electrodes on the muscle belly 2 cm apart from each other. After filtering (antialiasing filter) between 0.16 Hz and 1 kHz, EMG was recorded with 5 kHz sampling rate and downsampled to 1 kHz by the BrainAmp Amplifier (Kraus et al., 2016).

155 *Electroencephalography (EEG)*

156 Throughout the experiment, Ag/AgCl electrodes and BrainVision software with DC
157 amplifiers and an antialiasing filter (BrainAmp, Brainproducts GmbH, Germany) were
158 used to record electroencephalography (EEG) signals in a 32 channel setup that
159 complied with the international 10–20 system (Fp1, Fp2, F3, Fz, F4, FT7, FC5, FC3,
160 FC1, FC2, FC4, FC6, FT8, C5, C3, C1, Cz, C2, C4, C6, TP7, CP5, CP3, CP1, CPz,
161 CP2, CP4, CP6, TP8, P3, P4, POz with FCz as reference). For each experiment,
162 impedances at all electrodes were set below 10 kΩ. After filtering (antialiasing filter)
163 between 0.16 Hz and 1 kHz, EEG was recorded with 5 kHz sampling rate and
164 downsampled to 1 kHz by the BrainAmp Amplifier (Kraus et al., 2016). The EEG
165 signals were, then, transferred for online analysis to BCI2000 software, where they
166 were later stored offline (Schalk et al., 2004; Kraus et al., 2016)

167 *TMS protocol*

168 We used a navigated TMS stimulator (eXimiaR, Nexstim, Helsinki, Finland) with a
169 biphasic current waveform connected to a Figure-8 eXimia Focal Bipulse Coil (5 cm
170 mean winding diameter) during the intervention (Figure 1D). Prior to the experiment,
171 a 3-tesla Siemens TIM Trio MRI system (Siemens AG, Germany) was used to obtain
172 anatomical T1 weighted magnetic resonance imaging (MRI) sequences for each
173 participant. Images were loaded into the eXimia NBS system for coregistration with
174 the participant's head. Subjects were seated in a comfortable reclining chair. The
175 representation of the left extensor digitorium carpi (EDC) in the right M1 was
176 determined for each subject prior to the onset of the first experiment. As initial
177 intensity, we used 40% of maximum stimulator output and the anatomically defined
178 'hand knob' of M1. Whenever the initial stimulator output did not suffice to elicit
179 MEPs, we increased output in steps of 5%. We ensured that the orientation of the coil

remained perpendicular to the central sulcus and defined the coil site that consistently elicited the largest MEPs as our stimulation site. Having determined this 'hotspot', we varied the orientation of the coil in steps of roughly 10° around the original orientation to ascertain which orientation elicited the largest MEP at this site. The optimal coil orientation and location remained constant throughout the session. We then determined the resting motor threshold (RMT) by the relative frequency method, i.e., by detecting the minimum stimulus intensity (closest 2% of maximum stimulator output (MSO)) that resulted in MEPs >50 μV in the peak-to-peak amplitude in at least 5 out of 10 consecutive trials (Groppa et al., 2012).

Study design

The general design of the experiment is illustrated in Figure 1A. The experiment consisted of a forty-minute intervention; an isometric motor task (5 min) was performed before and after the intervention, which consisted of 15 runs. Each run lasted approximately 2.5 min and included 11 trials. Each trial started with a 6 s rest phase followed by a 2 s preparation phase and a 6 s motor imagery phase (Figure 1D). During the motor imagery phase, subjects performed a kinesthetic motor imagery task of finger extension. They were instructed to imagine and to sense the finger extension during the opening of their left hand from a first-person perspective without actually moving it. To prevent active movement, the hand was attached to an immobile hand orthosis throughout the experiment. The motor-imagery feedback consisted of a *red* cross in the middle of a computer screen. During the motor-imagery phase, this cross changed to *green* whenever ERD was detected. In the rest phases, the subjects were asked to count backward from ten without paying any attention to their left hand. The subjects were, moreover, asked to sustain or

reestablished the *green cross* whenever it turned red during the imagery phase by reinitiating motor-imagery of finger extension.

A biphasic single TMS pulse was used to stimulate the EDC ‘hotspot’ of the right M1 with 110% RMT for cortical brain-state dependent stimulation (experimental group). Whenever event-related desynchronization (ERD) was observed in the beta-band (16–22 Hz) during the motor imagery phase, the BCI2000 software triggered cortical stimulation (Gharabaghi et al., 2014). This frequency band was selected on the basis of previous work in our group on beta-band oscillatory circuits in the extended motor network (Khademi et al., unpublished observation). If ERD was sustained or reestablished after the first stimulus, more than one TMS pulse was applied during the motor imagery phase (Figure 1D). On average, 331 ± 77 TMS pulses were applied per subject. The minimum interstimulus interval was set at 500 ms. ERD detection was confined to electrodes FC4, C4 and CP4 over the right sensorimotor area (McFarland et al., 2000).The method that was used to detect ERD has been described in detail elsewhere (Gharabaghi et al., 2014; Kraus et al., 2016). Prior to the experiment, a desynchronization task, consisting of three motor-imagery training runs without stimulation, was performed for calibration to account for each subject’s ability for desynchronization (Kraus et al., 2016). In the primary data analysis (Kraus et al., 2016), the stimulus-locked EEG time-frequency analysis revealed frequency-contingency of TMS pulses during the intervention in comparison to control, i.e., indicating ERD specificity in the 16-22 Hz range before the TMS-pulses.

In the control group, cortical non-specific brain stimulation, cortical stimulation was not triggered by ERD. The stimulation intensity relative to RMT, a number of stimuli and the sequential pattern of cortical stimulation pulses in this measurement

were recorded from the experimental group and were therefore identical in both groups (Figure 1B). This ensured that the same number and pattern of cortical stimuli were applied in experimental and control group, but independent of the ongoing brain activity in the latter. The subjects in the control group were instructed not to perform motor imagery and to maintain muscle relaxation throughout the intervention (Kraus et al., 2016).

During the isometric motor task, a horizontal target bar was presented on a screen 150 cm in front of the subjects and oscillated vertically with a frequency of 0.1 Hz (i.e., cycles of 10 s length). The vertical position of a simultaneously presented cursor could be controlled by the participant via the force of the fingers (digit II–V) which were connected to the robotic orthosis via small magnets attached to the fingertips (Amadeo®, Tyromotion, Graz, Austria). During this isometric motor task, subjects were instructed to control the cursor through flexion and extension to follow the moving horizontal target bar on the screen as quickly and accurately as possible (Figure 1C). This task consisted of 15 trials (10 s each) per each run (2 runs), each of which had one flexion (5 s) and one extension (5 s) phase (Kraus et al., 2016; Naros et al., 2016).

EEG/EMG analysis

The data analysis in this study was different from the previous one (Kraus et al., 2016), which studied motor evoked potentials only. Here, we intended to capture network modulations during the intervention and the motor task thereafter. Data were analyzed offline using the MATLAB (The MathWorks, Inc., Natick, Massachusetts, United States) and FieldTrip open source MATLAB toolbox (http://fieldtrip.fcdonders.nl/; MathWorks). To study the synchronous oscillatory activity of the cortical networks, we applied two complementary methods. We investigated (i) transcranial stimulation evoked potentials (TEP) during the TMS intervention, and (ii) corrected imaginary part of the coherence (ciCOH) both during the intervention and the isometric motor task afterward. Additionally, we investigated (ii) cortico-muscular coherence (CMC) both during the intervention and the isometric motor task to study the synchronous oscillatory activity of EEG and EMG. We, furthermore, explored the phase-frequency relationships within the cortico-muscular network.

Data preprocessing

First, the TMS artifact was cut out, i.e. from -5 ms to +15 ms with respect to the TMS onset. Then, the data during the intervention was cut into 1 s epochs preceding and following each TMS pulse, respectively. If another TMS pulse occurred within this period, i.e. -1 s to +1 s, this epoch was not considered for further analysis to avoid interferences of different stimuli. Thereby, on average of 167 ± 80 epochs were removed from the 331 ± 77 TMS pulses, which were applied per subject. Then, the remaining epochs were visually inspected and excluded, when ocular and muscular artifacts occurred; thereby, on average 45 ± 30 epochs had to be removed. This yielded on average 148 ± 39 TMS pulses (and respective epochs) per subject for further analysis. In the primary data analysis (Kraus et al., 2016), we have already

tested that there was no significant difference in the EMG activity of the two experiments during the intervention and that the induced differences in cortico-spinal excitability after the intervention were not related to different EMG activity in the experiments.

For the isometric motor task, each trial (10 s) was divided into ten 1 s segments. They were visually inspected and excluded, when ocular and muscular artifacts occurred, yielding on average 246 ± 32 epochs per subject, i.e., 25 ± 5 epochs per 1 s segment.

Assessing cortico-cortical connectivity with TEP

In line with former reports (Lioumis et al., 2009; Premoli et al., 2014a), we considered five different TMS-evoked EEG potential (TEP) components (Figure 3A), i.e., P25 (25-30 ms), N45 (35-60 ms), P70 (60-80 ms), N100 (85-140 ms), and P180 (150-230 ms).To assess the TEP peak amplitudes, the signals from each EEG channel were averaged after baseline correction and subtraction of the mean amplitude during an interval between -100 ms and -10 ms before TMS onset (Petrichella et al., 2017). Later, the mean of the amplitude for the specified latency was divided by the baseline absolute value to normalize the amplitude of TEP components for further analysis.

Assessing cortico-cortical connectivity with ciCOH

We used the corrected version of the iCOH function (ciCOH) as suggested by Ewald et al. (2012). The ciCOH shares the same properties as the original iCOH function but includes additional features, i.e., compensating for preference for remote interactions (Ewald et al., 2012). The ciCOH results in an increase in signal to noise ratio (SNR), which potentially leads to observations of interactions, which are otherwise hidden in the noise when studying connectivity between sensors. The

imaginary part of coherence was computed by using the cross-spectral density matrix frequency analysis between the C4 channel and all other EEG channels. The cross-spectral density matrix was calculated frequency-wise using the multi-tapper method (9 tappers) over the frequency range from 2 to 46 Hz in steps of 1 Hz. Then, the imaginary part of coherence was normalized according to the square root of the real part and was Fisher z-transformed to fit a Gaussian distribution (Nolte et al., 2004; Rosenberg et al., 1989). For contrasting conditions, the absolute value of the ciCOH was used. The contrast between pre- and post-TMS ciCOH indicated the induced cortico-cortical coherence, which was used for further analysis.

Assessing cortico-muscular connectivity with CMC

Cortico-muscular coherence (CMC) was computed by using the cross-spectral density matrix frequency analysis between EEG and a rectified signal of EMG channels. The cross-spectral density matrix was calculated using the multi-tapper method (9 tappers) over the frequency range of 2 to 46 Hz in steps of 1 Hz. We obtained the magnitude of the coherence values by normalizing the magnitudes of the summed cross-spectral density matrix for each frequency to the corresponding power values at that frequency. Then the CMC magnitudes were Fisher z-transformed to fit a Gaussian distribution (Nolte et al., 2004; Rosenberg et al., 1989). The contrast between pre- and post-TMS CMC indicated the induced cortico-muscular coherence, which was used for further analysis.

Assessing the relationship between ciCOH and CMC

We used Spearman's rank correlation to evaluate the relationship between ciCOH and the corresponding CMC across subjects. The statistically significant clusters of the previous analyses for ciCOH and CMC (see above) were chosen for this

estimation. Specifically, the maximum ciCOH/CMC value from each cluster was subtracted from the median value of the respective cluster for each subject individually to compensate for variability. Per subject, one pair of ciCOH/CMC was used for further analysis.

Assessing the CMC phase-frequency relationships

The phase-frequency relationships (PFR) were estimated frequency-wise (every 1 Hz) following the CMC estimation (Witham et al., 2011) PFR were estimated for pre- and post-TMS epochs. The phase was estimated by taking the argument from the estimated EEG-EMG cross-spectrum. The phase delays were calculated by fitting a line to the phase–frequency plot by using linear regression over the frequency range, which showed a significant increase in the CMC magnitude (Witham et al., 2011).

Statistical analysis

Testing significance of cortico-cortical connectivity with TEP

Cluster-based randomization test statistic (Maris et al., 2007) was chosen to quantify the significance of the difference between experimental and control groups. The null hypothesis was that there is no difference between the amplitude of TEP components of experimental and control groups. The student t-test (p=0.05) was chosen for the selection of significant channels. When the t-statistic exceeded the threshold (p=0.05), adjacent EEG channels were clustered in the same set. Cluster-level statistics were, then, conducted by taking the sum of the t-statistics from the EEG channels. In case multiple clusters were observed, the cluster with the maximum cluster-level statistics was used for later comparisons. The p-value to reject the null hypothesis was the proportion of cluster-based randomizations that resulted in larger

test statistics than the observed one (without randomization). The same procedure was used to quantify the significance of the difference between start and end of intervention for each group, separately.

Testing significance of cortico-cortical connectivity with ciCOH and cortico-muscular connectivity with CMC

The artifact rejection led an unequal d.f. for the epochs during the intervention 2953 ± 646 and the motor task (443 ± 82). We, therefore, estimated a Z-statistic of the induced coherence difference in the course of the intervention before nonparametric statistical evaluation (Maris et al., 2007).

Having the null hypothesis that the observed increase in ciCOH/CMC was not the effect of the intervention, we used cluster-based randomization test statistic to randomize (1000 times) ciCOH/CMC values between experimental and control groups. We used a cluster-based nonparametric statistic to assess the significant coherence modulation of neighboring EEG channels. The cluster-based randomization test was performed for each frequency band of interest. The frequency bands were selected to cover the frequency band targeted by the intervention (16-22 Hz) and the neighboring frequency bands with the same bandwidth (9-15 Hz, 23-29 Hz, and 30-36 Hz) for balanced statistical comparisons.

In each step of randomization, we calculated the Z-statistic frequency-wise. For every frequency band, adjacent EEG channels were clustered in the same set when the maximum of Z-statistics from the respective frequency band exceeded the threshold of $Z>1.65$ ($p<0.05$, Maris et al., 2007). Cluster-level statistics were, then, calculated by taking the sum of the Z-statistics from the corresponding frequency band for each cluster. In case of multiple clusters, the maximum cluster-level statistic

was used for later comparisons. The p-value to reject the null hypothesis was the proportion of cluster-based randomizations that resulted in a larger test statistic than the observed one (with no randomization). We reject the null hypothesis for $p \leq 0.0001$.

Testing significance of the phase-frequency relationships

We calculated the mean of the estimated CMC phase for each frequency across subjects, yielding one phase-frequency spectrum. We, then, fitted a line to the phase-frequency plot using a linear regression (i.e., over a range of frequencies with significant CMC) and estimated the contrast of the estimated regression slope between pre- and post-TMS phase spectra. The estimated regression slope was significantly different from zero for $p<0.05$.

Results

The experimental group showed a significant increase in the positivity of the P180 TEP component as compared to the control group (Figure 3A, B). Moreover, this TEP component was the only one increasing in the course of the intervention; this evolution was specific for the experimental group (Figure 3C). The cortical topography of the P180 TEP component showed an *inter*-hemispheric pattern when comparing the experimental and control groups (Figure 3B; F3, FC5, FC3, C5, C3, C1, CP5, CP3, CP1, and P3; $p<0.0001$; cluster-based randomization test; 1000 repetitions); the experimental group showed, furthermore, an *intra*-hemispheric pattern to posterior areas in the course of the intervention (Figure 3C; Figure 3C; FC5, FC3, C5, CP5, CP3, CPz, CP2, Cp4, CP6, and P4; $p<0.0001$; cluster-based randomization test; 1000 repetitions).

This inter- and intra-hemispheric pattern was also observed in the coherence analysis. Specifically for the targeted frequency band (16-22 Hz), the induced cortico-cortical functional connectivity (ciCOH) was significantly higher in the experimental group than the control group (Figure 4A; FC2, FC4, FC6, C2, C6,CP5, CP3, CP1, CPz,CP2, CP4, and P4; $p<0.0001$; cluster-based randomization test; 1000 repetitions). This connectivity pattern was paralleled by significantly increased cortico-muscular coherence (CMC) in the targeted frequency band (16-22 Hz) from bilateral sensorimotor areas to the left EDC muscle (Figure 4B, FC6, C5, C3, Cz, C2, C4, C6, CP5, CP3, CP1, CPz, CP2, CP4, and P4;$p< 0.0001$; cluster-based randomization test; 1000 repetitions).

The induced CMC in the experimental group was paralleled by a significant change in the phase-frequency relationships (PFR). The PFR showed different directionality for each hemisphere, i.e., there was a negative and positive slope significantly different from zero ($p<0.05$; F-statistic) for the right and left hemisphere, respectively (Figure 4C). This indicated a leading direction of interaction from cortex to muscle in the right hemisphere, i.e., ipsilateral to the site of TMS (C2, C6, and CP4), and from muscle to cortex in the left hemisphere, i.e., contralateral to the site of TMS (C5, C3, CP5, CP3, and CP1). The average PFR phase delays were 19.33 ± 9.07 ms and 19.80 ± 5.11 for the right and left hemisphere, respectively.

Spearman's rank correlation showed a significant relationship between the induced bilateral cortico-cortical (ciCOH) and cortico-muscular (CMC) coherence in the experimental group (Figure 4D, E; $r=0.65$ $p=0.013$; Spearman's rank correlation, nonparametric randomization test, 1000 repetitions).

The connectivity pattern induced in the experimental group during the intervention persisted afterward during the motor task, i.e., in the absence of TMS,

revealing an inter-hemispheric pattern in the coherence analysis. Specifically for the targeted frequency band (16-22 Hz), the induced cortico-cortical functional connectivity (ciCOH) was significantly higher in the experimental group than the control group (Figure 5A; FC5, FC3, FC1, C5, C3, C1, Cz, CP5, CP3, and CP1; $p=0.026$; cluster-based randomization test; 1000 repetitions). This connectivity pattern was paralleled by significantly increased cortico-muscular coherence (CMC) in the targeted frequency band (16-22 Hz) from bilateral sensorimotor areas to the left EDC muscle (Figure 5B; FC2, FC4, FC6, C5, C3, C1, C2,C6, CP5,Cp3,Cp1,CPz, Cp2,Cp4, and P4; $p<0.0001$; cluster-based randomization test; 1000 repetitions).

Importantly, both ciCOH and CMC connectivity modulations occurred in the same movement interval of the motor task, i.e., during initiation of the finger extension movement.

Discussion

In this study with healthy subjects, we investigated a novel stimulation protocol that applied intrinsic brain states during motor-imagery of finger extension to trigger transcranial magnetic stimulation to the respective cortical motor representation within a brain-computer interface environment. The state-dependent approach – but not the same number and pattern of stimuli applied during rest - resulted in a significant and frequency-specific enhancement of cortico-spinal and cortico-cortical motor network connectivity in the course of the intervention and thereafter. This network plasticity was task-specific, i.e., occurred in the subsequent motor task only during initiation of finger extension.

Methodological considerations

This study differed from previous work in several methodological regards: (i) The stimulation protocol was applied during a cognitive task. (ii) The induced local and network-based plasticity was evaluated task-dependent as well. (iii) Both online effects and aftereffects of the stimulation were captured in the same way, i.e., by cortico-spinal and cortico-cortical connectivity. (iv) Both local and network-level effects were measured with the same neurophysiological parameter, i.e., the coherence of oscillatory activity.

(i) Previous TMS protocols for plasticity induction were applied at rest (Bestmann et al., 2003; 2005; Veniero et al., 2013; Nettekoven et al., 2014, Volz et al., 2016) or during overt movement (Bütefisch et al., 2004; Thabit et al., 2010; Bütefisch et al., 2011; Narayana et al., 2014). In this study, we stimulated the activated motor system, but in the absence of an actual movement; single TMS pulses were applied during self-regulation of the intrinsic brain state via motor imagery of finger extension. In future patient studies, this approach may provide a useful activity-triggered stimulation protocol for targeting brain circuits of lost motor function.

(ii) Previously, the TMS-induced plasticity of motor networks has been evaluated at rest as well (Bestmann et al., 2003; 2005; Veniero et al., 2013; Nettekoven et al., 2014; Volz et al., 2016). Motor network connectivity is, however, known to be state-dependent (Rehme et al., 2013). Activity-dependent properties of the cortical motor system before the intervention were, furthermore, shown to be indicative of the resulting excitability changes (Cardenas-Morales et al., 2014). It was therefore plausible to assume that stimulation protocols applied during different activity states (i.e., MI vs. rest) will impact task-related motor network connectivity

differentlly - both with regard to online effects and after effects. This study provided empirical support for this hypothesis. The same number and pattern of stimuli applied during MI resulted in significantly enhanced motor network connectivity as compared to the control application during rest. One possible explanation for this findings is that stronger activity-dependent synaptic transmission increases the susceptibility of the stimulated motor network for an external stimulus and Hebbian-like plastic changes.

(iii) Potential neurophysiological mechanisms of motor network plasticity could be elucidated by capturing the same connectivity parameters both during the intervention and thereafter. This approach revealed, in particular, the frequency-selectivity of the motor network entrainment by the state-dependent stimulation protocol. Importantly, this frequency-selectivity persisted during the subsequent motor task for both cortico-spinal and cortico-cortical connectivity.

(iv) Previous studies on motor network plasticity measured local and systems-level plasticity usually by different means, e.g., cortico-spinal excitability by TMS induced MEPs and cortical connectivity changes by the resting BOLD signal, respectively (Bestmann et al., 2003; 2005; Nettekoven et al., 2014; Volz et al., 2016). Applying the same neurophysiological parameter, i.e., the magnitude of coherence between oscillatory activity for both cortico-muscular and cortico-cortical connectivity allowed studying their interaction with regard to the cortical topology and spectral characteristics. Moreover, this approach provided additional motor state-dependent information to elucidate the task-specificity, i.e. for finger extension, of the motor network entrainment on a moment-to-moment basis during the isometric motor task (Mehrkanoon et al., 2014).

Neurophysiological considerations

The brain state-dependent stimulation paradigm applied here has already been shown to induce M1 plasticity, i.e., increased cortico-spinal excitability (indexed by the MEP amplitude) that outlasted the stimulation itself (Kraus et al., 2016). In this study, we demonstrated that this local plasticity was paralleled by frequency-selective and task-specific network-level plasticity as well:

Single-pulse TMS applied to the primary motor cortex during rest has been shown to induce synchronization, likely reflecting phase-resetting, of ongoing β-band oscillations - which are amplified by the thalamus- for several hundred milliseconds in the vicinity of the stimulation site (Paus et al. 2001; van der Werf and Paus, 2006; Chung et al. 2015). When increasing the intensity of the TMS pulse applied to the primary motor cortex, the induced oscillatory activity did not occur at the targeted site only but extended to distant cortical areas such as the frontal and parietal cortex of the ipsilateral hemisphere as well (Fuggetta et al., 2005). When comparing these TMS induced oscillatory activity with movement-related spectral perturbations such as event-related sensorimotor desynchronization (ERD), the same study revealed a larger magnitude of modulation and a relevant involvement, i.e. functional connectivity, of both hemispheres for the latter. However, TMS and the ERD-task were not applied simultaneously but in different experiments, leaving the open question how TMS induced oscillatory synchronization would interact with task-related desynchronization, e.g., during motor-imagery.

In this study, the TMS stimuli were applied during a cognitive task of MI and neurofeedback that has previously been shown to modulate both ERD and cortico-cortical connectivity in a frequency-specific way (Vukelic and Gharabaghi, 2015 a, b; Naros et al., 2016). In this data, the self-regulated ERD before the TMS pulses was

frequency-specific as well, i.e., in the 16-22 Hz range that was reinforced by the neurofeedback task (Kraus et al., 2016).

The state-dependent stimulation resulted in a significant intra- and interhemispheric TEP increase in the course of the intervention; specifically, to the parietal and sensorimotor area ipsi- and contralateral to the site of stimulation, respectively (Figure 3C). There was no TEP change in the control condition. This observation suggests a facilitation of signal propagation during the MI task and is consistent with previous task-related findings; during a memory task an increased spatial spread of the TMS-evoked activity to distal brain regions and increased phase reset of oscillatory activity as compared to the stimuli applied at rest was detected (Johnson et al., 2012). The contrast between intervention and control in the present study was particularly characterized by an inter-hemispheric enhancement of effective connectivity, i.e., TEP (Figure 3B), potentially facilitated by the dense transcallosal connections. This phenomenon was specific to the P180 TEP-component (Figure 3A) and suggests, therefore, an MI task-related GABAergic modulation of long-interval intracortical inhibition at the motor network-level (Premoli et al., 2014 a, b). This extends and complements previous findings that demonstrated MI-related modulation of short-interval intracortical inhibition of the motor cortex at the local level (Abbruzzese et al., 1999; Stinear and Byblow, 2004).

Importantly, both the immediate and the subsequent entrainment of oscillatory interactions were specific for the targeted frequency (16-22 Hz); this suggests that the cognitive task during the intervention contributed to a shaping of the TMS induced phase reset within the motor network. One might speculate that the coactivation of these interconnected regions enhanced not only the signal transmission between them but also the synchronicity of the respective neural activity

(Nettekoven et al., 2014). The increased frequency-specific coherence of motor network connections persisted after the intervention and re-occurred during the subsequent motor task which was performed in the same way by both groups. This finding indicates that the observed differences in connectivity were - at least not completely - related to instantaneous attentional differences between conditions during the intervention. While attention has been shown to influence PAS protocols (Stefan et al., 2004), the present findings may reflect rather a Hebbian-like modulation of specific circuits as suggested by the both the frequency-selectivity and the task-specificity of the connectivity changes. This specificity is most parsimoniously explained by the fact that the kinesthetic MI task applied here activates similar neuronal correlates to those during motor execution (Lotze et al., 1999; Neuper et al., 2005), increases cortico-spinal excitability and decreases short intracortical inhibition in a muscle- and task-specific way (Stinear and Byblow, 2004; Roosink and Zijdewind, 2010). This would open the interesting possibility to functionally target and enhance specific circuits with a state-dependent stimulation paradigm, e.g. during MI of finger extension, in order to restore (and not only to compensate for) a lesioned motor network that does not lead to an overt movement yet (Small et al., 2013).

Limitations and future directions

Future work needs to clarify several questions: do the observed effects last for longer periods than examined in the present study, are they dose-dependent and would ultimately lead to behavioral gains as well. Future studies may explore this paradigm during other movements as well to better delineate the task-specificity of the effects. To strengthen the brain state-dependency of the observation, future studies may also include event related synchronization (ERS)-related TMS as a control condition. To

confirm the frequency-selectivity of the effects, other frequency bands, e.g., the α-band which gates information by inhibiting task-irrelevant regions (Jensen and Mazaheri, 2010) should also be explored.

In conclusion, functional enhancement of task-specific motor network interactions may be achieved when the cortical input is paired with self-regulated intrinsic brain states. These findings are probably mediated via a Hebbian mechanism and are potentially important for developing closed-loop brain stimulation for the treatment of hand paralysis after stroke.

References

Abbruzzese G, Assini A, Buccolieri A, Marchese R, Trompetto C (1999) Changes of intracortical inhibition during motor imagery in human subjects. Neurosci Lett 263:113-116.

Bauer R, Fels M, Vukelić M, Ziemann U, Gharabaghi A (2015) Bridging the gap between motor imagery and motor execution with a brain-robot interface. Neuroimage 108:319-327.

Bestmann S, Baudewig J, Siebner HR, Rothwell JC, Frahm J (2003) Subthreshold high-frequency TMS of human primary motor cortex modulates interconnected frontal motor areas as detected by interleaved fMRI-TMS. Neuroimage 20:1685-1696.

Bestmann S, , Siebner HR, Rothwell JC, Frahm J (2005) BOLD MRI responses to repetitive TMS over human dorsal premotor cortex. Neuroimage 28:22-29.

Bütefisch CM (2004) Plasticity in the human cerebral cortex: lessons from the normal brain and from stroke. Neuroscientist 10:163-173.

Bütefisch C, Heger R, Schicks W, Seitz R, Netz J (2011) Hebbian type stimulation during robot-assisted training in patients with stroke. Neurorehabil Neural Repair 25:645–655.

Cárdenas-Morales L, Volz LJ, Michely J, Rehme AK, Pool EM, Nettekoven C, Eickhoff SB, Fink GR, Grefkes C (2014) Network connectivity and individual responses to brain stimulation in the human motor system. Cereb Cortex 24:1697-1707.

596 Chung SW, Rogasch NC, Hoy KE, Fitgeraled PB (2015) Measuring brain stimulation
597 induced changes cortical properties using TMS-EEG. Brain Stimul 8:1010-
598 1020.

599 Dayan E, Cohen LG (2011) Neuroplasticity subserving motor skill learning. Neuron
600 72:443-454.

601 Ewald A, Marzetti L, Zappasodi F, Meinecke FC, Nolte G (2012) Estimating true brain
602 connectivity from EEG/MEG data invariant to linear and static transformations
603 in sensor space. NeuroImage 60:476–488.

604 Fox MD, Raichle ME (2007) Spontaneous fluctuations in brain activity observed with
605 functional magnetic resonance imaging. Nat Rev Neurosci 8:700-711.

606 Fuggetta G, Fiaschi A, Manganotti P (2005) Modulation of cortical oscillatory
607 activities induced by varying single-pulse transcranial magnetic stimulation
608 intensity over the left primary motor area: a combined EEG and TMS study.
609 Neuroimage 27:896-908.

610 Gharabaghi A, Kraus D, Leão MT, Spüler M, Walter A, Bogdan, M, Rosenstiel W,
611 Naros G, Ziemann U (2014) Coupling brain–machine interfaces with cortical
612 stimulation for brain-state dependent stimulation: enhancing motor cortex
613 excitability for neurorehabilitation. Front Hum Neurosci 8:122.

614 Groppa S, Schlaak BH, Münchau A, Werner-Petroll N, Dünnweber J, Bäumer T, van
615 Nuenen BF, Siebner HR (2012) The human dorsal premotor cortex facilitates
616 the excitability of ipsilateral primary motor cortex via a short latency cortico-
617 cortical route. Hum Brain Mapp 33:419-430.

618 Hebb DO (1949) The Organization of Behavior: A Neuropsychological Theory. New
619 York:Wiley.

620 Jensen O, and Mazaheri A (2010) Shaping Functional Architecture by Oscillatory
621 Alpha Activity: Gating by Inhibition. Front in Human Neurosci 4: 186.

622 Johnson JS, Kundu B, Casali AG, Postle BR (2012) Task-dependent changes in
623 cortical excitability and effective connectivity: a combined TMS-EEG study. J
624 Neurophysiol 107:2383-2392.

625 Kraus D, Naros G, Bauer R, Khademi F, Leão MT, Ziemann U, Gharabaghi A (2016)
626 Brain state-dependent transcranial magnetic closed-loop stimulation controlled
627 by sensorimotor desynchronization induces robust increase of cortico-
628 muscular excitability. Brain Stimul 9:415-424.

629 Lioumis P, Kicić D, Savolainen P, Mäkelä JP, Kähkönen S (2009) Reproducibility of
630 TMS-Evoked EEG responses. Hum Brain Mapp 30:1387-1396.

631 Lotze M, Montoya P, Erb M, Hülsmann E, Flor H, Klose U, Birbaumer N, Grodd W
632 (1999) Activation of cortical and cerebellar motor areas during executed and
633 imagined hand movements: an fMRI study. J Cogn Neurosci 11:491-501.

634 Maris E, Schoffelen JM, Fries P (2007) Nonparametric statistical testing of coherence
635 differences. J Neurosci Methods 163:161-175.

636 McFarland DJ, Miner LA, Vaughan TM, Wolpaw JR (2000) Mu and beta rhythm
637 topographies during motor imagery and actual movements. Brain Topogr
638 12:177–186.

639 Mehrkanoon S, Breakspear M, Boonstra TW (2014) The reorganization of
640 corticomuscular coherence during a transition between sensorimotor state.
641 Neuroimage100:692:702.

642 Miller KJ, Leuthardt EC, Schalk G, Rao RPN, Anderson NR, Moran DW, Miller JW,
643 and Ojemann JG (2007) Spectral Changes in Cortical Surface Potentials
644 during Motor Movement. J Neurosci 27: 2424–2432.

645 Miller, KJ., Schalk G, Fetz EE, Den Nijs M, Ojemann JG, Rao RP (2010) Cortical
646 activity during motor execution, motor imagery, and imagery-based online
647 feedback. Proceedings of the National Academy of Sciences 107:4430-4435.

648 Murphy TH, Corbett D (2009) Plasticity during stroke recovery: from synapse to
649 behaviour. Nat Rev Neurosci 10:861-872.

650 Narayana S, Zhang W, Rogers W, Strickland C, Franklin C, Lancaster JL, Fox PT
651 (2014) Concurrent TMS to the primary motor cortex augments slow motor
652 learning. Neuroimage 3:971-984.

653 Naros G, Naros I, Grimm F, Ziemann U, Gharabaghi A (2016) Reinforcement
654 learning of self-regulated sensorimotor β-oscillations improves motor
655 performance. Neuroimage 134:142-152.

656 Nettekoven C, Volz LJ, Kutscha M, Pool EM, Rehme AK, Eickhoff SB, Fink GR,
657 Grefkes C (2014) Dose-dependent effects of theta burst rTMS on cortical
658 excitability and resting-state connectivity of the human motor system. J
659 Neurosci 34:6849-6859.

660 Neuper C, Scherer R, Reiner M, Pfurtscheller G (2005) Imagery of motor actions:
661 differential effects of kinesthetic and visual-motor mode of imagery in single-
662 trial EEG. Brain Res Cogn Brain Res 25:668-677.

663 Nolte G, Bai O, Wheaton L, Mari Z, Vorbach S, Hallett M (2004) Identifying true brain
664 interaction from EEG data using the imaginary part of coherency. Clin
665 Neurophysiol 115:2292–2307

666 Oldfield RC (1971) The assessment and analysis of handedness: the Edinburgh
667 inventory. Neuropsychologia 9:97–113.

668 Paus T, Sipila PK, Strafella AP (2001) Synchronization of neuronal activity in the
669 human primary motor cortex by transcranial magnetic stimulation: an EEG
670 study. J Neurophysiol 86:1983-1990.

671 Petrichella S, Johnson N, He B (2017) The influence of corticospinal activity on TMS-
672 evoked activity and connectivity in healthy subjects: A TMS-EEG study. PLoS
673 ONE12: e0174879.

674 Pfurtscheller G, Neuper, C (1997) Motor imagery activates primary sensorimotor area
675 in humans. Neuroscience letters 239: 65-68.

676 Premoli I, Castellanos N, Rivolta D, Belardinelli P, Bajo R, Zipser C, Espenhahn S,
677 Heidegger T, Mueller-Dahlhaus F, Ziemann U (2014a) TMS-EEG signatures of
678 GABAergic neurotransmission in the human cortex. J Neurosci 34:5603-5612.

679 Premoli I, Rivolta D, Espenhahn S, Castellanos N, Belardinelli P, Ziemann U, Müller-
680 Dahlhaus F (2014b) Characterization of GABAB-receptor mediated
681 neurotransmission in the human cortex by paired-pulse TMS-EEG.
682 Neuroimage 103:152-162.

683 Rehme AK, Eickhoff SB, Grefkes C (2013) State-dependent differences between
684 functional and effective connectivity of the human cortical motor system.
685 Neuroimage 67:237–246.

686 Rossi S, Hallett M, Rossini PM, Pascual-Leone A, The Safety of TMS Consensus
687 Group (2009) Safety, ethical considerations, and application guidelines for the
688 use of transcranial magnetic stimulation in clinical practice and research. Clin
689 Neurophysiol 120:2008‑2039.

690 Roosink M, Zijdewind I (2010) Corticospinal excitability during observation and
691 imagery of simple and complex hand tasks: implications for motor
692 rehabilitation. Behav Brain Res 213:35-41.

693 Rosenberg JR, Amjad AM, Breeze P, Brillinger DR, Halliday DM (1989) The Fourier
694 approach to the identification of functional coupling between neuronal spike
695 trains. Prog Biophys Mol Biol 53:1–31

696 Schalk G, McFarland DJ, Hinterberger, T, BirbaumerN,Wolpaw JR (2004) BCI2000: a
697 general-purposebrain–computerinterface (BCI) system. IEEE Trans Biomed
698 Eng 51:1034–1043.

699 Schnitzler A, Gross J (2005) Normal and pathological oscillatory communication in
700 the brain. Nat Rev Neurosci 6:285-296.

701 Small SL, Buccino G, Solodkin A (2013) Brain repair after stroke--a novel
702 neurological model. Nat Rev Neurol 9:698-707.

Stefan K, Wycislo M, Classen J (2004) Modulation of associative human motor cortical plasticity by attention. J Neurophysiol 92:66-72.

Stinear CM, Byblow WD (2004) Modulation of corticospinal excitability and intracortical inhibition during motor imagery is task-dependent. Exp Brain Res 157:351-358.

Suppa A, Quartarone A, Siebner H, Chen R, Di Lazzaro V, Del Giudice P, Paulus W, Rothwell JC, Ziemann U, Classen J (2017) The associative brain at work: Evidence from paired associative stimulation studies in humans. Clin Neurophysiol 128:2140-2164.

Takemi M, Masakado Y, Liu M, Ushiba J (2013) Event-related desynchronization reflects downregulation of intracortical inhibition in human primary motor cortex. J Neurophysiol 110:1158-1166.

Thabit MN, Ueki Y, Koganemaru S, Fawi G, Fukuyama H, Mima T (2010) Movement-related cortical stimulation can induce human motor plasticity. J Neurosci 30:11529-1136.

Van Der Werf YD, Paus T (2006) The neural response to transcranial magnetic stimulation of the human motor cortex. I. Intracortical and cortico-cortical contributions. Exp Brain Res 175:231-245.

Veniero D, Bortoletto M, Miniussi C (2012) Cortical modulation of short-latency TMS-evoked potentials. Front Hum Neurosci 6:352.

Volz LJ, Rehme AK, Michely J, Nettekoven C, Eickhoff SB, Fink GR, Grefkes C (2016) Shaping Early Reorganization of Neural Networks Promotes Motor Function after Stroke. Cereb Cortex 26:2882-2894.

Vukelić M, Bauer R, Naros G, Naros I, Braun C, Gharabaghi A (2014) Lateralized alpha-band cortical networks regulate volitional modulation of beta-band sensorimotor oscillations. Neuroimage 87:147-153.

Vukelić M, Gharabaghi A (2015a) Oscillatory entrainment of the motor cortical network during motor imagery is modulated by the feedback modality. NeuroImage 111:1–11.

Vukelić M, Gharabaghi A (2015b) Self-regulation of circumscribed brain activity modulates spatially selective and frequency specific connectivity of distributed resting state networks. Front Behav Neurosci 9.

Witham CL, Riddle CN, Baker MR, Baker SN (2011) Contributions of descending and ascending pathways to corticomuscular coherence in humans. J Physiol 589:3789-3800.

738 Ziemann U, Paulus W, Nitsche MA, Pascual-Leone A, Byblow WD, Berardelli A,
739 Siebner HR, Classen J, Cohen LG, Rothwell JC (2008) Consensus: Motor
740 cortex plasticity protocols. Brain stimul 1:164–182.

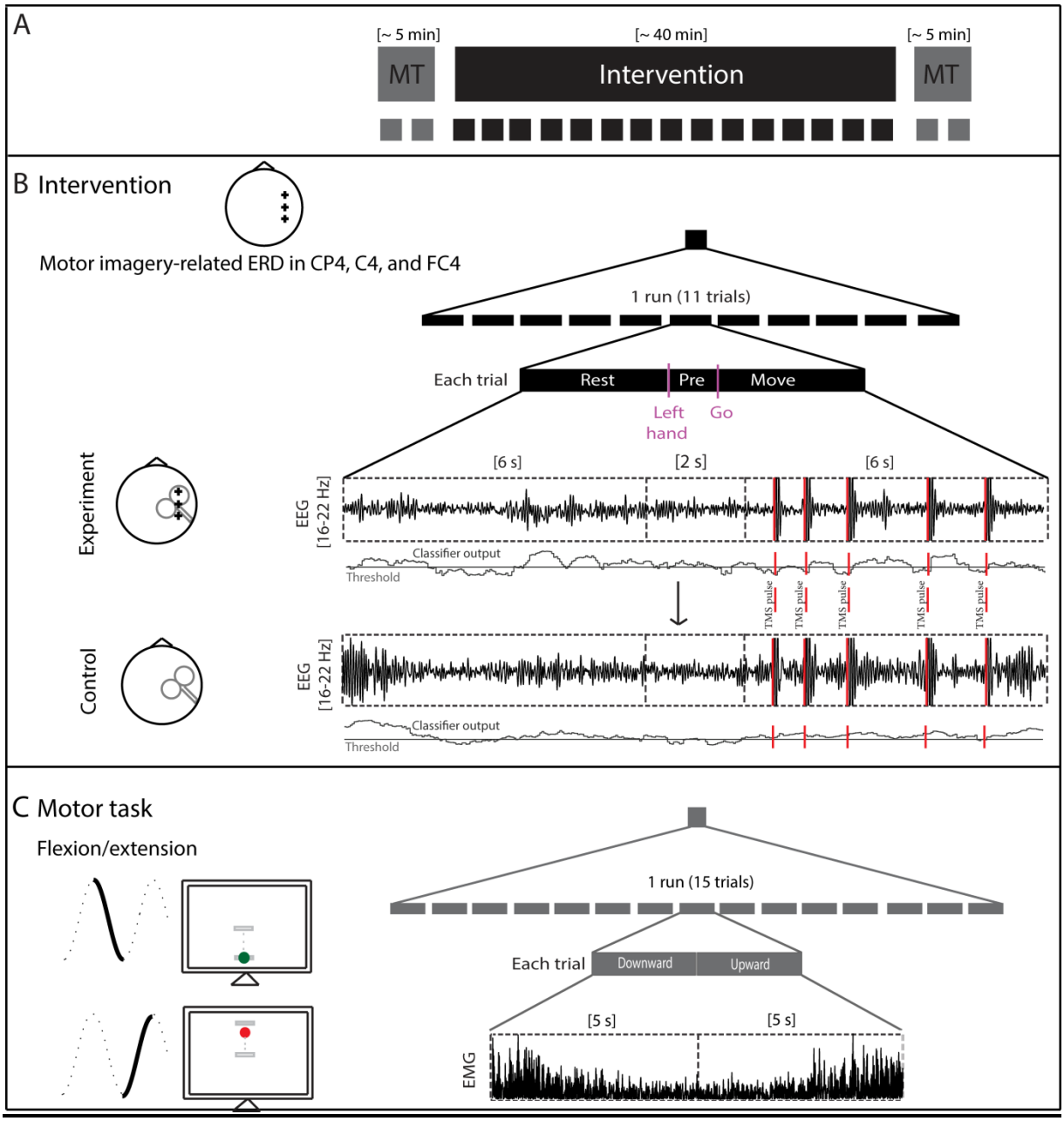

Figure 1. *Experimental design and example data*. ***A,*** Schematic illustration of the experimental design and timeline. ***B,*** Participants underwent a neurofeedback intervention of modulating beta-activity (16-22 Hz) in circumscribed premotor and sensorimotor regions (marked by '+' on the topography, i.e., FC4, C4, and CP4) of the right hemisphere by kinesthetic motor imagery (MI). Participants received single-pulse TMS with one of two different modalities. In the experimental group (n=11), TMS pulses were applied contingent to motor imagery-associated beta desynchronization. In the control group (n=11), TMS pulses were applied independent of the brain state but with the identical pattern, which was recorded from the experimental group. ***C,*** Participants performed a motor task (~5 minutes) before

and after the intervention. An oscillating target (0.1 Hz) was presented on a screen. Participants were instructed to follow the target by a cursor which was controlled by isometric flexion and extension of the left hand that was attached to a hand orthosis.

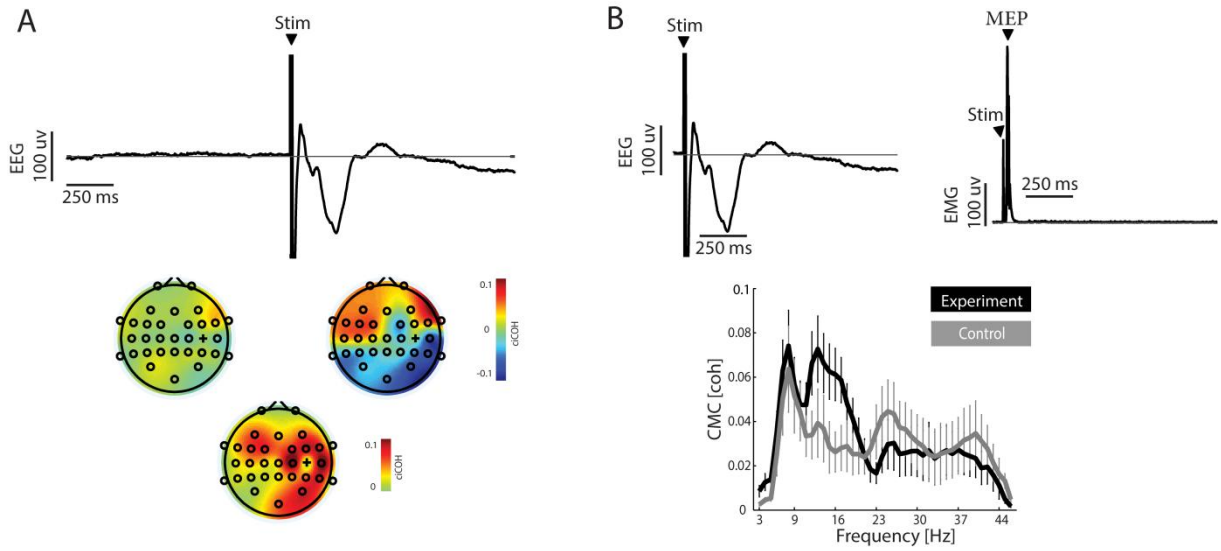

Figure 2. *Example data of pre/post-TMS oscillatory activity (EEG/EMG) and MEP.* ***A,*** The raw EEG signals were cut into epochs of ±1s around the TMS pulse to estimate the pre-TMS (left topography) and post-TMS (right topography) networks connected to the site of stimulation, i.e., C4 channel (indicated by '+'). The contrast between these two networks indicated the induced cortico-cortical coherence(lower topography). ***B,*** The raw EEG (upper left plot) and EMG (upper right plot) signals were cut into epochs of 1s after the TMS pulse to estimate the post-TMS CMC between cortex and EDC muscle. The CMC spectra (lower plot) demonstrate group results of the induced CMC between the C4 channel and EDC muscle for experimental (black) and control (gray) groups, respectively.

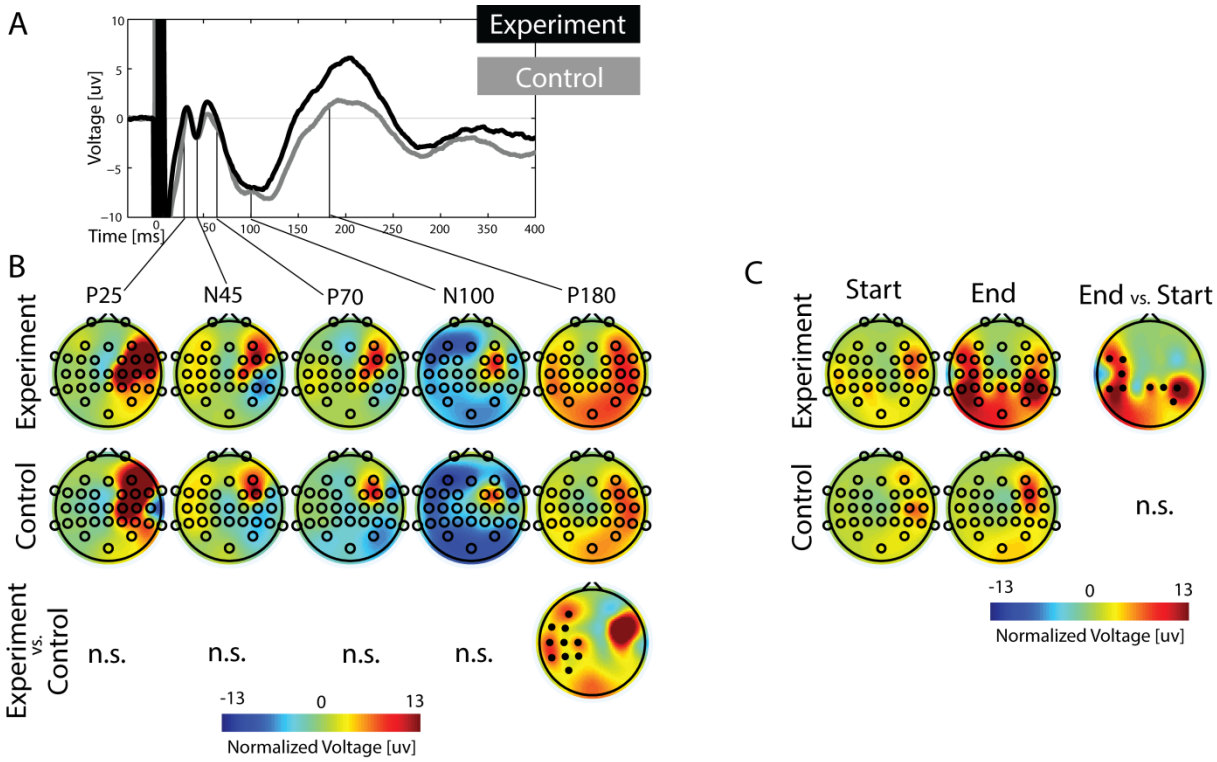

769

770 **Figure 3.** *TMS evoked cortical potentials*. ***A,*** Average of TEPs (over FC3, C3, and
771 CP3 electrodes) induced by TMS to the right motor cortex at the hotspot of the left
772 EDC muscle. TEP components are labeled according to their polarity and
773 approximate latency. ***B,*** Topographical distributions of surface voltages were
774 presented for the most pronounced TEP components (P25, N45, P70, N100, P180)
775 for the experimental (upper topographies) and control group (middle topographies)
776 and the significant difference between groups (lower topography), respectively. Black
777 circles indicate clusters with statistically significant modulation (cluster-base test
778 statistic). Red represents an increase in positivity. N.s. stands for not significant. ***C,***
779 Same as ***B*** but comparison between start and end of the intervention for each group
780 separately.

781

782

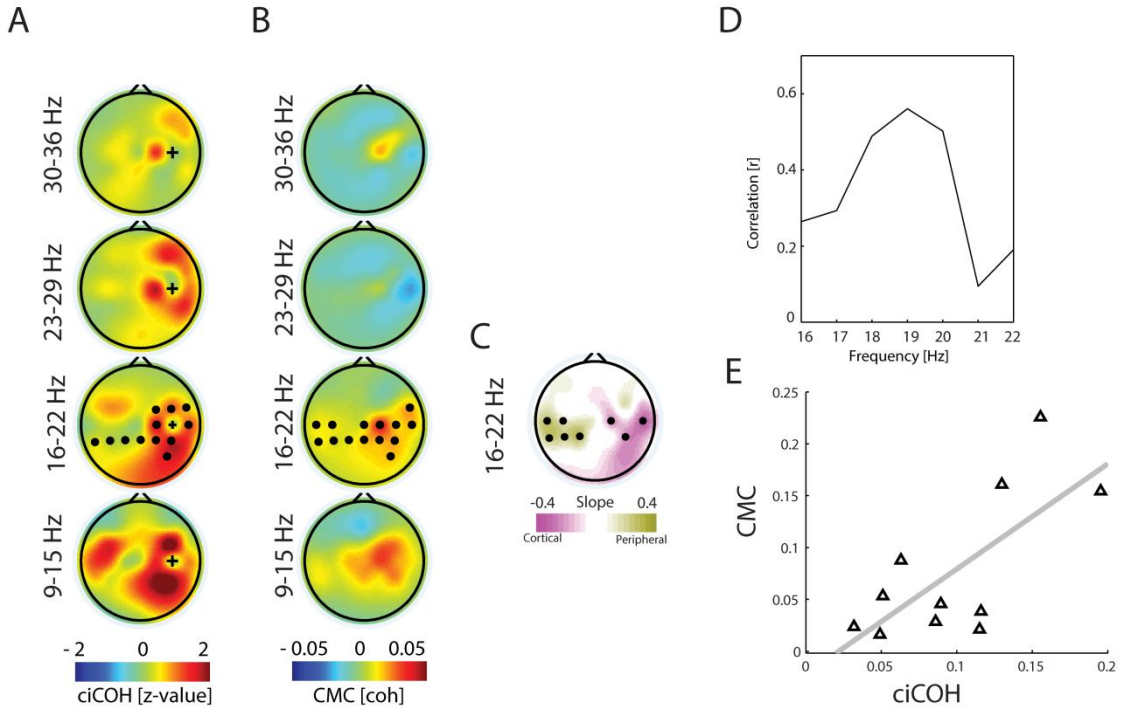

Figure 4. TMS induced c*ortico-cortical and cortico-muscular coherence.* ***A,*** Group data of the TMS induced ciCOH for four frequency bands (9-15 Hz, 16-22 Hz, 23-29 Hz, and 30-36 Hz). Black circles indicate clusters with statistically significant modulation (cluster-base test statistic) in the course of the intervention as a contrast between experimental and control groups. ***B,*** Same as ***A*** but for the TMS induced CMC. ***C,*** Topography of the *regression slope of phase spectra* for 16-22 Hz (group result; contrast between pre- and post TMS phase spectra of the experimental group). Magenta and dark yellow colors indicate the directionality of information flow from cortex to periphery and from periphery to cortex, respectively. Black circles represent the EEG channels, which have a regression slope that is significantly different from zero. ***D,*** Spearman's rank correlation between induced ciCOH (A) and CMC (B) for 16-22 Hz in the experimental group. ***E,*** Same as ***D*** but for the peak of the correlation coefficient 19 ±1 Hz; r=0.65p=0.013. Each triangle represents one subject.

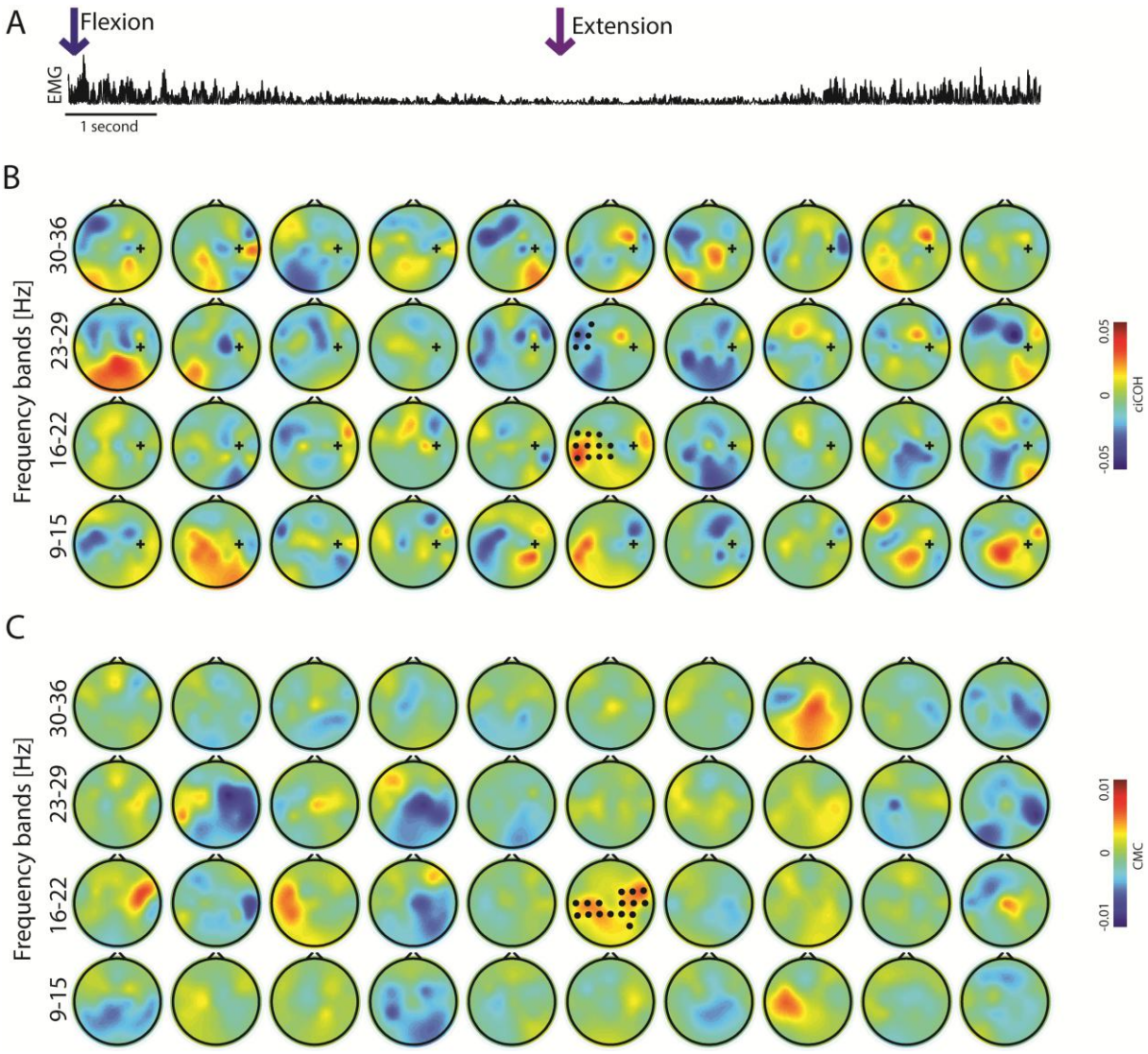

Figure 5. *Cortico-cortical and cortico-muscular coherence during the motor task*. ***A,*** The average of the EMG activity of the EDC muscle across all subjects. Blue and purple arrows represent the start of flexion and extension, respectively. ***B,*** Group data of cortical connectivity (i.e., ciCOH) as the contrast between experimental and control groups.Black circles indicate clusters with statistically significant modulation (cluster-base test statistic). ***C,*** Same as ***B*** but for CMC.

frontiers in
BEHAVIORAL NEUROSCIENCE

METHODS ARTICLE
published: 09 December 2014
doi: 10.3389/fnbeh.2014.00429

Learned self-regulation of the lesioned brain with epidural electrocorticography

Alireza Gharabaghi[1,2]*, Georgios Naros[1,2], Fatemeh Khademi[1,2], Jessica Jesser[1,2], Martin Spüler[3], Armin Walter[3], Martin Bogdan[3,4], Wolfgang Rosenstiel[3] and Niels Birbaumer[5,6,7]

[1] *Division of Functional and Restorative Neurosurgery and Division of Translational Neurosurgery, Department of Neurosurgery, Eberhard Karls University Tuebingen, Tuebingen, Germany*
[2] *Neuroprosthetics Research Group, Werner Reichardt Centre for Integrative Neuroscience, Eberhard Karls University Tuebingen, Tuebingen, Germany*
[3] *Department of Computer Engineering, Wilhelm-Schickard Institute for Computer Science, Eberhard Karls University Tuebingen, Tuebingen, Germany*
[4] *Department of Computer Engineering, University of Leipzig, Leipzig, Germany*
[5] *Institute for Medical Psychology and Behavioural Neurobiology, Eberhard Karls University Tuebingen, Tuebingen, Germany*
[6] *Ospedale San Camillo, IRCCS, Venice, Italy*
[7] *DZD, Eberhard Karls University Tuebingen, Tuebingen, Germany*

Edited by:
Christoph M. Michel, University of Geneva, Switzerland

Reviewed by:
John H. Gruzelier, Goldsmiths, University of London, UK
Tomas Ros, University of Geneva, Switzerland

****Correspondence:***
Alireza Gharabaghi, Division of Functional and Restorative Neurosurgery and Division of Translational Neurosurgery, Department of Neurosurgery, Eberhard Karls University Tuebingen, Otfried-Mueller-Str. 45, 72076 Tuebingen, Germany
e-mail: alireza.gharabaghi@uni-tuebingen.de

Introduction: Different techniques for neurofeedback of voluntary brain activations are currently being explored for clinical application in brain disorders. One of the most frequently used approaches is the self-regulation of oscillatory signals recorded with electroencephalography (EEG). Many patients are, however, unable to achieve sufficient voluntary control of brain activity. This could be due to the specific anatomical and physiological changes of the patient's brain after the lesion, as well as to methodological issues related to the technique chosen for recording brain signals.

Methods: A patient with an extended ischemic lesion of the cortex did not gain volitional control of sensorimotor oscillations when using a standard EEG-based approach. We provided him with neurofeedback of his brain activity from the epidural space by electrocorticography (ECoG).

Results: Ipsilesional epidural recordings of field potentials facilitated self-regulation of brain oscillations in an online closed-loop paradigm and allowed reliable neurofeedback training for a period of 4 weeks.

Conclusion: Epidural implants may decode and train brain activity even when the cortical physiology is distorted following severe brain injury. Such practice would allow for reinforcement learning of preserved neural networks and may well provide restorative tools for those patients who are severely afflicted.

Keywords: electrocorticography, neuroprosthetics, epidural implant, brain-machine interface, neurofeedback, cortical lesion, stroke

INTRODUCTION

Specific feedback and reward of brain activity allows learning of self-regulation strategies. Operant conditioning of electroencephalography (EEG) and of blood-oxygen-level-dependent (BOLD) signal activity has been applied to reduce disorder-specific symptoms in a variety of neurological and neuropsychiatric conditions (Wyckhoff and Birbaumer, 2014). When neurofeedback is coupled to external devices such as brain-machine interfaces (BMI), the volitional control of brain activity can often be attained, opening up novel training opportunities for the very severely brain-injured and even paralyzed (Buch et al., 2008, 2012; Ang et al., 2011, 2014; Gomez-Rodriguez et al., 2011; Ramos-Murguialday et al., 2012, 2013); first results using EEG-based BMI were promising (Ang et al., 2011, 2014; Ramos-Murguialday et al., 2013). Some -even healthy- participants, however, fail to achieve volitional control of brain activity (Vidaurre and Blankertz, 2010) because of subject-specific anatomical (Halder et al., 2011; Buch et al., 2012; Várkuti et al., 2013) and physiological (Blankertz et al., 2010; Grosse-Wentrup et al., 2011; Vukelić et al., 2014) limitations of the brain, or methodological issues of brain signal recording (Leuthardt et al., 2009). In the context of rehabilitation, additional neurophysiological considerations might contribute to limitations of EEG-based BMI: previous approaches have chosen those frequency bands and algorithms which differentiated best between "motor imagery" and "rest", e.g., the mu/alpha-band and/or modified common spatial filter algorithms to optimize the selection of temporo-spatial discriminative EEG characteristics (Buch et al., 2008, 2012; Ang et al., 2011, 2014; Ramos-Murguialday et al., 2013). Although even larger groups of stroke patients have participated in BMI training with this approach, a more restricted feature space, e.g., perturbations

in the beta-band over selected sensorimotor electrode contacts, might be preferred as a reinforced therapeutic target for restorative purposes (Gharabaghi et al., 2014a,b), despite the fact that they might be less optimal from classification purposes, e.g., to differentiate movement-related brain states in stroke patients (Gomez-Rodriguez et al., 2011; Rossiter et al., 2014).

In general, EEG-based approaches have a characteristically low spatial resolution and a low signal-to-noise ratio because of signal attenuation caused by the skull, possible contamination by muscle artifacts and external electrical activity. These approaches might therefore be specifically challenged in cases of an intentionally limited feature space due to therapeutic purposes. Moreover, they often require a relatively long period of training before subjects can gain real-time control of devices (Birbaumer et al., 1999; Leuthardt et al., 2009; Gharabaghi et al., 2014b).

By contrast, electrocorticographic (ECoG) neurofeedback approaches may be able to surmount such difficulties thanks to their proximity to the neural signal source. We recently proposed a new approach which is less invasive than the classical implanted approaches with *subdural* grids (Yanagisawa et al., 2011, 2012; Wang et al., 2013) or even brain penetrating electrodes (Hochberg et al., 2012; Collinger et al., 2013). This novel approach entailed the application of *epidural* ECoG to decode volitional brain activity in patients with locked-in syndrome suffering from amyotrophic lateral sclerosis (Bensch et al., 2014), with chronic pain as a result of upper limb amputation (Gharabaghi et al., 2014c), and with hemiparesis following subcortical hemorrhagic stroke (Gharabaghi et al., 2014b). In all of these cases, however, most of the cortical tissue of the patients was preserved.

Essential questions with regard to the clinical usefulness of implantable brain-computer interfaces based on epidural ECoG remain unanswered. For instance, would this technique also be applicable in patients with extended cortical lesions? Are these patients able to learn consistent online-control of brain activity? Would high intensity neurofeedback training in these patients be possible? Would ECoG neurofeedback be applicable in patients who are not using volitional control of their brain oscillations with a standard EEG-based approach?

We therefore investigated a brain-machine interface based on epidural ECoG and examined its practicability for neurofeedback training in a patient with an extended ischemic lesion of motor cortical areas who did otherwise not adequately engage in voluntary modulation of brain activity based on EEG recordings.

METHODS

PATIENT

The patient, a 52-year-old man, had suffered an ischemic stroke of the right hemisphere with extended cortical lesions (see **Figure 1**) 13 years prior to implantation. This caused a persistent severe hemiparesis and he no longer had control of his left upper extremity (Medical Research Council motor scale < 2).

Several months before surgery, the patient underwent twenty sessions of EEG-based BMI neurofeedback similar to the training described earlier (Ramos-Murguialday et al., 2012; Vukelić et al., 2014) with the same study design that was later used for ECoG-based BMI neurofeedback (see Section Experimental Procedure and **Figure 2**). Offline evaluation of the EEG data revealed artifacts in the recorded brain signals induced by muscle contraction, i.e., showing EEG amplitudes which exceeded the mean cortical activity by at least two standard deviations. For each feedback electrode (FC4, C4 and CP4) we calculated, separately for the "move" and "rest" period of each trial, the percentage of artifacted samples per session and compared their evolution over time with the respective BMI performance evaluated by the area under the recipient operating characteristics curve (AUC).

Several months later, the patient participated in a different, long-term study for motor cortex stimulation with epidural implants simultaneously with rehabilitation training to improve upper limb motor function following the stroke. The study protocol, approved by the ethics committee of the Medical Faculty of the University of Tuebingen, also involved a four-week evaluation period immediately subsequent to implantation, with electrodes externalized with percutaneous extensions to assess the patient's cortical physiology for optimization of stimulation. The data shown below is derived from this period.

Following implantation of the electrode array, i.e., several months after the preoperative evaluation with EEG, the patient was subjected to several different experiments for parameter selection and optimization of motor cortex stimulation (not part of the present report) which included altogether 30 ECoG-based neurofeedback sessions with a mean of $\sim$108 feedback trials per session. Due to their heterogeneity these sessions are not suited to evaluate the evolution of BMI performance during this period, however, they may serve as a valuable source of information for estimating the influence of muscle artifacts, which were visually detected during offline analysis, and the feasibility and reliability of ECoG-based neurofeedback.

EPIDURAL ELECTROCORTICOGRAPHY

The epidurally implanted 4×4 electrode array consisted of four electrode leads for chronic application (Resume II, Medtronic, Minneapolis, USA) with four platinum iridium electrode contacts, each (4 mm diameter, 10 mm center-to-center distance) covering parts of the right primary motor, somatosensory cortex and premotor cortex. During the evaluation period, the electrode grid was externalized with percutaneous extensions which were connected to a recording and processing unit and a robotic hand orthosis. A monopolar amplifier (BrainAmp MR plus, BrainProducts, Munich, Germany) with 1 kHz sampling rate and a high-pass filter (cutoff frequency at 0.16 Hz) and a low-pass filter (cutoff frequency at 1000 Hz) was used for ECoG recording. Online processing of brain signals was performed using the BCI 2000 framework (Schalk et al., 2004) extended with custom-built features to control an electromechanical hand orthosis (Amadeo, Tyromotion GmbH, Graz, Austria). The data was collected batch-wise, i.e., every 40 ms, the recording computer received a batch of data that contained 40 samples per channel (Walter et al., 2012; Gharabaghi et al., 2014a). The reference electrode was chosen from the contacts on the somato-sensory

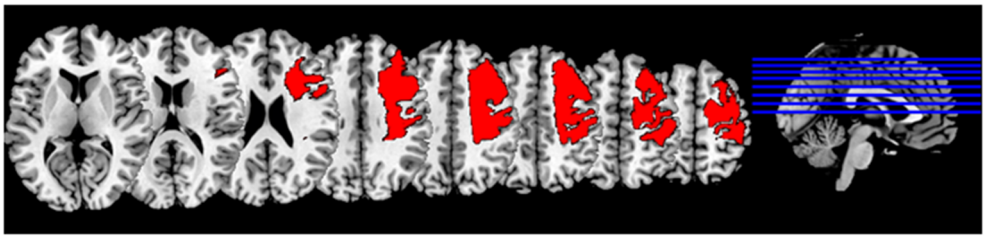

FIGURE 1 | Lesion mask: Normalized lesion mask displayed on MNI (Montreal neurological institute) brain in standard space (Fonov et al., 2009).

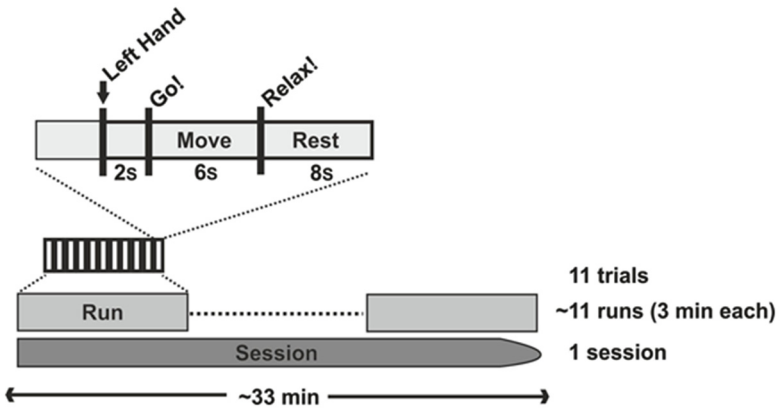

FIGURE 2 | Study design.

cortex, i.e., medio-posterior or latero-posterior corner of the grid.

EXPERIMENTAL PROCEDURE

We used closed-loop, orthosis-assisted opening of the paralyzed left hand which was triggered online by ipsilesional oscillatory brain activity during cued kinesthetic motor imagery of hand opening (Walter et al., 2012; Gharabaghi et al., 2014a). Each session contained 4–16 runs (average 10.86 ± 4.5 runs). Each of the runs had a duration of circa 3 min and consisted of 11 trials. Each trial began with a preparation phase of 2 s, followed by a 6 s movement imagination phase and an 8 s rest phase (see **Figure 3**). Preparation, imagination and rest phases were instigated by a recorded female voice that gave the commands "left hand", "go" and "rest" respectively.

A hand orthosis passively opened the affixed left hand as soon as motor imagery-related event-related desynchronization (ERD) in the beta-band (17–23 Hz) was identified during the movement imagination phase. An epoch was regarded as ERD-positive only when the output of the classifier exceeded a threshold. The latter and the electrode selection were determined individually from three training runs before the test sessions (Walter et al., 2012; Gharabaghi et al., 2014a). The spectral power was calculated using an autoregressive model with an order of 16 (McFarland and Wolpaw, 2008) over a normalized 500 ms sliding window shifting every 40 ms. In order to sidestep a noisy control signal for the orthosis, i.e., giving robust and harmonic feedback, we initiated or discontinued orthosis-assisted movement only when

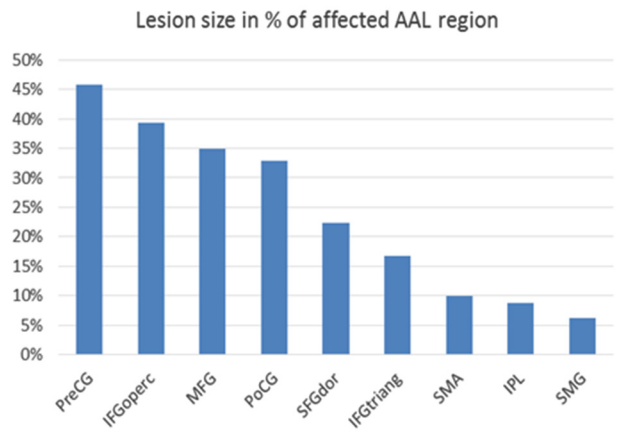

FIGURE 3 | Lesion size in percentage of affected cortical AAL (=automated anatomical labeling) region (Tzourio-Mazoyer et al., 2002): Affected cortical regions are named according to the AAL brain atlas labels: PreCG = precentral gyrus, IFGoperc = pars opercularis of inferior frontal gyrus, MFG = middle frontal gyrus, PoCG = postcentral gyrus, SFGdor = superior frontal gyrus, dorsolateral, IFGtriang = pars triangularis of inferior frontal gyrus, SMA = supplementary motor area, IPL = inferior parietal lobule, SMG = supramarginal gyrus.

five consecutive 40 ms epochs (i.e., 200 ms) where classified as ERD-positive or negative, respectively.

PERFORMANCE EVALUATION

To determine the patient's ability to modulate his brain activity contingent on the BMI feedback task, we determined the percentage of trials with orthosis movement (i.e., ERD) and the average time with orthosis movement (i.e., ERD) divided by the total feedback duration phase (Gharabaghi et al., 2014b,c).

We also measured a baseline condition to supervise spontaneous perturbations of brain activity which could cause fluctuations in the online performance during the feedback task, i.e., could start the orthosis movement independent of motor-imagery. This baseline condition entailed several ECoG recordings which were taken while the patient rested, i.e., one run with eyes open and one run with eyes closed before each session throughout the whole study period. All in all, we recorded approximately 20 min of such spontaneous baseline ECoG activity for offline analysis, segmented it into trials of the same structure and processed it in the same way as in the feedback sessions (Gharabaghi et al., 2014b,c). For statistical analysis, we used the Matlab toolbox (Wilcoxon rank-sum test) to compare the distribution of performance values per run in each feedback session with the distribution of performance values for the baseline data.

IMAGING EVALUATION

Before implantation magnetic resonance imaging (MRI) was performed on a 3.0-Tesla Siemens Trio Scanner (TR 1.95 s, TE 2.26 ms, 176 slices of 1 mm slice thickness). For lesion segmentation MRIcron software[1] was used to manually delineate the lesion. The anatomical image and the mask were normalized to MNI space using SPM 8 (Statistical Parametric Mapping, The Wellcome Department of Imaging Neuroscience, Institute of Neurology, University College London, UK). The overlap of the Automated Anatomical Labeling (AAL) atlas regions and the normalized lesion mask were calculated.

RESULTS

Lesion segmentation revealed that extended parts of the right hemisphere were affected by the stroke, in particular the primary motor and somatosensory cortex with 45% and 33% lesion size and higher motor areas with 35% (middle frontal gyrus) and 22% (superior frontal gyrus) lesion size with respect to the AAL atlas. The basal ganglia were not affected by the lesion (**Figure 3**).

EEG analysis of the non-invasive training showed a systematic change of the number of muscle artifacts. In the course of the training, there was an increase of artifacted samples in the "rest" period of each trial and a decrease in the respective "move" periods. The patient learned to increase and decrease muscle tension in the rest period and in the move period of each trial, respectively (see **Figures 4A,B**).

These changes correlated significantly ($p < 0.05$) with the BMI performance for all channels and both conditions (rest and move), i.e., channel FC4 $r = 0.8905$ for rest and $r = -0.8254$ for move; channel C4: $r = 0.7045$ for rest and $r = -0.8447$ for move; channel CP4: $r = 0.8878$ for rest and $r = -0.8386$ for move (Pearsons correlation coefficient). As a result of the increasing difference between the rest and move condition, there was an increase of BMI control (see **Figure 4B**), i.e., the increased baseline activity in "rest" made it easier to reach the desynchronization threshold in the "move" period for controlling the BMI. Thus, the patient did not volitionally control his oscillatory brain activity for the neurofeedback training.

In contrast, ECoG analysis of the implant based training showed no systematic change in the number of muscle artifacts. Due to the low distance of the two recording channels, the number of artifacted samples was identical. In the course of the training, there was a fluctuating amount of artifacted samples both in the "rest" period and in the "move". Similar to the EEG experiment there were more artifacts in the rest period, but showed no evolution over time. Thus, although muscle tension was not completely eliminated, it did not influence the volitional control of oscillatory brain activity (see **Figure 5**).

Accordingly, in the ECoG-based approach, the patient modulated his motor-imagery related ERD contingent on the BMI feedback task, i.e., initiated the orthosis movement in a mean of $90.49 \pm 13.73\%$ of all trials (baseline condition: $32.72 \pm 9.77\%$), thus retaining significant control of brain activity throughout the whole study period (see **Figure 6**).

In fact, he controlled the orthosis movement (i.e., ERD) for a mean of $37.15 \pm 15.27\%$ of the feedback duration in each trial. Thus, his performance in this online closed-loop paradigm was constant and significantly higher than in the baseline condition ($14.52 \pm 7.30\%$) throughout the study period (see **Figure 7**).

DISCUSSION

The patient presented here—with an extended ischemic lesion of the cortex—learned control of high intensity neurofeedback training based on self-regulation of brain oscillations recorded from the epidural space by ECoG. Although the ECoG based approach enabled the patient to maintain consistent control of his sensorimotor rhythms in the beta-band in an online closed-loop paradigm throughout the study period, his performance in controlling the neurofeedback device in ∼30–40% of the feedback duration was—while significantly better than baseline (∼15%)—nonetheless markedly lower than comparable ECoG-based (Gharabaghi et al., 2014b) or EEG-based (Ramos-Murguialday et al., 2013) approaches in other similarly affected patients who had attained control rates of ∼50–60% of the feedback duration. These variations in performance might be explained by physiological and morphological differences: The respective patients showed strikingly different baseline conditions, i.e., spontaneous perturbations of brain activity in the beta-band could start the orthosis movement independent of motor-imagery during ∼15% vs. ∼30% of the feedback period in the present and in previous cases (e.g., Gharabaghi et al., 2014b), respectively. These physiological baseline differences could be explained by the different lesion characteristics, namely extended cortical vs. circumscribed subcortical lesions, respectively. Since this brain activity is known to originate from primary motor and

[1] http://www.mccauslandcenter.sc.edu/mricro/mricron/install.html

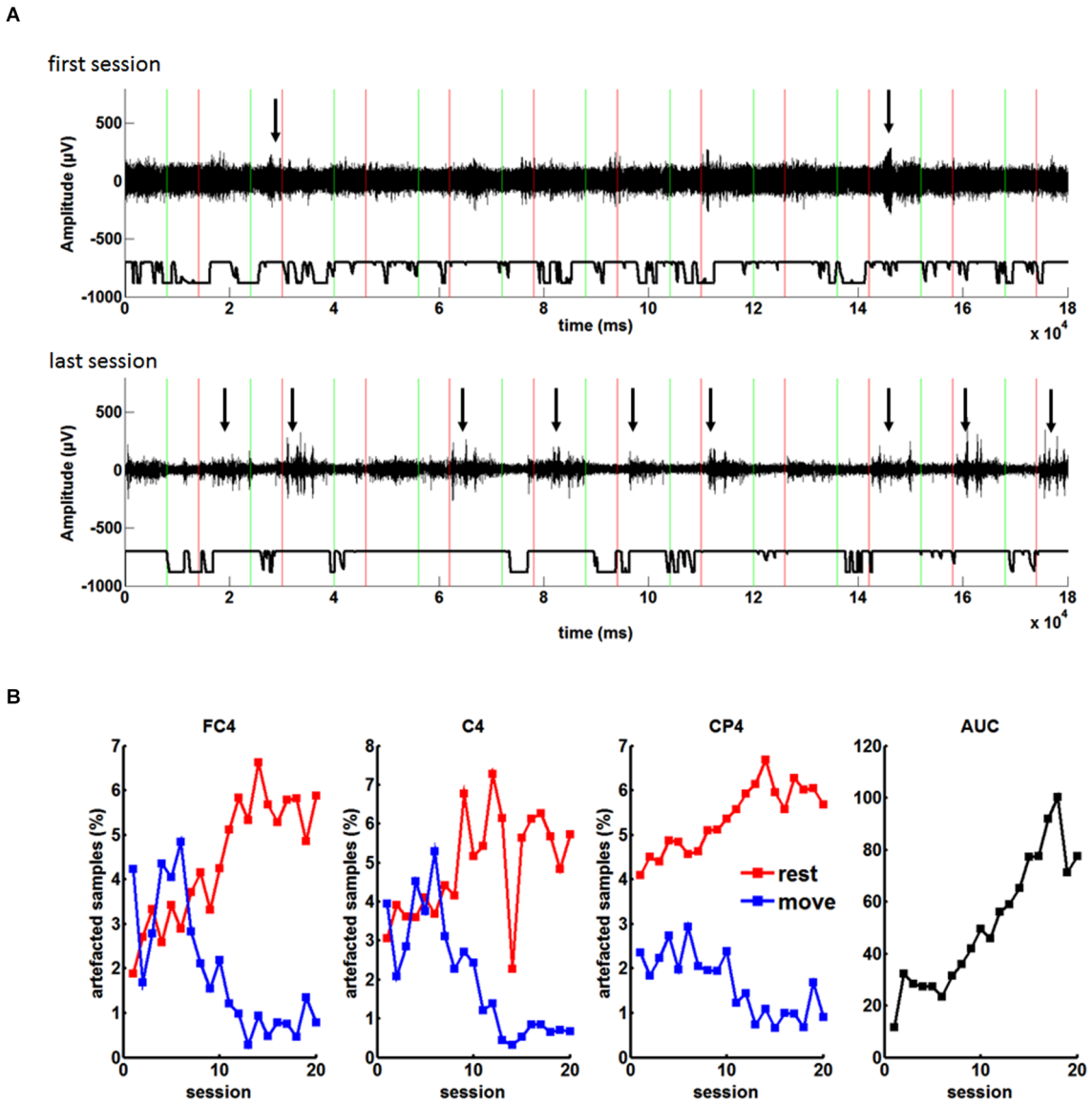

FIGURE 4 | (A) EEG recordings during the feedback task with the orthosis before grid implantation: Green and red lines indicate "Go" and "Rest" cues during each trial, respectively. Arrows highlight muscle artifacts during the run. From the first to the last session the number of the artifacts in the rest period of each trial increased. **(B)** Percentage of artifacted samples during the rest and move condition for the three feedback electrodes (FC4, C4, CP4) in the course of twenty sessions. As a result of the increasing difference of artifacts in the rest and the move condition, there was an increase of BCI control measured by the area under the recipient operating characteristics curve (AUC).

somatosensory as well as from secondary motor areas, the most plausible explanation for the decrease of spontaneous perturbations in the presented case is that they have been affected by the lesion. Our results are in line with recent findings that movement-related beta desynchronization in the contralateral primary motor cortex was found to be significantly reduced in stroke patients compared to controls, while within this patient group, smaller desynchronization has been seen in those with more motor impairment (Rossiter et al., 2014). Moreover, these observations support our general strategy, applied in the present case as well, to choose beta-band desynchronisation as a therapeutic target for restorative interventions in severely affected stroke patients (Gharabaghi et al., 2014a,b).

An intriguing insight gained in this study was that the epidural ECoG technique enabled the patient to engage in feedback exercises based on voluntary modulation of brain activity despite the fact that he did otherwise not use properly a standard EEG-based approach. Interestingly enough, prior to using the implanted brain interface, the patient learned to increase and decrease muscle tension in the rest period and in the move period of each trial, respectively, for BMI control. This alternative conditioning probably occurred because the extent of his

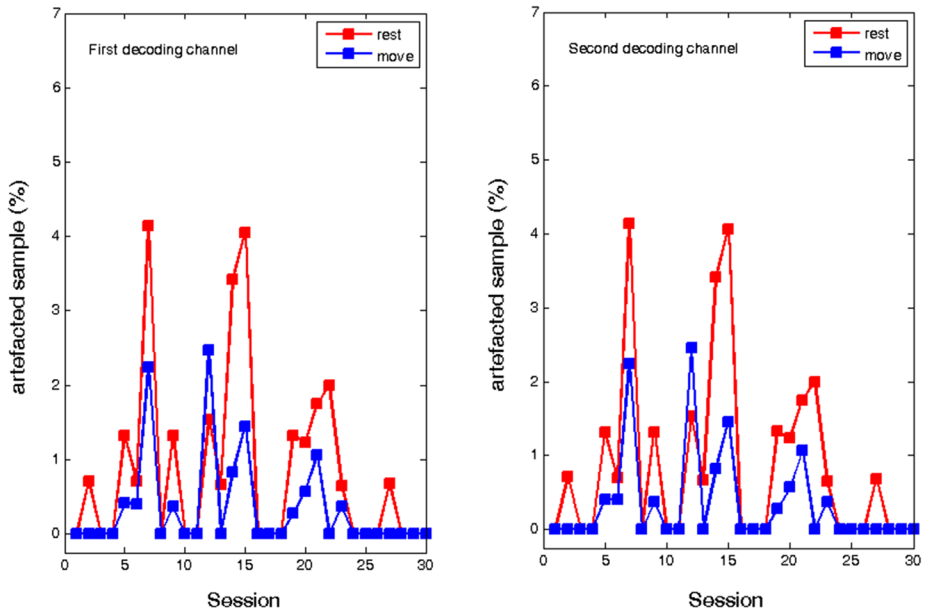

FIGURE 5 | Percentage of artifacted samples during the rest and move condition of the ECoG recordings for two epidural feedback electrodes in the course of thirty sessions.

own voluntary modulation of brain activity was too insignificant to be detected by EEG whereas the muscle contractions could sufficiently be detected and were reinforced by feedback and reward. This alternative control strategy applied by the patient was unexpected. The participants in this study and in previous studies with healthy subjects (Vukelić et al., 2014) and similarly severely affected stroke patients (Ramos-Murguialday et al., 2012) were instructed to avoid blinking, chewing, head and body compensation movements. Along with visual inspection and feedback by an experienced examiner this approach proved to be a sufficient method to prevent alternative BMI control in the past. Moreover, the examiners were prepared to detect compensatory movements *during* the "move" phase of the feedback task as this is the most commonly observed strategy to pretend volitional modulation of ERD, and not *before* the actual task in the "rest" phase. Therefore, increasing baseline activity in "rest" through elevated muscle tension and concurrent reduced muscle tension in the "move" period, have in future to be considered as subtle bypassing strategies to reach the desynchronization threshold more easily.

For this purpose, online detection of EMG contamination with dedicated spectral and topographical analyses might be necessary to prevent alternative BMI control in future. Previous work in this field was conducted without such precautions most probably due to the fact that lower frequency bands were applied for BMI control, which are usually less affected by muscle artifacts (Goncharova et al., 2003). However, due to their relevance for sensorimotor control (Kilavik et al., 2013; Brittain et al., 2014), motor learning (Herrojo Ruiz et al., 2014) and corticospinal excitability (Takemi et al., 2013) as well as due to their correlation with the extent of functional impairments after stroke (Rossiter et al., 2014), higher frequency bands in the beta

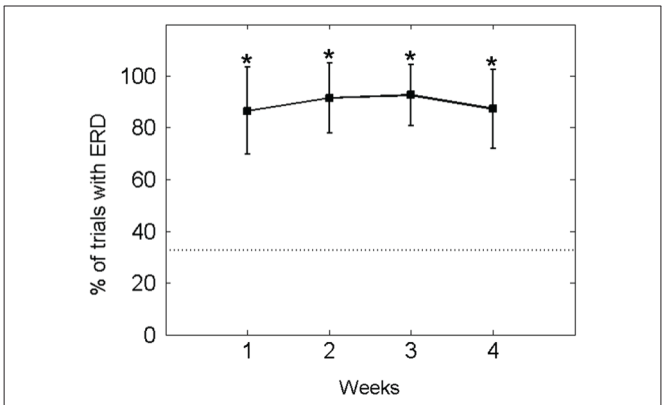

FIGURE 6 | Percentage of EcoG trials with orthosis movement (i.e., event-related desynchronisation [ERD] in the beta-band): The mean ± standard deviation of the performance measure per week is indicated by solid lines. The mean of the baseline data is indicated as a dotted line. An asterisk (*) marks weeks in which the mean of the performance measure differs significantly ($p < 0.05$) from the mean of the baseline value.

range might be considered in future more often as therapeutic targets for restorative EEG neurofeedback and motor rehabilitation (Gharabaghi et al., 2014a,b), necessitating the consideration of even subtle EMG contamination as observed in the presented case. EMG artifact detection may include relatively simple methods such as rejection of EEG segments that exceed a predefined amplitude threshold or more sophisticated methods such as factor decomposition using principal component or independent component analysis with or without source reconstruction algorithms (Goncharova et al., 2003; Hipp and Siegel, 2013). In any case,

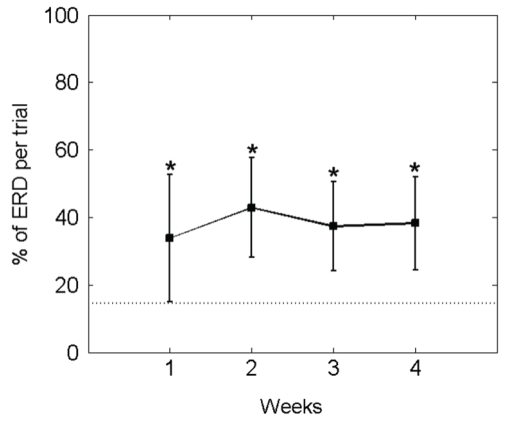

FIGURE 7 | Percentage of average ECoG-based orthosis movement (i.e., event-related desynchronisation [ERD] in the beta-band) divided by the total feedback duration phase: The mean ± standard deviation of the performance measure per week is indicated by solid lines. The mean of the baseline data is indicated as a dotted line. An asterisk (*) marks weeks in which the mean of the performance measure differs significantly ($p < 0.05$) from the mean of the baseline value.

applicable approaches need to work even with only few available channels within a narrow frequency band and have to provide real time processing and low computational complexity (Tiganj et al., 2010).

Should EMG artifacts turn out to be too difficult to mitigate (yet not explicitly addressed by this study) or should the targeted physiological brain state, e.g., motor imagery-related beta-band desynchronisation, be too weak to be robustly detected in the EEG of severely affected stroke patients, implantable approaches might provide an alternative. In this context, the ECoG approach has two advantages over EEG: On account of its proximity to the neural signal source, it surmounts difficulties related to signal attenuation caused by the skull. It is also less susceptible to contamination by muscle artifacts, and, in this case, benefits from the signal attenuation caused by the skull. In this vein, simultaneously recorded ECoG and EEG activity in motor cortical areas revealed that invasively measured signals had a twenty to hundred times better brain signal quality than signals that were acquired non-invasively (Ball et al., 2009).

The technique presented here is limited by the necessity to connect the intracranial implant to an external online processing framework for recording and neurofeedback training via extension leads which are externalized through the skin (Gharabaghi et al., 2014b,c). Future applications of this brain self-regulation approach will require wireless devices capable of fast and reliable information transfer (Borton et al., 2013; Piangerelli et al., 2014). This would facilitate the application of this intervention on a day-patient basis or even in the patient's home environment.

However, before drawing definite conclusions regarding effectiveness of various neurofeedback approaches, future studies need to directly compare ECoG-based techniques to EEG-based methods which control for EMG artifacts. This research needs to consider further aspects such as direct and indirect costs, complications, learning curve, motivation, applicability for long-term use and the possibility of performing training independent of professional support. Based on the respective findings, patients with different impairment levels might then be referred to the specific treatment modality best suited for the individual pathophysiological state.

In conclusion, epidural implants could provide reliable feedback interfaces for brain self-regulation in patients in whom non-invasive approaches fail on account of signal attenuation caused by the skull or due to the underlying pathophysiology. This could establish them as valuable tools in the context of reinforcement learning in a variety of neurological and neuropsychiatric conditions.

ACKNOWLEDGMENTS

Alireza Gharabaghi is supported by grants from the German Research Council, Deutsche Forschungsgemeinschaft [DFG GH 94/2-1, DFG EC 307], and from the Federal Ministry for Education and Research [BFNT 01GQ0761, BMBF 16SV3783, BMBF 03160064B, BMBF V4UKF014]. Fatemeh Khademi is supported by the Graduate Training Centre of Neuroscience, International Max Planck Research School, Tuebingen, Germany. Niels Birbaumer is supported by the Deutsche Forschungsgemeinschaft (Reinhard Koselleck Project) and by Brain Products GmbH, Munich, Germany. We thank Ramin Azodi Avval for his support with the figures and Dr. Mathias Vukelić and Vladislav Royter for fruitful discussions.

REFERENCES

Ang, K. K., Chua, K. S. G., Phua, K. S., Wang, C., Chin, Z. Y., Kuah, C. W. K., et al. (2014). A randomized controlled trial of EEG-based motor imagery brain-computer interface robotic rehabilitation for stroke. *Clin. EEG Neurosci.* 42, 253–258. doi: 10.1177/1550059414522229

Ang, K. K., Guan, C., Chua, K. S. G., Ang, B. T., Kuah, C. W. K., Wang, C., et al. (2011). A large clinical study on the ability of stroke patients to use EEG-based motor imagery brain-computer interface. *Clin. EEG Neurosci.* 42, 253–258. doi: 10.1177/155005941104200411

Ball, T., Kern, M., Mutschler, I., Aertsen, A., and Schulze-Bonhage, A. (2009). Signal quality of simultaneously recorded invasive and non-invasive EEG. *Neuroimage* 46, 708–716. doi: 10.1016/j.neuroimage.2009.02.028

Bensch, M., Martens, S., Halder, S., Hill, J., Nijboer, F., Ramos, A., et al. (2014). Assessing attention and cognitive function in completely locked-in state with event-related brain potentials and epidural electrocorticography. *J. Neural Eng.* 11:026006. doi: 10.1088/1741-2560/11/2/026006

Birbaumer, N., Ghanayim, N., Hinterberger, T., Iversen, I., Kotchoubey, B., Kübler, A., et al. (1999). A spelling device for the paralysed. *Nature* 398, 297–298. doi: 10.1038/18581

Blankertz, B., Sannelli, C., Halder, S., Hammer, E. M., Kübler, A., Müller, K. R., et al. (2010). Neurophysiological predictor of SMR-based BCI performance. *Neuroimage* 51, 1303–1309. doi: 10.1016/j.neuroimage.2010.03.022

Borton, D. A., Yin, M., Aceros, J., and Nurmikko, A. (2013). An implantable wireless neural interface for recording cortical circuit dynamics in moving primates. *J. Neural Eng.* 10:026010. doi: 10.1088/1741-2560/10/2/026010

Brittain, J.-S., Sharott, A., and Brown, P. (2014). The highs and lows of beta activity in cortico-basal ganglia loops. *Eur. J. Neurosci.* 39, 1951–1959. doi: 10.1111/ejn.12574

Buch, E. R., Modir Shanechi, A., Fourkas, A. D., Weber, C., Birbaumer, N., and Cohen, L. G. (2012). Parietofrontal integrity determines neural modulation associated with grasping imagery after stroke. *Brain* 135, 596–614. doi: 10.1093/brain/awr331

Buch, E., Weber, C., Cohen, L. G., Braun, C., Dimyan, M. A., Ard, T., et al. (2008). Think to move: a neuromagnetic brain-computer interface (BCI) system for chronic stroke. *Stroke* 39, 910–917. doi: 10.1161/STROKEAHA.107.505313

Collinger, J. L., Wodlinger, B., Downey, J. E., Wang, W., Tyler-Kabara, E. C., Weber, D. J., et al. (2013). High-performance neuroprosthetic control by an individual with tetraplegia. *Lancet* 381, 557–564. doi: 10.1016/S0140-6736(12)61816-9

Fonov, V. S., Evans, A. C., McKinstry, R. C., Almli, C. R., and Collins, D. L. (2009). Unbiased nonlinear average age-appropriate brain templates from birth to adulthood. *Neuroimage* 47(Suppl. 1), S102. doi: 10.1016/s1053-8119(09)70884-5

Gharabaghi, A., Kraus, D., Leão, M. T., Spüler, M., Walter, A., Bogdan, M., et al. (2014a). Coupling brain-machine interfaces with cortical stimulation for brain-state dependent stimulation: enhancing motor cortex excitability for neurorehabilitation. *Front. Hum. Neurosci.* 8:122. doi: 10.3389/fnhum.2014.00122

Gharabaghi, A., Naros, G., Walter, A., Grimm, F., Schuermeyer, M., Roth, A., et al. (2014b). From assistance towards restoration with epidural brain-computer interfacing. *Restor. Neurol. Neurosci.* 32, 517–525. doi: 10.3233/RNN-140387

Gharabaghi, A., Naros, G., Walter, A., Roth, A., Bogdan, M., Rosenstiel, W., et al. (2014c). Epidural electrocorticography of phantom hand movement following long-term upper-limb amputation. *Front. Hum. Neurosci.* 8:285. doi: 10.3389/fnhum.2014.00285

Gomez-Rodriguez, M., Peters, J., Hill, J., Schölkopf, B., Gharabaghi, A., and Grosse-Wentrup, M. (2011). Closing the sensorimotor loop: haptic feedback facilitates decoding of motor imagery. *J. Neural Eng.* 8:036005. doi: 10.1088/1741-2560/8/3/036005

Goncharova, I. I., McFarland, D. J., Vaughan, T. M., and Wolpaw, J. R. (2003). EMG contamination of EEG: spectral and topographical characteristics. *Clin. Neurophysiol.* 114, 1580–1593. doi: 10.1016/s1388-2457(03)00093-2

Grosse-Wentrup, M., Schölkopf, B., and Hill, J. (2011). Causal influence of gamma oscillations on the sensorimotor rhythm. *Neuroimage* 56, 837–842. doi: 10.1016/j.neuroimage.2010.04.265

Halder, S., Agorastos, D., Veit, R., Hammer, E. M., Lee, S., Varkuti, B., et al. (2011). Neural mechanisms of brain-computer interface control. *Neuroimage* 55, 1779–1790. doi: 10.1016/j.neuroimage.2011.01.021

Herrojo Ruiz, M., Brücke, C., Nikulin, V. V., Schneider, G.-H., and Kühn, A. A. (2014). Beta-band amplitude oscillations in the human internal globus pallidus support the encoding of sequence boundaries during initial sensorimotor sequence learning. *Neuroimage* 85, 779–793. doi: 10.1016/j.neuroimage.2013.05.085

Hipp, J. F., and Siegel, M. (2013). Dissociating neuronal gamma-band activity from cranial and ocular muscle activity in EEG. *Front. Hum. Neurosci.* 7:338. doi: 10.3389/fnhum.2013.00338

Hochberg, L. R., Bacher, D., Jarosiewicz, B., Masse, N. Y., Simeral, J. D., Vogel, J., et al. (2012). Reach and grasp by people with tetraplegia using a neurally controlled robotic arm. *Nature* 485, 372–375. doi: 10.1038/nature11076

Kilavik, B. E., Zaepffel, M., Brovelli, A., MacKay, W. A., and Riehle, A. (2013). The ups and downs of beta oscillations in sensorimotor cortex. *Exp. Neurol.* 245, 15–26. doi: 10.1016/j.expneurol.2012.09.014

Leuthardt, E. C., Schalk, G., Roland, J., Rouse, A., and Moran, D. W. (2009). Evolution of brain-computer interfaces: going beyond classic motor physiology. *Neurosurg. Focus* 27:E4. doi: 10.3171/2009.4.FOCUS0979

McFarland, D. J., and Wolpaw, J. R. (2008). Sensorimotor rhythm-based brain-computer interface (BCI): model order selection for autoregressive spectral analysis. *J. Neural Eng.* 5, 155–162. doi: 10.1088/1741-2560/5/2/006

Piangerelli, M., Ciavarro, M., Paris, A., Marchetti, S., Cristiani, P., Puttilli, C., et al. (2014). A fully integrated wireless system for intracranial direct cortical stimulation, real-time electrocorticography data transmission and smart cage for wireless battery recharge. *Front. Neurol.* 5:156. doi: 10.3389/fneur.2014.00156

Ramos-Murguialday, A., Broetz, D., Rea, M., Läer, L., Yilmaz, O., Brasil, F. L., et al. (2013). Brain-machine interface in chronic stroke rehabilitation: a controlled study. *Ann. Neurol.* 74, 100–108. doi: 10.1002/ana.23879

Ramos-Murguialday, A., Schürholz, M., Caggiano, V., Wildgruber, M., Caria, A., Hammer, E. M., et al. (2012). Proprioceptive feedback and brain computer interface (BCI) based neuroprostheses. *PLoS One* 7:e47048. doi: 10.1371/journal.pone.0047048

Rossiter, H. E., Boudrias, M. H., and Ward, N. S. (2014). Do movement-related beta oscillations change following stroke? *J. Neurophysiol.* 30, 2053–2058. doi: 10.1152/jn.00345.2014

Schalk, G., McFarland, D. J., Hinterberger, T., Birbaumer, N., and Wolpaw, J. R. (2004). BCI2000: a general-purpose brain-computer interface (BCI) system. *IEEE Trans. Biomed. Eng.* 51, 1034–1043. doi: 10.1109/tbme.2004.827072

Takemi, M., Masakado, Y., Liu, M., and Ushiba, J. (2013). Is event-related desynchronization a biomarker representing corticospinal excitability? *Conf. Proc. IEEE Eng. Med. Biol. Soc.* 2013, 281–284. doi: 10.1109/EMBC.2013.6609492

Tiganj, Z., Mboup, M., Pouzat, C., and Belkoura, L. (2010). "An algebraic method for eye blink artifacts detection in single channel EEG recordings," in *17th International Conference on Biomagnetism Advances in Biomagnetism-Biomag* (Springer Berlin Heidelberg), 175–178.

Tzourio-Mazoyer, N., Landeau, B., Papathanassiou, D., Crivello, F., Etard, O., Delcroix, N., et al. (2002). Automated anatomical labeling of activations in SPM using a macroscopic anatomical parcellation of the MNI MRI single-subject brain. *Neuroimage* 15, 273–289. doi: 10.1006/nimg.2001.0978

Várkuti, B., Guan, C., Pan, Y., Phua, K. S., Ang, K. K., Kuah, C. W., et al. (2013). Resting state changes in functional connectivity correlate with movement recovery for BCI and robot-assisted upper-extremity training after stroke. *Neurorehabil. Neural Repair* 27, 53–62. doi: 10.1177/1545968312445910

Vidaurre, C., and Blankertz, B. (2010). Towards a cure for BCI illiteracy. *Brain Topogr.* 23, 194–198. doi: 10.1007/s10548-009-0121-6

Vukelić, M., Bauer, R., Naros, G., Naros, I., Braun, C., and Gharabaghi, A. (2014). Lateralized alpha-band cortical networks regulate volitional modulation of beta-band sensorimotor oscillations. *Neuroimage* 87, 147–153. doi: 10.1016/j.neuroimage.2013.10.003

Walter, A., Ramos Murguialday, A., Spüler, M., Naros, G., Leão, M. T., Gharabaghi, A., et al. (2012). Coupling BCI and cortical stimulation for brain-state-dependent stimulation: methods for spectral estimation in the presence of stimulation after-effects. *Front. Neural Circuits* 6:87. doi: 10.3389/fncir.2012.00087

Wang, W., Collinger, J. L., Degenhart, A. D., Tyler-Kabara, E. C., Schwartz, A. B., Moran, D. W., et al. (2013). An electrocorticographic brain interface in an individual with tetraplegia. *PLoS One* 8:e55344. doi: 10.1371/journal.pone.0055344

Wyckhoff, S., and Birbaumer, N. (2014). "Neurofeedback and brain-computer interfaces," in *The Handbook of Behavioural Medicine*, ed D. I. Mostofsky (Hoboken, NJ: Wiley-Blackwell), 275–312.

Yanagisawa, T., Hirata, M., Saitoh, Y., Goto, T., Kishima, H., Fukuma, R., et al. (2011). Real-time control of a prosthetic hand using human electrocorticography signals. *J. Neurosurg.* 114, 1715–1722. doi: 10.3171/2011.1.JNS101421

Yanagisawa, T., Hirata, M., Saitoh, Y., Kishima, H., Matsushita, K., Goto, T., et al. (2012). Electrocorticographic control of a prosthetic arm in paralyzed patients. *Ann. Neurol.* 71, 353–361. doi: 10.1002/ana.22613

Conflict of Interest Statement: The authors declare that the research was conducted in the absence of any commercial or financial relationships that could be construed as a potential conflict of interest.

Received: 30 June 2014; accepted: 24 November 2014; published online: 09 December 2014.

Citation: Gharabaghi A, Naros G, Khademi F, Jesser J, Spüler M, Walter A, Bogdan M, Rosenstiel W and Birbaumer N (2014) Learned self-regulation of the lesioned brain with epidural electrocorticography. Front. Behav. Neurosci. ***8****:429. doi: 10.3389/fnbeh.2014.00429*

This article was submitted to the journal Frontiers in Behavioral Neuroscience.